Multivariable Thickness Control of a Hot Rolling Mill

Pedersen, Lars Malcolm

1995

Document Version:
Publisher's PDF, also known as Version of record

Department of Automatic Control
Lund Institute of Technology
P.O. Box 118
S-221 00 Lund Sweden

Document name
Licentiate Thesis

Date of issue
September 1995

Document Number
ISRN LUTFD2/TFRT--3214--SE

Author(s)
Lars Malcolm Pedersen

Supervisor
Björn Wittenmark

Sponsoring organisation
The Danish Steel Works Ltd. and The Nordic Fund for Technology and Industrial Development

Title and subtitle
Multivariable Thickness Control of a Hot Rolling Mill

Abstract

The purpose of this report is to design a thickness controller for a hot rolling mill. The thickness control problem is difficult and small improvements make large savings possible. It is therefore relevant to use advanced control strategies for controlling the plate thickness.

In the report a short introduction to the thickness control problem, and a description of how thickness control is done today, is first given. Then a physical model for the hot rolling process is developed, measurements are collected, and the parameters of this model are found using system identification. The model is used for finding a control strategy and to design a controller for the plate thickness. As control methods feedback linearization and eigenspace design are used. The performance of the controller is investigated using computer simulations. Furthermore, the stability is analyzed and the effects of the present parameter variations is also investigated.

The main effort has been spent on developing the model for the rolling mill and identifying the parameters of this model. Modeling is a recursive procedure and after the first iteration several changes of the model were necessary to obtain proper results. Since there are many things to vary in the model and in the way of doing the system identification, it is a complicated procedure to find the right set-up.

It should be recognized that besides the control strategy many other things have been gained from the work with the problem. For instance the knowledge of the nature of the rolling process have increased significantly in connection with the modeling and system identification.

Key words
Hot rolling mill, Rolling process, Thickness control, System identification, Modeling, Controller design

Classification system and/or index terms (if any)

Supplementary bibliographical information

ISSN and key title
0280–5316

ISBN

Language
English

Number of pages
152

Recipient's notes

Security classification

Multivariable Thickness Control of a Hot Rolling Mill

LARS MALCOLM PEDERSEN

The Danish Steel Works Ltd.

and

Department of Automatic Control
Lund Institute of Technology

Life starts at 40.
Danish saying

Life starts at 200.
Bikers' saying

Contents

Preface

This report is the result of three years work at The Danish Steel Works Ltd., Frederiksværk, Denmark and the Department of Automatic Control, Lund Institute of Technology, Sweden. The project has been supported financially by The Nordic Fund for Technology and Industrial Development and The Danish Steel Works Ltd. It is directed towards control engineers with interest in the hot rolling process, but the report might also be of interest for other technicians working with the hot rolling process.

Beside this report the work has been published in the technical report [Pedersen, 1993] and the conference papers [Pedersen, 1994], [Pedersen, 1995], [Pedersen, 1996], and [Pedersen and Wittenmark, 1996]. The last paper is though not yet accepted. Furthermore 60 course credits equivalent to one and a half years of study time have been collected as a necessary part of the Swedish lic. tech. degree.

I would like to thank the management at The Danish Steel Works Ltd, Birgitte Rolf Jacobsen at the Danish Academy of Technical Sciences, and professors Björn Wittenmark and Karl Johan Åström at the Department of Automatic Control for making this project possible and for the freedom I have had in planning and carrying out the project work. I would furthermore like to thank all my colleagues at The Danish Steel Works and at The Department of Automatic Control for making these nice places to work.

At The Danish Steel Works I would like to thank Henrik Kudsk and Kirsten Erichsen for being good colleagues, always prepared to discuss various problems, Carsten Villadsen for the help with the data collec-

tion and Niels Uhrbrand for, despite various accidents, allowing me to collect the data necessary for this project. I would furthermore like to thank my advisor at the Steel Works, Ole Abildgaard for helping me with the modeling and Troels Andersen for showing general interest in my work and for proofreading this report.

At the Department of Automatic Control I would like to thank my advisor Björn Wittenmark for all his work in connection with this project, Bo Bernhardsson for proofreading this report several times, and Anders Rantzer and Ulf Jönsson for helping me out on the stability analysis. I would furthermore like to thank Per Hagander for answering my questions on linear systems and Rolf Johansson for helping me with the system identification.

1

Introduction

When I first started to work with the control systems on the hot rolling mill at The Danish Steel Works, I was impressed by the complexity of the computer system planning the rolling. I was also surprised by the simplicity of the control laws used for controlling the actuators of the rolling mill. Even if there is a lot of control equipment, all the control loops are single-input single-output, and are mostly controlled by PI-controllers.

The simple control algorithms usually work well, are easy to understand and can be tuned on-line. The use of more complex controllers can however lead to better performance. This is especially relevant for actuators with a direct impact on product quality. Better control of these actuators could be an easy and cheap way of improving the product quality and reduce production costs.

The thickness control system is used for ensuring that the plate thickness meets the customers' specifications. Since the plate thickness can not be changed after the rolling, the performance of the thickness control system has a direct impact on the product quality. Furthermore, the increasing level of automation in the industry increases the demands on high thickness accuracy of steel plates. The thickness control therefore qualifies as one of the key processes where the advanced methods are relevant. A more accurate control of the plate thickness will, beside the quality improvement, also make it possible to reduce the target thickness of the plates and hereby save material. Even small improvements make substantial savings possible. Therefore high accuracy thickness control is a worthwhile and challenging

problem.

Beside the economical reasons the rolling process is also interesting from a technical point of view. Several things make the control of the plate thickness difficult:

- The output of the process – the plate thickness – can not be measured with a sufficient accuracy because of the harsh environment near the rolling mill.
- The process is multivariable, that is, it has several important inputs and outputs.
- The material characteristics of the steel plate vary with time.

This makes the process difficult to handle using simple control strategies. The simple control algorithms have the following difficulties:

- They can not handle asymmetric characteristics of the steel plate.
- The fact that the thickness can not be measured introduces problems with the stability of the control loop.
- The variations of the material makes the performance of the controller vary with time.

Further details are given in Chapter 2 and Chapter 3. The above problems make the thickness control of the hot rolling mill a good process for using advanced control methods.

1.1 Problem formulation

The modeling in this report is made from a control engineer's point of view. Normally control engineers work with relatively simple dynamical models for the processes. The relatively simple models make it possible to use some more or less advanced mathematics for analysis and design. The point of view in this work will therefore be different from the traditional rolling theory, where static nonlinear models normally are used.

To be able to design better controllers, better models are needed. Therefore, development of suitable models and determining the parameters

of these models will be a key subject. To be able to design an advanced control strategy we need a dynamical multivariable model. To minimize the number of parameters of the model and to ensure a good understanding, a physical model will be derived. Using the model it will be possible to evaluate the performance of the new control strategy using computer simulations. In the light of the problems described above, an investigation of the stability of the control loop and the effects of the varying material characteristics will be made after the controller design.

We thus arrive at the following problem formulation:

> *The purpose of this report is to improve the performance of the thickness control for a hot rolling mill. The improvement will done by:*
>
> - *deriving a dynamical multivariable model for the hot rolling process;*
> - *designing an advanced control strategy on the basis of the model.*
>
> *The performance of the improved control strategy will be evaluated by computer simulations. The stability of the control loop and the effects of variation of the material characteristics will also be investigated in connection with the controller design.*

It is usually hard to find a good mathematical model for a process at the first attempt. Process modeling therefore often is an iterative procedure. An initial modeling is necessary to decide which input and output signals to collect for the system identification where the parameters of the model are found. Using the results from the identification, the model is adjusted. Usually it is not necessary to collect new data. The controller will be designed when the model is ready. Sometimes the model is also changed in the controller design when the characteristics of the model are evaluated again. Inspired by [Gustavsson, 1975] we can illustrate the modeling and design procedure by Figure 1.1. We will not work with the implementation of the controller in this report, but it is included in the figure for completeness.

Even if we end up with a controller for the thickness control process

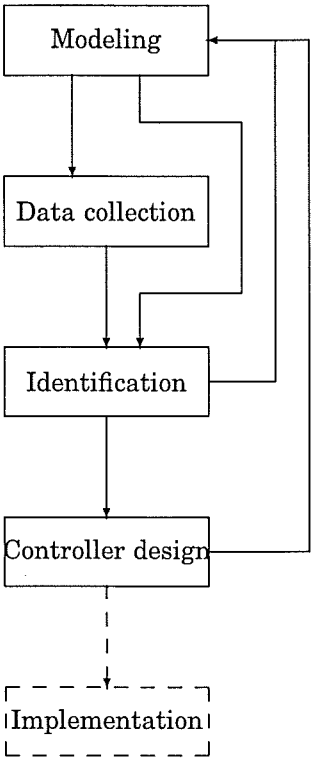

Figure 1.1 Flow diagram for the work in connection with the modeling and controller design. The figure illustrates the iterative nature of the modeling process.

and it performs well in the computer simulations, this does not mean that we are ready for implementation. A lot of work on verifying the theoretical analysis, possible improvements of measurements, and developing and implementing the sequence control of the thickness control remain. This requires people with additional experience of implementation of thickness controllers. The work of this thesis aim to serve as a theoretical basis for a new and improved thickness control system, not as a solution ready for implementation in practice.

It should be mentioned that my knowledge of how the thickness control problem is solved today, comes from the control laws used at The Danish Steelworks and a fairly large, but probably not complete, literature study. It is therefore not only possible, but also likely that there exists more advanced solutions of the thickness control problem, than the one described as the state of the art in this report.

1.2 Outline of the report

The task of this report is to develop models and control strategies for the thickness control for a hot rolling mill. To give a background for this, two introductory chapters are included as an introduction to the modeling and design. The contents of the report are as follows:

Chapter 2: **The thickness control problem**. This chapter gives a basic description of the hot rolling mill and the thickness control problem.

Chapter 3: **Thickness control of hot rolling mills**. Here it is described how the plate thickness is controlled today. The state of the art solution is analyzed and an example of where the traditional control fails is given.

Chapter 4: **Modeling of the rolling mill**. In this chapter the new mathematical models for the rolling mill are derived. The models are later used for the system identification, the controller design, and the computer simulations.

Chapter 5: **Data collection and preprocessing**. To find the parameters of the models, measurements of the input and output

variables are needed. The measurement procedure and the processing of the measurements are described here.

Chapter 6: **System identification**. The parameters of the model are determined. When this is done the models are ready for controller design, and computer simulations.

Chapter 7: **Controller design**. The control law for the thickness control is designed. The performance of the controller is evaluated using computer simulations. The stability and effect of the time varying material characteristics are also investigated.

The conclusions on the work done in this report are given in Chapter 8. The variables used throughout the report are listed in Appendix A and the physical parameters used in connection with the modeling are derived in Appendix B.

2

The thickness control problem

In this chapter a more detailed description of the hot rolling process is given. The description will serve as a basis for the work in the following chapters. The main purposes are to give the reader a feeling for the problem and to introduce the necessary concepts. It should here be noted that this is a description of the rolling process seen from a control engineer's point of view and therefore a lot of details are left out. For more detailed descriptions of the process the reader should read the references as a supplement.

In the following, hot rolling is first described in general and a short introduction to the planning of the rolling sequence is given. The functionality of the rolling mill, relevant for the thickness control, is also described. After this the thickness control problem is described in more detail.

2.1 Hot rolling of steel plates

The purpose of the hot rolling process is to turn preheated steel blocks into plates, that is to make them longer and thinner. The steel blocks are called *slabs*. The thickness of the slab is reduced by pulling it through two parallel rolls, see Figure 2.1.

Each time time the plate is pulled through the rolls is called a *pass* and

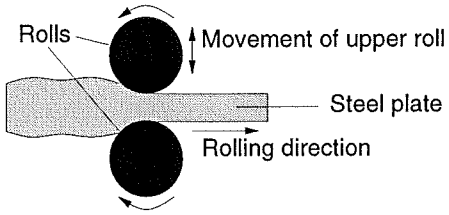

Figure 2.1 The principle of the hot rolling process. The thickness of the steel plate is reduced by pulling it through two parallel rolls.

the difference between the ingoing and outgoing thickness is called the *thickness reduction*. As seen from the figure it is possible to change the outgoing thickness by moving the upper roll. Due to physical limitations the thickness reduction in one pass is limited. It is therefore necessary with several passes before the plate has obtained the desired thickness. In practice this is done by reversing the rolls when the pass is finished and then rolling the plate in the other direction. The series of passes from slab to finished plate is called a *pass schedule*. The above process is called *hot rolling* and the equipment performing the deformation of the steel plate is called a *hot rolling mill*.

The thickness of the slabs at The Danish Steel Works Ltd. are 100, 150, 210, or 260 mm before the rolling is started. Normally the width of the finished plates is between 2 m and 3 m, the length is between 10 m and 25 m, and the thickness is between 6 mm and 100 mm. The weight of one plate varies between 1,000 kg and 13,000 kg. The forces obtained during rolling are quite large, the maximal permitted vertical force, the *rolling force*, is 37.3 MN. This is equivalent to the weight of 1900 Volvos! To be able to handle these large forces the hot rolling mill is quite a solid construction, it is 13 m high, 5 m wide and the diameter of the rolls used for deforming the plate is 1 m. Even if the equipment is large it is possible to obtain quite accurate dimensions of the rolled plates, typical thickness tolerances for thin plates are in the range of ±0.2 mm.

A schematic diagram of the rolling mill is shown in Figure 2.2. When comparing to Figure 2.1 it is seen that a number of things are added.

The work rolls are the rolls used for deforming the steel plate, while the backup rolls are used for supporting the work rolls. This is to prevent excessive bending of the work rolls. The mill frame is used for holding the rolls and the equipment used for positioning the *upper roll pack*, which consists of the upper backup and work rolls. There are two ways of adjusting the position of the upper roll pack:

- using the screws;
- using the hydraulic positioning systems.

The screws are, as the name indicates, two large screws driven by two dc-motors while the hydraulic positioning systems are two grease cylinders placed between the screws and the upper roll pack. The screws are used for large position changes between passes while the hydraulic systems are used for small position changes between and during the passes. Note that it is possible to adjust the position of the roll pack independently at the north and south sides and we therefore have a multivariable system.

The main limitation of the rolling mill is the magnitude of the supply pressure of the hydraulic systems. If the pressure due to the rolling force exceeds this limit it is not possible for the hydraulic systems to operate and the rolling is terminated. This has to be taken into consideration when planning the thickness reductions of the pass schedule.

Using a minimum of time for rolling a plate has several advantages. One is that the rolling is finished while the plate still is hot and therefore soft. Another advantage is that the material flow through the rolling mill is maximized. Careful planning of the pass schedule to ensure maximal utilization of the rolling mill capacity is therefore an important matter. Here maximal utilization implies that all passes should be rolled with a rolling force as close to the limit as possible. Today the planning is handled by a computer control system which optimizes the thickness reduction in each pass to ensure that the rolling is done as fast as possible, for a description of a similar system see [Davies *et al.*, 1983]. This computer control system finds the desired set-points for the roll position, rolling force, and plate thickness. These set-points are transferred to the thickness control system, which operates in two modes:

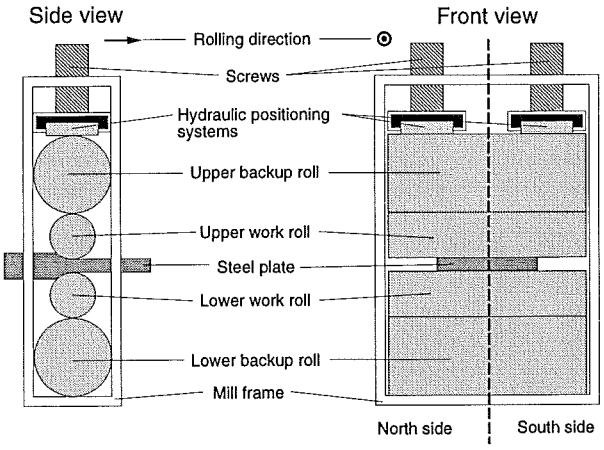

Figure 2.2 Principal diagrams of the rolling mill seen from the side and the front. The main thing to note here is the functionality of the positioning systems for the upper rolls.

- relative control, used in the first part of the pass schedule;
- absolute control, used in the last part of the pass schedule.

In relative control the task of the thickness control system is to keep the thickness close to the value obtained without thickness control in the beginning of the pass. The goal of the absolute control is to keep the thickness as close as possible to the value specified by the planning system. The purpose of the relative control is to prepare the plate for the absolute control.

2.2 Controlling the plate thickness

The reason why it is necessary to control the plate thickness during a pass is that the vertical forces obtained in connection with the deformation of the steel plate are sufficiently large for inducing an elastic deformation of the rolling mill. At the maximal rolling force the deformation of the rolling mill is 7 mm, which is of the same order of

magnitude as the plate thickness for the thin plates in the final passes. Due to the elastic deformation of the rolling mill, two different concepts for the roll gap are used, the *unloaded roll gap*, which is the roll gap between the passes, and the *loaded roll gap*, which is the roll gap during the pass.

The zero point of the unloaded roll gap varies with time. This is because of the thermal expansion of the rolls due to heating by the steel plates and wear of the work rolls. It is therefore necessary to find the zero point for the unloaded roll gap regularly. This is done is by pressing the rolls together with a large force. When the measured position is corrected for the mill deflection we have a reliable mean value for the zero point of the unloaded roll gap. Another thing that affects the zero point of the unloaded roll gap is the roll eccentricity and ovalness. These phenomena vary considerably faster with time than the wear and thermal expansion. Therefore more advanced methods are needed to compensate for the roll ovality and eccentricity.

Due to the bending of the rolls the plate is always thicker at the center than at the edges, this phenomenon is called *plate crown*. This results in an unnecessary use of material. To cancel this effect, to some extent, the work rolls are made thicker at the center than at the edges. This is referred to as *roll crown*.

If the rolling force during the pass was constant it would be possible to preset the position of the upper roll pack to ensure that the loaded roll gap was equal to the desired plate thickness. Unfortunately the rolling force is hard to predict and it varies during the pass. These variations are due to different characteristics of the steel plate along the plate length:

- variation of the ingoing plate thickness;
- variation of the plate hardness.

The variations of the ingoing plate thickness are due to imperfect thickness control and the variations of the plate hardness are mainly induced by variations of the plate temperature. The temperature variations are due to inhomogeneous heating by the reheating furnaces and cooling by the roller tables used for transporting the plate. As will be seen in the data collection in Chapter 5 these disturbances have a

significant influence on the plate thickness. The steady state gain and the dynamics of the rolling process vary with material properties, this will be investigated in Chapter 7. Apart from the material properties the rolling force also varies with the thickness reduction, see [Roberts, 1983].

The thickness of the steel plate is controlled by varying the position of the hydraulic systems during the pass, that is, the hydraulic systems are the actuators of the thickness control system. A main difficulty in connection with the thickness control is that it is not possible to measure the plate thickness during the rolling. It is simply not possible to build reliable equipment for measuring the plate thickness because of the heat radiation from the steel plate and the steam from the water used for cleaning the plate surface during rolling. Since it is not possible to measure the thickness during the the pass it is necessary to estimate it. This estimate can then be updated using a value of the thickness measured after the last pass, see [Ferguson *et al.*, 1986].

The available measurements for the thickness control are:

- the positions of the screws;
- the positions of the hydraulic systems;
- the rolling forces at the north and south sides.

These signals are usually available for the thickness control. The rolling force is interesting because it is an internal variable which is closely related to the plate thickness. Since it is possible to get a reliable measurement of the rolling force it is often used for the thickness control, see [Wood *et al.*, 1977].

2.3 Summary

With the above basic description of the control problem in mind we conclude that the thickness control mainly is a regulator problem where the main task of the thickness control is to eliminate the effects of process disturbances. An additional difficulty, which makes the thickness control problem non-standard, is that it is not possible to measure the process output in connection with the control.

A natural question to be asked now is: *How is the thickness control problem solved today?*. This subject will be treated in the following chapter.

3

Thickness control of hot rolling mills

The purpose of this chapter is to describe the state of the art of thickness control for hot rolling mills. This is done to prepare the reader for the fundamental ideas used in the following chapters.

First a general statement of the thickness control problem is given and a general controller structure is derived. After this the state-of-the-art model is described and using this model the structure of the thickness controller is found. The performance and stability of this control structure is then analyzed. The thickness control laws rely on a fundamental symmetry assumption and in the last section an example is presented of what happens if the symmetry assumption is not fulfilled. This is done to illustrate the potential advantages of a multivariable control strategy.

3.1 What is needed?

Inspired by Chapter 2 we formulate the thickness control problem for hot rolling mills:

> *The purpose of the thickness control for a hot rolling mill is to maintain the specified thickness despite:*
>
> - *variations of the plate hardness;*

- *variations of the ingoing thickness.*

Since the plate thickness can not be measured during the pass it has to be estimated.

We conclude that we need a model for the controller design, a controller able to cancel the above disturbances, and an observer for estimating the plate thickness during the rolling. Two models will be used. One for the controller design and one used in the observer for estimating the plate thickness. The reason for using two different models is that the rolling force measurement is available when implementing the controller, but is not of much use when designing the controller since it is just an internal variable of the rolling mill and not an independent input of the process. As will be seen later the rolling force is of good use when the thickness is to be estimated, and it is therefore used as an input for the observer.

At our disposal we have the signals

- the roll positions at the north and the south sides, which are the sums of the screw and the hydraulic positions, $z^T = [z_n \quad z_s]$;
- the rolling force measurements at the north and south sides, $f^T = [f_n \quad f_s]$.

The principal structure of the thickness controller is shown in Figure 3.1. This controller structure is used both for the existing control strategy and the new control strategy developed in this report. In the figure v_e is the output of the observer, r is the reference for the plate thickness and x_{vr} is the control signal for the hydraulic positioning systems. The controlled output is the plate thickness v.

3.2 What is done already?

Looking at the existing thickness control strategies described in various articles and papers we conclude that the models and observers used for control purposes for the rolling stand are static and scalar, see for instance [Choi *et al.*, 1994], [Edwards, 1978], [Asada *et al.*, 1986], [Bryant *et al.*, 1975], [Ferguson *et al.*, 1986], [Ginzburg, 1984],

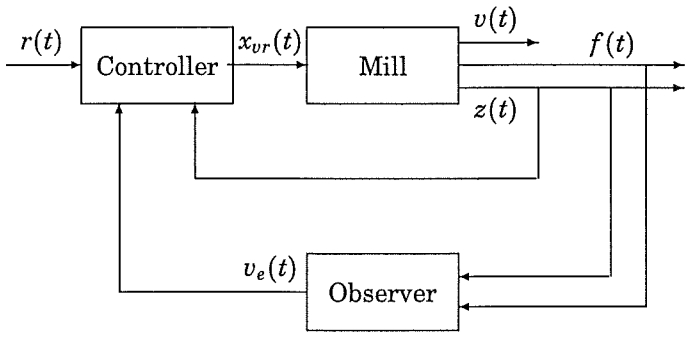

Figure 3.1 General structure of the thickness controller. Here f is the rolling force measurement, z is the roll position measurement, v is the plate thickness, r is the thickness reference, v_e is the estimate of the plate thickness, and x_{vr} is the control signal for the positioning systems. The observer is necessary since it is not possible to measure the plate thickness during rolling.

[Atori *et al.*, 1992], [Nakagawa *et al.*, 1990], [Saito *et al.*, 1981], [Teoh *et al.*, 1984], and [Yamashita *et al.*, 1976]. The scalar models are found by using the mean values of the variables at the north and south sides.

Normally the rolling mill is modeled as a nonlinear spring $K(f,w)$ where w is the plate width f are the rolling forces. The plate is modeled as a time varying spring $a_m(t)$. Since a_m and K are spring constants they are real and positive.

Assuming that the plate thickness is equal to the loaded roll gap we find that the mean value of the deflection of the rolling mill is the difference between the mean value of the plate thickness $\overline{v}$ and the mean value of the roll position $\overline{z}$:

$$\overline{v}(t) - \overline{z}(t) - o(t),$$

where $\overline{z} = \frac{1}{2}(z_n + z_s)$, o is the roll eccentricity and ovalness, and $\overline{v} = \frac{1}{2}(v_n + v_s)$. v_n is the plate thickness at the north edge and v_s is the plate thickness at the south edge.

The deflection of the plate is equal to the thickness reduction:

$$\overline{v}_{-1}(t) - \overline{v}(t),$$

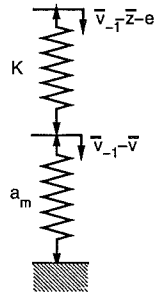

Figure 3.2 The state-of-the-art model used for thickness control today. The steel plate and the rolling mill are modeled as springs.

where $\overline{v} = \frac{1}{2}(v_{-1n} + v_{-1s})$. v_{-1n} is the ingoing thickness at the north edge and v_{-1s} is the ingoing thickness at the south edge.

Since the rolling mill and the plate are modeled as springs we find the mean value of the rolling force $\overline{f}$ by multiplying the deflection of the rolling mill by the mill spring coefficient K and the deflection of the plate by the plate hardness a_m. As illustrated by Figure 3.2 these two forces are equal and we therefore arrive at the equation

$$\overline{f}(t) = a_m(t)(\overline{v}_{-1}(t) - \overline{v}(t)) = K(f,w)(\overline{v}(t) - \overline{z}(t) - o(t)), \tag{3.1}$$

where $\overline{f} = \frac{1}{2}(f_n + f_s)$. We are now able to derive the equations for the mean value of plate thickness $\overline{v}$, where we suppress the arguments for convenience

$$\overline{v} = \frac{1}{K}\overline{f} + \overline{z} + o \tag{3.2}$$

$$= \frac{K}{K + a_m}(\overline{z} + o) + \frac{a_m}{K + a_m}\overline{v}_{-1}. \tag{3.3}$$

We now see why the mean value of the force $\overline{f}$ is used for the thickness estimation. Using the rolling force it is possible to estimate the plate thickness without knowing the plate hardness a_m and the ingoing thickness $\overline{v}_{-1}$. The roll eccentricity and ovalness o still enters (3.2) as an unmeasurable disturbance. Eq. (3.2) is often referred to as the

gaugemeter equation. Note that the gain of the relation between mean value of the thickness $\bar{v}$ and the mean value of the position $\bar{z}$ in (3.3) is time varying due to the variations of the plate hardness a_m and the mill spring coefficient K.

The hydraulic systems are usually controlled using a separate controller, see for instance [Huzyak and Gerber, 1984], [Ginzburg, 1984], [Saito *et al.*, 1981], and [Nakagawa *et al.*, 1990]. We consequently here model the hydraulic systems as a second order system, with unit steady state gain

$$\bar{z}_h = G_h \bar{z}_r = \frac{\omega_h^2}{p^2 + 2\zeta_h \omega_h p + \omega_h^2} \bar{z}_r \tag{3.4}$$

where $\bar{z}_r$ is the reference for the positioning system from the thickness controller and $\bar{z}_h$ is the mean position of the hydraulic systems found using G_h. $p = \frac{d}{dt}$ is the differential operator, and G_h is the transfer function for the hydraulic system.

Using (3.2) we obtain the observer for the thickness estimation

$$\bar{v}_e = \frac{1}{\overline{K}} \bar{f} + \bar{z} + o_e,$$

where $\overline{K}$ is an estimate of the mill spring coefficient K, o_e is an estimate of the roll eccentricity and ovalness o, and $\bar{v}_e$ is an estimate of the mean value of the thickness $\bar{v}$. Using this for estimating the plate thickness we have the control law

$$\bar{z}_r = C_v (\bar{r} - \bar{v}_e) = C_v \left(\bar{r} - \frac{1}{\overline{K}} \bar{f} - \bar{z} - o_e \right), \tag{3.5}$$

where C_v is the transfer function for the thickness controller and $\bar{r}$ is the reference for the mean thickness $\bar{v}$.

The structure of the control system is shown in Figure 3.3. For more detailed descriptions of the thickness control problem, see [Middleton and Goodwin, 1990] and [Grimble and Johnson, 1988].

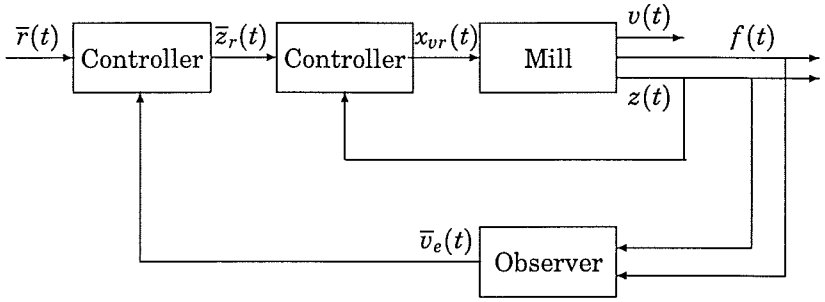

Figure 3.3 The state-of-the-art thickness control. $\overline{r}$ is the reference for the mean value of the plate thickness $\overline{v}$, $\overline{v}_e$ is the estimate of the mean value of the thickness, $\overline{z}_r$ is the reference for the position controllers, and x_{vr} are the control signals for the positing systems. The output signals are the roll positions z, the rolling forces f, and the plate thicknesses v. In this solution the hydraulic positioning systems are controlled by separate controllers.

3.3 Analysis of the state-of-the-art solution

Introducing $\overline{z}_h$ for $\overline{z}$ in (3.5) and using (3.4) and (3.1) we find that

$$\overline{z} = \frac{G_h C_v}{1 + G_h C_v}\left(\overline{r} - \frac{a_m}{\overline{K}}(\overline{v}_{-1} - \overline{v}) - o_e\right).$$

Inserting this for $\overline{z}$ in (3.3) and assuming that the material hardness a_m varies slowly and that the estimate of the mill spring coefficient $\overline{K}$ is kept constant during the pass we find that

$$(1 - \varphi G_t)\overline{v} = \frac{K}{a_m + K} G_t \overline{r} + \frac{K}{a_m + K}(o - G_t o_e) + \frac{a_m}{a_m + K}\left(1 - \frac{K}{\overline{K}} G_t\right)\overline{v}_{-1}, \quad (3.6)$$

where $G_t = (G_h C_v)/(1+G_h C_v)$ and $\varphi = (K/\overline{K})a_m/(a_m+K)$. Normally an integrator is included in the thickness controller C_v and therefore the steady state gain of G_t will be 1.

Performance

Several things can be concluded from (3.6). If $\overline{K} = K$ we will have full compensation for the mill deflection ($\overline{v} = \overline{r}$) at steady state, since $1 - \varphi G_t$ reduces to $K/(a_m + K)$ and the term on v_{-1} vanishes. However if $o_e = 0$ then the roll eccentricity and ovalness o affects the mean value of the plate thickness $\overline{v}$ with a gain of 1 if $\overline{K} = K$. It can be seen from (3.3) that without the thickness control o is reduced by a factor $K/(a_m + K)$. The thickness control therefore tends to amplify the effect of roll eccentricity and ovalness. For a more detailed analysis of the accuracy of the thickness control, see [Kokai *et al.*, 1985]

The left side of (3.6) shows that the thickness control uses positive feedback. This stems from the fact that if the plate thickness for some reason becomes too large it is necessary to close the roll gap which increases the rolling force and thereby the plate thickness by a factor φG_t. Since $\varphi < 1$, for $\overline{K} = K$ the plate thickness $\overline{v}$ will however still be reduced by closing the roll gap in this case. The positive feedback can also be seen from the fact that a too large rolling force makes it necessary to close the roll gap which makes the force even larger – this also illustrates the fact that the thickness control tends to amplify the rolling force variations.

The problem of eliminating the effects of the roll eccentricity and ovalness o has been given much attention. There are two main groups of methods to reduce the impact of o:

- Traditional methods, where it is exploited that o can be observed as small periodic variations in the rolling forces f. Here band-stop filters and dead-zones are used to prevent the thickness control to react to these variations in the rolling force. These two methods only compensate partly for the roll eccentricity. An other possibility is to add an inner force control loop to ensure that the small variations of the rolling are cancelled. This method is able to compensate fully for the roll eccentricity and ovalness. For a comparison of these methods see [Edwards, 1978].
- Advanced methods, where o_e is estimated and used in the thickness control, as in (3.5).

Quite advanced methods have been used for the last alternative, see

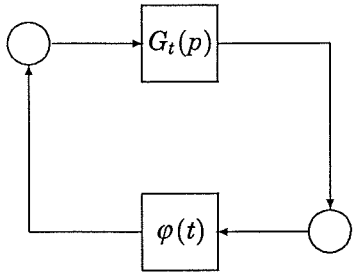

Figure 3.4 Standard representation of thickness control problem for using the small gain theorem to determine the stability.

for instance [Kitamura *et al.*, 1987], [Yeh *et al.*, 1991], and [Edwards *et al.*, 1987].

Stability

To illustrate the stability problem we represent the characteristic polynomial on the form shown in Figure 3.4. Assuming that G_t is stable, and using the small gain theorem, see [Desoer and Vidyasagar, 1975], we find that the closed loop will be stable if

$$\begin{aligned} \gamma_1 &\geq \sup_{s=j\omega} |G_t(s)| \\ \gamma_2 &\geq \sup_{t} |\varphi(t)| \\ \gamma_1\gamma_2 &< 1. \end{aligned}$$

Even if it by the controller design is ensured that $\gamma_1 \leq 1$, the mill spring coefficient K can vary approximately ±20%, which makes it necessary to increase the value of the estimate of the mill spring coefficient $\overline{K}$ to ensure that $\gamma_2 < 1$. Normally $\overline{K}$ is made 20 % larger than K, this is called *detuning* and deteriorates the performance of the thickness control system. Note that the problem with the instability is introduced by the fact that it is necessary to estimate the plate thickness using an observer.

3.4 What can be improved? – An example

A general comment to the way thickness control is done today could be that the rolling mill is quite a complex structure which is modeled by a spring which is a simple mechanical structure. Several questions about the dynamics and multivariable structure of the process can be asked. We concentrate on this and will therefore not look at the compensation for roll eccentricity and ovalness, since this subject is considered well developed already.

The models described above use the mean values of the variables of the north and south sides. The implicit assumption is that the rolling process is symmetric around the vertical symmetry line of the rolling mill. This symmetry can be disturbed if the plate is not centered in the mill or if the temperature of one side of the plate deviates from the temperature of the other side. The variations of the plate hardness is typically induced by inhomogeneous heating by the reheating furnaces and inhomogeneous cooling by the roller tables.

The consequence of such asymmetric effects are shown Figure 3.5. Here the more advanced model derived in the following chapters is used for simulating the case where the plate hardness across the plate width is asymmetric. In the simulations asymmetric conditions in the plate hardness of ±20 % between the plate edges are introduced at $t = 0.5$. For more details refer to Chapter 7.

As seen from the figure the traditional control system does not react properly, since the mean value of the plate thickness is not changed. Worse is the fact that the plate length of the two sides will be different due to the different thickness reductions – this will give the plate an undesired curved shape.

To compensate for the hardness asymmetry we need:

- a multivariable model;
- a multivariable observer;
- a controller which can handle the multivariable case.

Due to the nonzero mass of the roll pack and the damping of the rolling process the rolling mill is also a dynamical system. We will thus de-

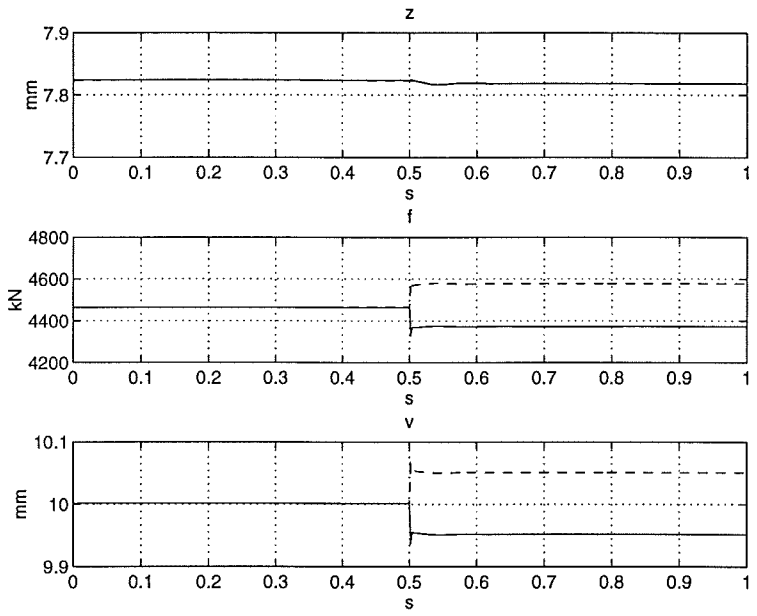

Figure 3.5 The effect of asymmetric material hardness using the traditional thickness controller. Top plot, full: roll position north side z_n and dashed: roll position at the south side z_s. Middle plot, full: rolling force north side f_n and dashed: rolling force at the south side f_s. Bottom plot, full: plate thickness at north edge v_n and dashed: plate thickness at south edge v_s. It is seen that the thickness errors due to the asymmetric material conditions remains unaffected. The small change in the roll position is due to a slight change of the sum of the rolling forces.

velop dynamical multivariable models for the rolling mill in the following.

Since we are not able to measure the plate thickness we use the principle illustrated by Figure 3.1 – the main difference will be that we increase the complexity of the observer, and the model used for the thickness control. Since we can not measure the process output we are not able to use a standard observer. We will therefore use an open loop observer for estimating the plate thickness from the roll positions z and the rolling forces f.

3.5 Summary

We have now described how the thickness control problem is solved today. The state of the art is a controller and an observer based on static scalar models. Investigating the thickness control system we find that special stability and performance problems occur since it is necessary to estimate the controlled output.

Since the thickness controllers today rely on a symmetry assumption, asymmetric rolling conditions cause errors in the control of the plate thickness. More complex models and controllers are necessary to handle this case. The derivation of these models and control strategies are the purposes of the work presented in this report.

4

Modeling of the rolling mill

The purpose of this chapter is to derive physical models for the rolling mill, which is divided into two subsystems:

- the hydraulic systems used for positioning the roll pack;
- the rolling stand used for deforming the steel plate.

The model for the hydraulic systems is more or less standard, see [Gou, 1991], while the other is new and it will therefore be described in more detail.

In the beginning of this chapter the model for the hydraulic systems is derived. This is done by explaining how the real systems works and from this form a physical model which describes the main characteristics of interest. Using the physical model the nonlinear differential equations for the hydraulic systems are found.

A model for the controller design and an observer for the thickness estimation are derived. The difference between the two is whether the force measurements are available or not. The above idea with the physical model is again exploited. It is used to find energy functions for the rolling stand. From these the partial differential equations for the stand are found and ordinary differential equations are derived using modal truncation.

In the final part of the chapter the models for the hydraulic systems and the model for the rolling stand are combined to a total model for the entire system.

Aspects connected with the system identification, such as parametriza-

tion and identifiability, will be treated later, since they depend on which realization of the models that is appropriate for describing the real system.

4.1 Hydraulic system

The modeling of the hydraulic systems has already been done by several authors. The suggested nonlinear models do not differ much. For application to rolling mills see, for instance, [Ginzburg, 1984], [Paul, 1975], and [Gou, 1991].

There are two hydraulic systems on the rolling mill, one for each side. The two systems are identical and therefore only the north system is considered in the following. The hydraulic system can be divided into three main parts, see Figure 4.1:

- servo valve – controls the oil flow to the system;
- oil cylinder – positioning of common piston;
- grease cylinder – positioning of grease piston and roll pack.

Since the compressibility of grease is smaller than the compressibility of oil it is possible to use a higher working pressure in the grease cylinder. This makes it possible to reduce the area of the grease piston, which increases the stability of the mechanical construction. The common piston, which connects the oil and grease cylinders, reduces the pressure from the grease to the oil side and works as a mechanical amplifier.

The servo valve is used for controlling the velocity of the common piston. This is done by varying the flow "through" the oil cylinder. The velocity of the grease piston is controlled by adjusting the level in the grease cylinder using the common piston. To ensure a low back pressure when adjusting the roll pack downwards the right side of the oil cylinder is drained for oil. Note that since the grease system is single acting the entire system is single acting. That the system is single acting implies that it is only possible to push the roll pack downwards with a large force.

The available measurements are, see Figure 4.1:

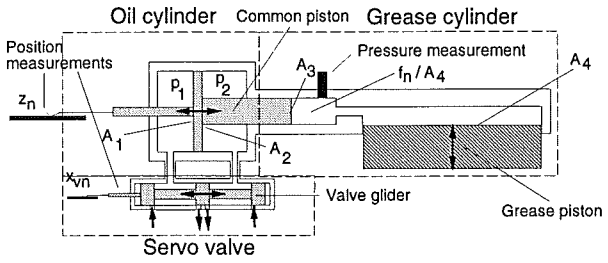

Figure 4.1 Schematic diagram of the main parts of the hydraulic system. The servo valve controls the oil flow to the oil cylinder. The oil cylinder is connected to the grease cylinder by the common piston. The grease piston moves the roll pack.

- position of valve glider of the servo valve x_{vn},
- position of the common piston z_n,
- rolling force f_n.

Note that even if it is the position of the grease piston we want to control it is the position of the common piston that is measured. The two positions can though easily be related by assuming that the grease is incompressible and using the ratio of the areas of the common piston.

The measurement of the grease pressure is used as a rolling force measurement. The load on the hydraulic system is not directly included in the model, it enters through the north rolling force f_n. The most significant part of the load is the friction between the work rolls and the mill frame. This implies that that this measurement also includes the frictional forces from the movement of the upper roll pack, see [Zeltkalns *et al.*, 1977]. Generally, backlash is not a problem when the plate is in the mill since the mechanical system is pressed together with a large force. Furthermore, the positioning system is lubricated with grease. Backlash and friction will therefore not be considered here.

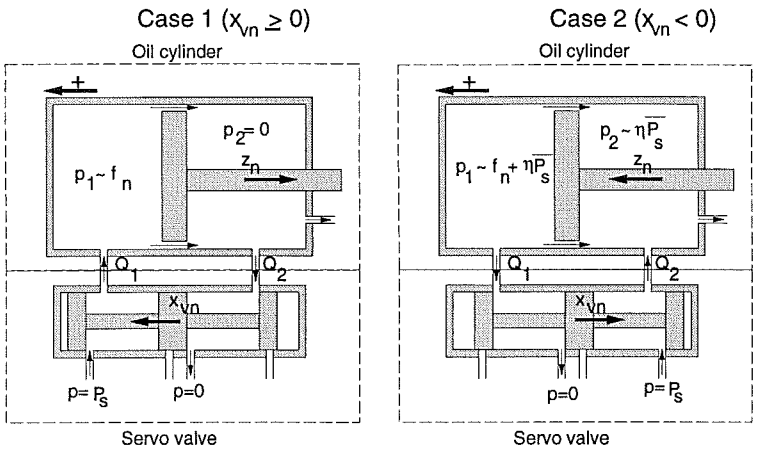

Figure 4.2 The physical model for the hydraulic systems. The model illustrates the effects we want to include.

Physical model

To be able to derive a mathematical model we first build a physical model, which includes the properties of the hydraulic systems we want to model, see Figure 4.2. Since it is not possible to measure the position of the grease piston only the oil side is included in the physical model. The mass and friction of the rest of the hydraulic system will therefore be included in the load. Furthermore, the function of the servo valve is not considered since it is not essential for the functionality of the hydraulic system.

The positive direction of the flow of the left side of the oil cylinder Q_1 is into the cylinder and the positive direction of the flow of the right side of the oil cylinder Q_2 is out of the cylinder. Note the leak flow between the piston and the cylinder wall. Note furthermore that the pressures of the return paths of the servo valve are set to zero and the supply pressure P_s is assumed constant.

To derive a model we need to know the pressure at both sides of the oil piston. To model the oil compressibility it is also necessary to know

the time derivative of these pressures. Since the pressure is measured at the grease side only a linear combination of the pressures at the oil side can be measured, neglecting mass and friction of the common piston the relation is

$$\frac{A_3}{A_4} f_n(t) = A_1 p_1(t) - A_2 p_2(t), \tag{4.1}$$

where p_1 and p_2 are the pressures at the left and right sides of the oil cylinder, respectively, and f_n is the rolling force. A_1, A_2, and A_3 are the areas of the common piston corresponding to p_1, p_2, and f_n/A_4 and A_4 is the area of the grease piston.

Since the oil is drained from the right side of the oil cylinder, we have an additional leak flow. This makes it hard to find the values of the flow Q_2 and the pressure p_2. When the valve glider position $x_{vn} > 0$ and the positioning system is moving downwards there is no flow into the right side of the cylinder and we might assume that the this side is drained for oil in this case. This leads us to the assumption

$$\begin{aligned} A_1 p_1(t) &\approx \frac{A_3}{A_4} f_n(t) \\ A_2 p_2(t) &\approx 0. \end{aligned} \tag{4.2}$$

When the valve glider position $x_{vn} < 0$ and the positioning system therefore moves upwards there is an oil flow into the right side of the cylinder and we can no longer assume that it is drained for oil. We here make the simple assumption that the pressure $p_2 \approx \eta P_s$. Intuitively the coefficient η tells us how much of the pressure at the servo valve that is applied at the common piston. The assumption leads to the equations

$$\begin{aligned} A_1 p_1(t) &\approx A_2 \eta P_s + \frac{A_3}{A_4} f_n(t) \\ A_2 p_2(t) &\approx A_2 \eta P_s, \end{aligned} \tag{4.3}$$

which have been shown to work well in practice. Note that since the areas $A_1 \approx A_2$ (4.1) is still approximatively fulfilled.

Derivation of model

The model is derived by combining the flow through the servo valve and the cylinder. Using [Trostmann, 1987] and [Gou, 1991] we find that the flows through the servo valve can be modeled as

$$\text{Case 1: } x_{vn}(t) \geq 0$$

$$\begin{cases} Q_1(t) = k_1 x_{vn}(t)\sqrt{p_1(t)} = \overline{k}_1 x_{vn}(t)\sqrt{\overline{P}_s - f_n(t)} \\ Q_2(t) = k_1 x_{vn}(t)\sqrt{p_2(t)} = 0 \end{cases} \tag{4.4}$$

$$\text{Case 2: } x_{vn}(t) < 0$$

$$\begin{cases} Q_1(t) = k_1 x_{vn}(t)\sqrt{p_1(t)} = \overline{k}_1 x_{vn}(t)\sqrt{\eta\overline{P}_s + f_n(t)} \\ Q_2(t) = k_1 x_{vn}(t)\sqrt{p_2(t)} = \overline{k}_1 x_{vn}(t)\sqrt{\eta\overline{P}_s}, \end{cases} \tag{4.5}$$

where k_1 is a positive constant. The supply pressure $\overline{P}_s$ and $\overline{k}_1$ have been transformed to equivalent constants assuming that $A_1 \approx A_2$. The zero point for the valve glider is at the middle position and the positive direction of movement is from the right to the left. The two sets of equations comes from the different flow paths depending on the position of the valve glider. The equations are derived using Bernoulli's laws for flow through an orifice – which in this case is the variable opening area of the servo valve.

Choosing the zero point for the common piston in the lowermost (to the right) position and the positive direction of movement to be upwards (from the right to the left), the flow through the oil cylinder can be modeled as

$$Q_1(t) + Q_2(t) = -(A_1 + A_2)\dot{z}_n(t) + A_1 k_2 (z_t - z_n(t))\dot{f}_n(t) + k_3 f_n(t), \tag{4.6}$$

where z_t is the top position of the common piston, z_n is the position of the common piston and k_2 and k_3 are positive constants. The first term is the flow due to the movement of the piston. The second term is due to the compressibility of the hydraulic oil which is proportional to the volume. This explains the appearance of $A_2(z_t - z_n)$ which is

the volume of the left side as a function of the position z_n. The third term is the leak flow between the common piston and oil cylinder wall, which is assumed proportional to the pressure difference between the two sides which by (4.2) and (4.3) is proportional to the rolling force f_n.

Combining (4.4), (4.5), and (4.6) we obtain the following differential equations for the hydraulic system, where we introduce the variable z_{h_n} as the output of the model

Model for hydraulic system

$$-\dot{z}_{h_n}(t) = a_{hn1}\xi_n(t) - a_{hn2}(z_t - z_{h_n}(t))\dot{f}_n - a_{hn3}f_n(t), \qquad (4.7)$$

where

$$\xi_n(t) = \begin{cases} x_{vn}(t)\sqrt{\overline{P}_s - f_n(t)} & x_{vn}(t) \geq 0 \\ x_{vn}(t)(\sqrt{\eta\overline{P}_s} + \sqrt{\eta\overline{P}_s + f_n(t)}) & x_{vn}(t) < 0. \end{cases}$$

Inputs to the model are the valve glider position x_{vn} and the rolling force measurement f_n and the output is the position of the common piston z_{h_n}.

4.2 Rolling stand

As explained in Chapter 3 a model and an observer are needed for the thickness control. The difference between these two is that the rolling force measurements are available in the second case but not in the first. Output of the model is the thickness profile across the plate width, later more convenient outputs will be introduced. Furthermore, the force can also be used as an output for the model. The output of the observer will be the estimate of the states of the model.

The author has found no reports in the literature to build a multivariable dynamical model for the rolling stand. For descriptions of simpler models see, for instance, [Fujii and Saito, 1975], [Kokai *et al.*, 1985],

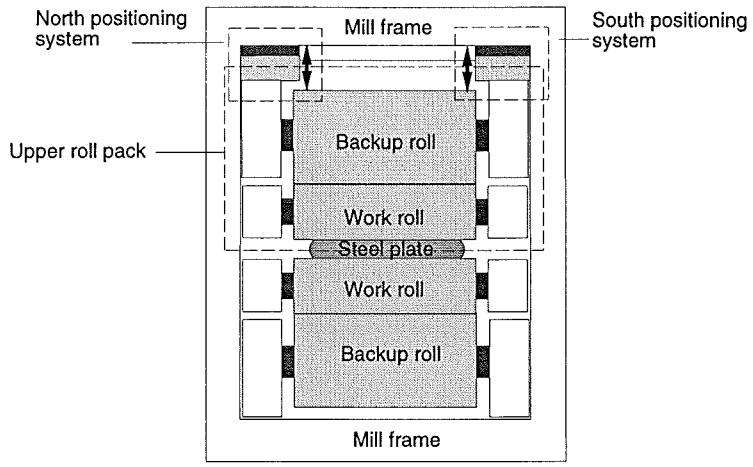

Figure 4.3 Diagram of the main parts of the rolling stand. The parts shown in the figure are the ones we want to include in the model.

[Mizuno,], and [Stone, 1969]. See also Chapter 2.

Physical model

The rolling stand consists of three main parts:

- roll pack – used for reducing the plate thickness;
- mill frame – holds the rolls;
- steel plate.

Since the border of the model for the hydraulic system is the common piston, the model for the rolling stand includes the grease cylinder. This implies that the compressibility and damping of the grease will be implicitly included in the mill model. A schematic diagram is shown in Figure 4.3

The main characteristic of interest in the modeling of the rolling stand is the elastic deflection of the roll pack and the mill frame and the plastic deformation of the steel plate. The model should cover the

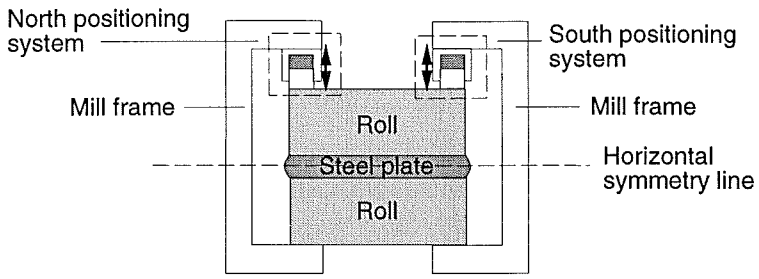

Figure 4.4 Diagram of the main parts of the rolling stand. Here the assumptions are illustrated and all unnecessary parts are removed.

behavior of both the rolling stand and the steel plate. We first assume that the mill frame does not deflect in the sidewise direction and that the plate is always centered in the rolling mill. Joining the work and backup roll to one roll makes it possible to make the simplified model shown in Figure 4.4. It is seen that the width of the rolling stand is set equal to the plate width. This makes it possible to use the mill spring coefficient K from the existing control system for the physical model. An other advantage is that all the parameters are independent of x, which results in a simpler structure of the mathematical model.

Considering plate halves above and below the horizontal symmetry line we see that the forces applied for deforming the two parts must be equal. This is the case since a difference in the two forces will result in an adjustment of the vertical position and thus reestablish the equality of the forces. Assuming that the hardness of the plate is the same for the top and bottom halves gives us the possibility to establish symmetry. This makes it only necessary to model one half of the rolling stand – we here choose to consider the top half.

Using the above assumptions and experience from the system identification the physical model shown on Figure 4.5 is developed. Here the rolling stand is modeled as two springs and the roll pack is modeled as an elastic beam. The springs and the beam are deflected when the beam is subjected to the pressure distribution from the material during rolling. Using the positioning systems the thickness of the plate can

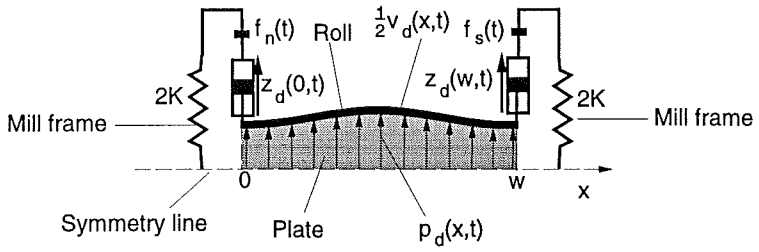

Figure 4.5 Physical model of the rolling stand. This figure is the basis for the energy functions and thus the mathematical model for the rolling stand.

be adjusted. Ideal plastic behavior is assumed, which implies that the thickness profile of the finished plate is the same as the roll profile. In the model the beam ends are built-in, this implies that the orientation of the beam ends are fixed. This gives two of the boundary conditions for the model derived below.

To obtain a two dimensional model it is assumed that the area of contact between rolls and plate is a line. The thickness profile of the plate is $\frac{1}{2}v_d(x,t)$ and $p_d(x,t)$ is the pressure distribution applied to the work roll by the plate. Note that $z_d(0,t)$ and $z_d(w,t)$ in the figure are not the positions of the hydraulic systems since the width of the rolling stand is set equal to the plate width – this will be taken into consideration when deriving the model.

The available measurements are also shown in Figure 4.5:

- positions of hydraulic systems at the plate edges $z_d(0,t)$ and $z_d(w,t)$;
- rolling forces $f(t) = [\, f_n(t) \quad f_s(t) \,]^T$;
- thickness profile of the plate in the width direction $\frac{1}{2}v_d(x,t)$.

Since we only derive a model for the top half of the plate, we work with half the plate thickness and half the roll position. The two first measurements are the same as for the hydraulic system while the thickness is measured after the rolling. The output of the model will be the thickness profile $\frac{1}{2}v_d(x,t)$.

The model

Deriving the model is complicated and it is therefore divided in the following steps:

- choice of material model;
- derivation of a partial differential equation (PDE) for the rolling stand;
- obtaining an ordinary differential equation (ODE) from the PDE.

The theoretical aspects are described during the derivation.

Material model Since the rolling force is not available in the model we need a model for how the pressure distribution depends on the plate thickness. This is a complex problem, but to preserve simplicity we here assume *plane strain*, which implies that there is no material flow in the sidewise direction and that the material is homogeneous in the sidewise direction. This implies that the pressure in one point is only dependent on the plate thickness at that point.

Generally, the material characteristics include a stiffness and a damping term. The input variables are thickness reduction and roll velocity, see [Roberts, 1983] and [Guo, 1994]. Traditionally the models are nonlinear functions of the reduction

$$r_d(x,t) = \frac{\frac{1}{2}v_{d-1}(x,t) - \frac{1}{2}v_d(x,t)}{\frac{1}{2}v_{d-1}(x,t)},$$

the strain rate (the time derivative of the reduction r_d), and plate temperature T. $\frac{1}{2}v_{d-1}$ is the thickness profile for the ingoing thickness. Using a nonlinear material model will result in a nonlinear PDE as a model for the rolling stand. This will be hard to handle and assuming that the thickness control works properly we choose to linearize the material model at a working point.

To prevent waves in the length direction the computer planning system tries to withhold a *constant relative crown*. This means that the shape of the thickness profile is keep constant in the last part of the pass schedule. This implies that we can assume that

$$\frac{1}{2}v_d(x,t) \approx \varpi(t)\frac{1}{2}v_{d-1}(x,t),$$

where ϖ always is smaller than 1.

Using the above and assuming that ϖ varies slowly we postulate that the external transverse force applied to the roll is

$$p_d(x,t) = -a_{m1}(t)(1-\varpi(t))\tfrac{1}{2}v_d(x,t) - a_{m2}(t)(1-\varpi(t))\frac{d}{dt}\tfrac{1}{2}v_d(x,t) + a_{m3}(t)v_r(t), \quad (4.8)$$

where v_r is the rotational speed of the work roll and a_{m1}, a_{m2}, and a_{m3} are positive parameters. In the following we will include the variations of ϖ in a_{m1} and a_{m2}. Note that the pressure profile will be a function of the thickness profile obtained in earlier passes, this gives the rolling process repetitive structure, see for instance [Foda and Agathoklis, 1992].

The variation of the material parameters is mainly due to the variations of the plate temperature T which does not change much during one pass. As seen from (4.8) the material model for the steel plate is time varying. The system identification will be based on data from one pass and the controller design will also be done for one pass at the time. The main demand on the model is therefore that it should be valid for one pass at the time and not for the entire rolling. We therefore assume that the material parameters a_{m1}, a_{m2}, and a_{m3} varies slowly compared to the dynamics of the rolling stand. This will make it possible assume that the material parameters are constant when doing the modeling, system identification and controller design and we will therefore be able to use methods for time invariant systems for these tasks.

PDE for the rolling stand Assuming that the roll packs behave as slender members we can model them as *Euler-Bernoulli beams*, see [Abildgaard, 1991] and [Crandall *et al.*, 1978]. This implies that there is no shear strain present when the roll is deflected. The bending moment of the roll pack is then given by

$$M_b = EI\frac{\partial^2 \frac{1}{2}v_d(x,t)}{\partial x^2},$$

where E is Youngs modulus of elasticity and I is the second moment of area of the work roll, see Appendix B. The roll pack is, however, not

exactly a slender member, but since the roll bending is small compared to the roll geometry the shear strain will be small compared to the normal strain when the roll is deformed. This justifies the assumptions.

Since a change in position at one side affects the thickness profile $\frac{1}{2}v_d(x,t)$ for all x we introduce the function

$$z_d(x,t) = \begin{bmatrix} 1 - \frac{x+\frac{1}{2}(l-w)}{l} & \frac{x+\frac{1}{2}(l-w)}{l} \end{bmatrix} \begin{bmatrix} \frac{1}{2}z_n \\ \frac{1}{2}z_s \end{bmatrix} \quad x \in [0,w],$$

where l is the width of the rolling stand. $z_d(x,t)$ describes the effect of a position change across the plate width.

The model for the rolling stand is found by forming the energy function for the mechanical structure shown in Figure 4.5 and then using the Euler-Lagrange equations on the energy functions, see [Meirovitch, 1980]. The method used here is the same as used in optimal control, here we introduce the performance function

$$\int_{t_1}^{t_2} L_l(t)dt = \int_{t_1}^{t_2} (T_l(t) - V_l(t))dt,$$

where T_l is the total kinetic energy and V_l is the total potential energy for the system. In order to fulfill the physical laws, the system will always be in the state minimizing the performance function L_l, see [Hansen, 1993].

The energy functions for the physical model in Figure 4.5 are found to be

$$\begin{aligned} T_l(t) &= \frac{1}{2}\int_0^w \rho A \tfrac{1}{2}(\dot{v}(x,t))^2 dx \\ V_l(t) &= \frac{1}{2}\int_0^w \left(\tfrac{1}{2}EI(v^{(2)}(x,t))^2 + a_{m1}\tfrac{1}{2}v(x,t)^2\right) dx \\ &\quad + \frac{1}{2}2K\left((\tfrac{1}{2}v_d(0,t) - z_d(0,t))^2 + (\tfrac{1}{2}v_d(w,t) - z_d(w,t))^2\right), \end{aligned}$$

where $^{(i)}$ denotes i times partial derivation with respect to to x, ρ is the mass density of steel, A is the cross sectional area of the roll pack and $2K$ is the spring constant for half a leg of the mill frame, see

Appendix B. The therm in T_l is the kinetic energy due to the velocity of the roll pack, the first term in V_l are the potential energy due to the bending of the roll pack, the second term is the potential energy used for deforming the steel plate and the two last terms is the energy used for deforming the springs of the sides of the rolling stand.

The original *Euler-Lagrange* formulation only covers conservative systems, i.e., systems without losses. To include the losses of the material model they are represented as non-conservative virtual work, see [Meirovitch, 1980]

$$\delta W(t) = \int_0^w \left(-a_{m2}\tfrac{1}{2}\dot{v}(x,t) + a_{m3}v_r(t)\right)\delta\tfrac{1}{2}v_d(x,t)dx,$$

and can in this way be included in the Lagrangian formulation.

Using Euler-Lagranges equations we obtain the PDE, see [Meirovitch, 1980]

$$EI\tfrac{1}{2}v_d^{(4)}(x,t) + a_{m1}\tfrac{1}{2}v_d(x,t) + \rho A\tfrac{1}{2}\ddot{v}_d(x,t) = \\ -a_{m2}\tfrac{1}{2}\dot{v}_d(x,t) + a_{m3}v_r(t),\ x \in (0,w)$$

with the boundary conditions

$$\begin{aligned} \tfrac{1}{2}v_d^{(1)}(0,t) &= 0 \\ \tfrac{1}{2}v_d^{(1)}(w,t) &= 0 \\ (EI/2K)\tfrac{1}{2}v_d^{(3)}(0,t) + \tfrac{1}{2}v_d(0,t) &= z_d(0,t) \\ -(EI/2K)\tfrac{1}{2}v_d^{(3)}(w,t) + \tfrac{1}{2}v_d(w,t) &= z_d(w,t). \end{aligned} \tag{4.9}$$

Note that since we have a 4th order PDE we have four boundary conditions. The first two boundary conditions state that the orientation of the beam ends are fixed while the two last imply that the forces at the beam ends should be equal to the force applied to the springs.

A problem is now that we have non-homogeneous boundary conditions.

This can be solved by the state transformation

$$\begin{aligned} u(x,t) &= \tfrac{1}{2}v_d(x,t) - \varepsilon(x)\tfrac{1}{2}z(t),\ x \in [0,w] \\ &= \tfrac{1}{2}v_d(x,t) - \tfrac{1}{2}\begin{bmatrix} (1+\cos(\frac{\pi}{w}x)) & (1-\cos(\frac{\pi}{w}x)) \end{bmatrix}\begin{bmatrix} z_d(0,t) \\ z_d(w,t) \end{bmatrix} \\ &= \tfrac{1}{2}v_d(x,t) - \left(\tfrac{1}{2} + \tfrac{w}{2l}\cos(\tfrac{\pi}{w}x)\right)\tfrac{1}{2}z_n(t) + \left(\tfrac{1}{2} - \tfrac{w}{2l}\cos(\tfrac{\pi}{w}x)\right)\tfrac{1}{2}z_s(t), \end{aligned} \tag{4.10}$$

where u is the new state variable. The state transformation moves the terms for the roll position $z_d(x,t)$ from the boundary conditions to the PDE and in this way we obtain an extra input.
Applying the state transformation we obtain the PDE

$$\begin{aligned} EIu^{(4)} + a_{m2}\dot{u} + a_{m1}u + \rho A\ddot{u} &= a_{m3}v_r - a_{m1}\varepsilon\tfrac{1}{2}z - EI\varepsilon^{(4)}\tfrac{1}{2}z \\ &\quad - a_{m2}\varepsilon\tfrac{1}{2}\dot{z} - \rho A\varepsilon\tfrac{1}{2}\ddot{z},\ x \in (0,w), \end{aligned} \tag{4.11}$$

with the (now homogeneous) boundary conditions

$$\begin{aligned} u^{(1)}(0,t) &= 0 \\ u^{(1)}(w,t) &= 0 \\ (EI/2K)u^{(3)}(0,t) + u(0,t) &= 0 \\ -(EI/2K)u^{(3)}(w,t) + u(w,t) &= 0. \end{aligned}$$

We now have the PDE with boundary conditions on standard form and can thus proceed with the solution of the problem.

Obtaining the ODE For the PDE we define the eigenvalue problem

$$\begin{aligned} L\phi_i(x) &= \lambda_i m\phi_i(x),\ i = 1,\ldots \\ \left(EI\frac{\partial^4}{\partial x^4} + a_{m1}\right)\phi_i(x) &= \lambda_i\rho A\phi_i(x). \end{aligned} \tag{4.12}$$

This equation is, in general, fulfilled for an infinite set of real eigenvalues λ_i and eigenfunctions ϕ_i which furthermore have to fulfill the

boundary conditions. Note that the eigenfunctions must belong to the same function space as the solution to the PDE (they both have the same number of continuous derivatives).

It can by partial integration and use of the boundary conditions be shown that the differential operator L is *self adjoint* ($< La, b >=< a, Lb >$) where $< \cdot >$ is the inner product in $L_2[0, w]$. This implies that the eigenfunctions are orthogonal and they furthermore form a complete set. Since the solution to the PDE also belongs to this space it can be expanded as

$$u(x,t) = \sum_{i=1}^{\infty} \phi_i(x) q_i(t),$$

where the q_i's are called *normal coordinates* and are continuous functions of t.

Since it is hard to work with an infinite series it is necessary to use an approximate method when obtaining the ODE's. The method which will be used here is *Galerkin's method.* This has the advantage that it preserves the symmetry of the system when the approximate solution is calculated. Furthermore, the method is simple to use and it is easy to understand the main idea.

It is first of all assumed that the approximate solution $\hat{u}$ is given by the finite series

$$\hat{u}(x,t) = [\phi_1(x)\ \phi_2(x) \cdots \phi_n(x)][q_1(t)\ q_2(t) \cdots q_n(t)]^T. \tag{4.13}$$

Introducing the approximate solution for u in the PDE, premultiplying with the eigenfunctions $[\phi_1\ \phi_2 \cdots \phi_n]^T$ and integrating with respect to x from 0 to w yields a set of differential equations for the normal coordinates q_i's.

We now proceed with finding the eigenfunctions from (4.12) and the boundary conditions. In order to satisfy (4.12) it is necessary that

$$\phi_i^{(4)}(x) = k\phi_i(x),\ i = 1, \ldots$$

where k is a real constant. The solution for this differential equation is

$$\phi_i(x) = c_{i1} \cos(\beta_i x) + c_{i2} \sin(\beta_i x) + c_{i3} \cosh(\beta_i x) + c_{i4} \sinh(\beta_i x),$$

which also is suggested in [Meirovitch, 1980]. We thus find that $\lambda_i = (EI\beta_i^4 + a_{m1})/\rho A$.
Inserting the solution in the boundary conditions results in the equation system

$$\begin{bmatrix} 0 & \beta_i & 0 & \beta_i \\ -\beta_i \sin(\beta_i w) & \beta_i \cos(\beta_i w) & \beta_i \sinh(\beta_i w) & \beta_i \cosh(\beta_i w) \\ 1 & -\beta_i^3 EI/2K & 1 & \beta_i^3 EI/2K \\ X_1 & X_2 & X_3 & X_4 \end{bmatrix} \begin{bmatrix} c_{i1} \\ c_{i2} \\ c_{i3} \\ c_{i4} \end{bmatrix} = 0,$$

where

$$\begin{aligned} X_1 &= \beta_i^3 (EI/2K) \sin(\beta_i w) - \cos(\beta_i w) \\ X_2 &= -\beta_i^3 (EI/2K) \cos(\beta_i w) - \sin(\beta_i w) \\ X_3 &= \beta_i^3 (EI/2K) \sinh(\beta_i w) - \cosh(\beta_i w) \\ X_4 &= \beta_i^3 (EI/2K) \cosh(\beta_i w) - \sinh(\beta_i w). \end{aligned}$$

The coefficients (up to a scaling constant) lie in the null space of the above matrix. For the null space to have a dimension larger than zero, the determinant of the system should be zero – this can be utilized to find the β_i's. Setting the determinant equal to zero yields the equation

$$\begin{aligned} &(8\beta_i^3 KEI \sinh(\beta_i w) - 8K^2 \cosh(\beta_i w)) \cos(\beta_i w) + \\ &8\beta_i^3 KEI \cosh(\beta_i w) - 4\beta_i^6 EI^2 \sinh(\beta_i w)) \sin(\beta_i w) + 8K^2 = 0, \end{aligned}$$

which is transcendental and therefore has to be solved numerically. To ensure uniqueness of the eigenfunctions the coefficients are normalized such that

$$\int_0^w \rho A \phi_i^2(x) dx = 1, \; i = 1, \ldots .$$

Inserting the values for the physical constants found in Appendix B we can find the eigenfunctions for one specific plate width w.
For us the two first eigenfunctions are the most interesting. The reason for this is that they describe the mean value and the skewness of

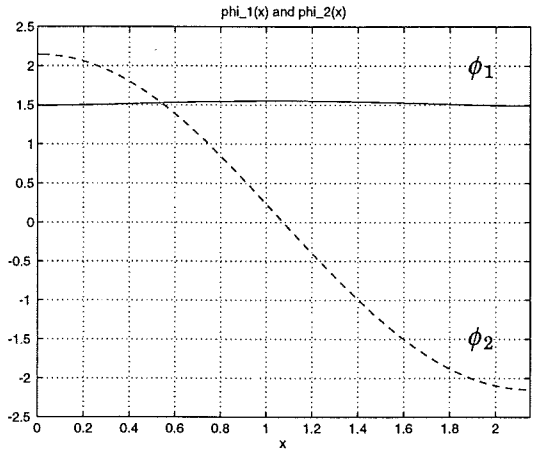

Figure 4.6 The first two eigenfunctions for the rolling stand. They describe the mean value and the skewness of the roll gap and are the ones that will be considered in the following.

the roll gap, see Figure 4.6. The β_i's are used in increasing magnitude when finding the eigenfunctions, this implies that the variations of the eigenfunctions as a function of x increases with i. The terms $\int_0^w \varepsilon\phi_i dx$, $\int_0^w \varepsilon^{(4)}\phi_i dx$, and $\int_0^w \phi_i dx$ therefore decrease with increasing i. This is because due to the more and more high frequency nature of the eigenfunctions and the fact that the mean values of all other eigenfunctions than ϕ_1 is zero.

Looking at the differential equation found later in this chapter we conclude that the steady state gains of the differential equations belonging to the eigenfunctions decrease with increasing i. Investing these steady state gains from $\frac{1}{2}z$ to q we find that they typically are of a order of magnitude 10^{-1} for the two first eigenfunctions ϕ_1 and ϕ_2, and then decrease by a factor 10^{-3} for the following eigenfunctions. The system identification has been performed using the three first eigenfunctions, but as indicated by the above, it was found that ϕ_3 hat little or no importance. We therefore only include the two first eigenfunctions in the model for the rolling stand.

Applying Galerkins method on (4.11) yields the *polynomial matrix description (PMD)*, see [Kailath, 1980]

$$\left(Ip^2 + a_{m2}\Gamma_1 p + EI\Gamma_2 + a_{m1}\Gamma_1\right) q(t) =$$
$$a_{m3}\Gamma_5 v_r(t) - \left(\rho A\Gamma_3 p^2 + a_{m2}\Gamma_3 p + a_{m1}\Gamma_3 + EI\Gamma_4\right) \tfrac{1}{2} z(t),$$

where

$$\Gamma_{1ij} = \int_0^w \phi_i(x)\phi_j(x)dx = \frac{1}{\rho A}\delta_{ij}$$
$$\Gamma_{2ij} = \int_0^w \phi_i^{(4)}(x)\phi_j(x)dx = \frac{\beta_i^4}{\rho A}\delta_{ij}$$

$$\Gamma_{3i} = \int_0^w \phi_i(x)\varepsilon(x)dx$$
$$\Gamma_{4i} = \int_0^w \phi_i(x)\varepsilon^{(4)}(x)dx$$
$$\Gamma_{5i} = \int_0^w \phi_i(x)dx.$$

δ is the unit pulse

$$\delta_{ij} = \begin{cases} 1, & \text{when } i = j \\ 0, & \text{otherwise} \end{cases}$$

The structure of the matrices is

$$\Gamma_i = \begin{bmatrix} \gamma_{i_1} & \gamma_{i_1} \\ \gamma_{i_2} & -\gamma_{i_2} \end{bmatrix}$$

for $i = 3, 4, 6$. This is due to the fact that the eigenfunction ϕ_1 is symmetric while the eigenfunction ϕ_2 is anti-symmetric around $w/2$. $\gamma_{4_1} = 0$ since ε and ϕ_1 are orthogonal. Γ_1 and Γ_2 are diagonal due the orthogonality of the eigenfunctions and the fact that $\phi_i^{(4)} = \beta_i^4\phi_i$.
Using the state transformation $y_{c_1} = q + \rho A\Gamma_3\frac{1}{2}z$ to remove the direct term and the methods given in [Kailath, 1980] we obtain the state space equations

The model

$$\left[\begin{array}{c}\dot{y}_{c_1}\\ \dot{y}_{c_2}\\ \hline q_c\end{array}\right] = \left[\begin{array}{c|c} A_c & B_c \\ \hline C_c & D_c\end{array}\right]\left[\begin{array}{c} y_c \\ \hline \frac{1}{2}z \\ v_r\end{array}\right]$$

$$= \left[\begin{array}{cc|cc} -a_{m2}\Gamma_1 & I & 0 & 0 \\ -EI\Gamma_2 - a_{m1}\Gamma_1 & 0 & EI(\rho A\Gamma_2\Gamma_3 - \Gamma_4) & a_{m3}\Gamma_5 \\ \hline I & 0 & -\rho A\Gamma_3 & 0\end{array}\right]\left[\begin{array}{c} y_{c_1} \\ y_{c_2} \\ \hline \frac{1}{2}z \\ v_r\end{array}\right] \tag{4.14}$$

The inputs are the roll positions z and the roll speed v_r, and the outputs are the normal coordinates q_c. $y_c = [\, y_{c_1} \quad y_{c_2}\,]$ are the states of the model. Since several state transformations are involved when finding the above model the state variables can not be given any direct physical relation.

The observer

The purpose of the observer is to estimate the states of the model (4.14) in an appropriate way. The difference is that we here have the rolling force measurements at our disposal.

Using the fact that the rolling force is equal to the shear force at the beam ends we have that

$$V_b(0,t) = -EIu^{(3)}(x,t) = 2Ku(0,t) = f_n(t) \tag{4.15}$$

$$V_b(w,t) = EIu^{(3)}(x,t) = 2Ku(w,t) = f_s(t). \tag{4.16}$$

Note that these are also the two last boundary conditions for (4.11).

It is in this way possible to use the rolling forces f for finding the normal coordinates q. Using the approximative relationship

$$u(x,t) \approx \phi_1(x)q_1(t) + \phi_2(x)q_2(t).$$

We can by (4.15) and (4.16) derive the matrix equation

$$\begin{bmatrix} f_n(t) \\ f_s(t)\end{bmatrix} \approx 2K\begin{bmatrix}\phi_1(0) & \phi_2(0) \\ \phi_1(w) & \phi_2(w)\end{bmatrix}\begin{bmatrix} q_1(t) \\ q_2(t)\end{bmatrix}. \tag{4.17}$$

Using the relationships found from (4.14)

$$q_c(t) = y_{c_1}(t) - \rho A \Gamma_3 \tfrac{1}{2} z(t) \tag{4.18}$$

$$\dot{y}_{c_1}(t) = -a_{m2}\Gamma_1 y_{c_1}(t) + y_{c_2}(t). \tag{4.19}$$

Introducing q_c for q in (4.17) and using this equation together with (4.18) and (4.19) it is possible to find an estimate for y_c. To simplify the structure of the observer we assume that $\dot{y}_{c_2}$ is small and obtain

The observer

$$y_e(t) = \begin{bmatrix} \Gamma_6 \\ a_{m2}\Gamma_1\Gamma_6 \end{bmatrix} f(t) + \begin{bmatrix} \rho A \Gamma_3 \\ a_{m2}\Gamma_3 \end{bmatrix} \tfrac{1}{2} z(t) \tag{4.20}$$

where

$$\Gamma_6 = \frac{1}{2K} \begin{bmatrix} \phi_1(0) & \phi_2(0) \\ \phi_1(w) & \phi_2(w) \end{bmatrix}^{-1}$$

Inputs are the roll positions z, the rolling forces f. y_e is the estimate of the states of the model y_c. The steady state gains of the model and the observer are the same.

4.3 Total model

As we have seen in (4.15) and (4.16) it is possible to find the rolling force from the model for the rolling stand. The rolling force and its time derivative are used in the model for the hydraulic systems this makes it possible to make a total model for simulation by combining the models for the hydraulic systems and the model for the rolling stand. Using (4.17) and inserting q_c for q we have that

$$f_c(t) = \begin{bmatrix} f_{c_n}(t) \\ f_{c_s}(t) \end{bmatrix} = 2KF \begin{bmatrix} q_{c_1}(t) \\ q_{c_2}(t) \end{bmatrix}, \tag{4.21}$$

where:

$$F = \begin{bmatrix} \phi_1(0) & \phi_2(0) \\ \phi_1(w) & \phi_2(w) \end{bmatrix}$$

By the above expression we can establish a connection between the *models for the hydraulic positioning systems*

$$-\dot{z}_{h_n}(t) = a_{hn1}\xi_n(t) - a_{hn2}(z_t - z_{h_n}(t))\dot{f}_n - a_{hn3}f_n(t)$$
$$-\dot{z}_{h_s}(t) = a_{hs1}\xi_s(t) - a_{hs2}(z_t - z_{h_s}(t))\dot{f}_s - a_{hs3}f_s(t)$$

where

$$\xi_n(t) = \begin{cases} x_{vn}(t)\sqrt{\overline{P}_s - f_n(t)} & x_{vn}(t) \geq 0 \\ x_{vn}(t)(\sqrt{\eta\overline{P}_s} + \sqrt{\eta\overline{P}_s + f_n(t)}) & x_{vn}(t) < 0 \end{cases}$$

$$\xi_s(t) = \begin{cases} x_{vs}(t)\sqrt{\overline{P}_s - f_s(t)} & x_{vs}(t) \geq 0 \\ x_{vs}(t)(\sqrt{\eta\overline{P}_s} + \sqrt{\eta\overline{P}_s + f_s(t)}) & x_{vn}(t) < 0 \end{cases}$$

and the *model*

$$\left[\begin{array}{c} \dot{y}_c \\ \hline q_c \end{array}\right] = \left[\begin{array}{cc|cc} -a_{m2}\Gamma_1 & I & 0 & 0 \\ -EI\Gamma_2 - a_{m1}\Gamma_1 & 0 & EI(\rho A\Gamma_2\Gamma_3 - \Gamma_4) & a_{m3}\Gamma_5 \\ \hline I & 0 & -\rho A\Gamma_3 & 0 \end{array}\right] \left[\begin{array}{c} y_c \\ \hline \frac{1}{2}z \\ v_r \end{array}\right].$$

By substituting f and $\frac{d}{dt}f$ with

$$f_c(t) = 2KFq_c(t)$$
$$\frac{d}{dt}f_c(t) = 2KF\frac{d}{dt}q_c(t).$$

Note that $\frac{d}{dt}q_c$ can be calculated using $\frac{d}{dt}y_c$ and the models for the hydraulic systems. A principal diagram of the model structure is shown in Figure 4.7. By joining the two models we have a system with the valve glider positions for the hydraulic systems x_v and the roll speed v_r as inputs and the normal coordinates q_c as outputs. The complete model will in the following be used for the simulations.

The controlled outputs, which are the thicknesses at a distance μ from the plate edges, see Chapter 7, can in the simulations be calculated

from

$$v_c(t) = \begin{bmatrix} v_{c_n}(t) \\ v_{c_s}(t) \end{bmatrix} = 2 \begin{bmatrix} \hat{u}(\mu,t) \\ \hat{u}(w-\mu,t) \end{bmatrix} + \begin{bmatrix} \varepsilon(\mu) z_h(t) \\ \varepsilon(w-\mu) z_h(t) \end{bmatrix}$$
$$= 2\Phi \begin{bmatrix} q_{c_1}(t) \\ q_{c_2}(t) \end{bmatrix} + \begin{bmatrix} \varepsilon(\mu) z_h(t) \\ \varepsilon(w-\mu) z_h(t) \end{bmatrix} \tag{4.22}$$

where

$$\Phi = \begin{bmatrix} \phi_1(\mu) & \phi_2(\mu) \\ \phi_1(w-\mu) & \phi_2(w-\mu) \end{bmatrix}.$$

In this way the plate thicknesses at the edges v_c can be found using the normal coordinates q_c and the roll positions z_h.

The *observer*

$$y_e(t) = \begin{bmatrix} \Gamma_6 \\ a_{m2}\Gamma_1\Gamma_6 \end{bmatrix} f_c(t) + \begin{bmatrix} \rho A \Gamma_3 \\ a_{m2}\Gamma_3 \end{bmatrix} \tfrac{1}{2} z_h(t)$$

will be used for estimating the states of the model for the rolling stand when implementing the controller in the simulations. Here the additional force measurements are available for a better estimate of the plate thickness. The estimate for the normal coordinates q_c can be calculated from

$$q_e(t) = [I \quad 0]\, y_e(t) - \rho A \Gamma_3 \tfrac{1}{2} z_h(t).$$

Again the thickness at the north and south edge v_{e_n} and v_{e_s} can be calculated using q_e and (4.22).

4.4 Summary

We have now derived models for the hydraulic systems and the rolling stand. The model for the hydraulic systems is nonlinear with the rolling force and controlled variable as inputs and the roll position as output. The model for the rolling stand is linear and multivariable

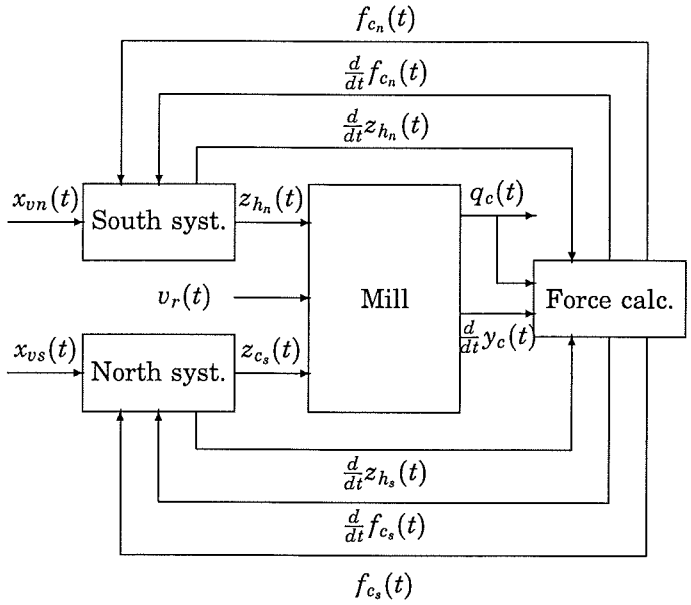

Figure 4.7 The total model for the rolling mill made by combining the models for the hydraulic systems and the model for the rolling stand. The rolling forces and their derivatives are calculated using two of the boundary conditions for the PDE.

with roll positions and rolling speed as inputs and normal coordinates for the eigenfunctions of the rolling stand as outputs. A static observer with roll positions and the rolling forces as inputs and the states of the model for the rolling stand as outputs is also found.

Using the boundary conditions for the rolling stand, the rolling forces can be calculated. This makes it possible to combine the model for the hydraulic systems and the model for the rolling stand into a total model for the whole rolling mill. The total model will be used for computer simulations.

The load of the hydraulic systems is included in the model for the rolling stand. Since we in this model have a linear model for the damping the, friction between the roll pack and the mill frame is indirectly modeled as viscous friction. That this and the other assumption in the modeling is reasonable will be investigated in the system identification.

To find the unknown parameters of the models for the hydraulic systems and the rolling stand it is necessary to perform a system identification. The collection and preparation of the data for the system identification is described in the next chapter.

5

Data collection and preprocessing

This chapter describes the data collection and the preprocessing of the data necessary before the system identification can be performed. The data have been collected during normal production and it has been chosen not to affect the experimental conditions.

It will later be seen that the excitation is not ideal – this could be improved by injecting an external input signal. Two things can be said against this. First of all, the bandwidths of the hydraulic systems are small in comparison to the interesting modes of the rolling stand, and secondly the rolling process is quite sensitive and there is a risk of destroying expensive equipment. Because of this it has been chosen to collect the data during normal operation. This also has the advantage that they are collected under realistic conditions.

The data shown in this chapter will all be from the same plate, which has a nominal thickness of 10 mm, a width of 2.15 m and a length of 10.5 m. The data from this plate will also be used for all the examples in the rest of this report.

5.1 Measurement equipment

From Chapter 4 we know that the relevant input and output signals for the models are:

- The positions of the servo valve gliders x_{vn} and x_{vs}.
- The positions of the common pistons z_n and z_s.
- The rolling forces f_n and f_s.
- The rotational speed of the upper work roll v_r.
- The plate thickness at the north edge, the center and the south edge $v_d(x_1, t)$, $v_d(x_2, t)$, and $v_d(x_3, t)$.

The plate thickness is measured at the edges and the center since these three measurements give us the possibility to determine the plate crown. The four first variable types exist as electrically measurable signals in the rolling mill control systems, while the thickness has to be measured after the rolling when the plate is cold. We thus need a measurement device for electrically measurable signals and a device for measuring the plate thickness.

Electrically measurable signals

For the data collection of the electrically measurable signals a Sharp transportable PC with Burr-Brown data acquisition equipment is used. The data collection software is Labtech Notebook, the measured signals are shown in Table 5.1. The sampling frequency is chosen to be 400 Hz since this is the maximal sampling rate for the measurement equipment. Furthermore, this value has proven to be sufficient to capture the bandwidths of the relevant signals in earlier tests.

The equipment has one A/D-converter with a multiplexer switching between the signals. The signals are ordered to minimize the delay between the related signals in the multiplexing. The typical multiplexing time between two channels is 76 μs, see [Bur, 1986]. The maximal distance between two related signals is 4 channels. This gives a maximal delay of 0.304 ms. Since the maximal bandwidth of the signals is found to approximately 15 Hz yielding a time constant of 11 ms we consider this delay neglectable compared to the system dynamics.

To avoid aliasing the signals are filtered using second order analog Butterworth filters with a cut-off frequency of 100 Hz, which is half the Nyquist frequency, see [Åström and Wittenmark, 1990]. Furthermore, the signals are amplified to ensure proper utilization of the 12-bit A/D converter of the measurement system.

Name	Variable
North valve glider position	x_{vn}
North hydraulic position	z_n
North rolling force	f_n
Roll speed	v_r
South valve glider position	x_{vs}
South hydraulic position	z_s
South rolling force	f_s

Table 5.1 The variables of the models which are possible to measure as electrical signals.

The measurements are done in the last pass for the relevant plates, an example of the signals is shown in Figure 5.1. Since the measurement of the valve glider positions is quite noisy we measure the reference signal for the valve glider position instead. In this pass the thickness control is in *absolute mode* which yields the best excitation since this gives that largest variations in force and position. It is also the signals for the last pass which are related to the plate thickness measured after the rolling. Note the poor excitation of z_n and z_s, furthermore, note that it is only possible to collect data for approximately 4 s for the plate before the pass ends.

Thickness measurement

It is not possible to measure the thickness of the plate during rolling, see Chapter 2. Furthermore, the accuracy of the existing thickness measurement device, which is placed after the rolling mill, is not sufficient. It is therefore necessary to measure the plates after the rolling when the plate is cold.

It was first tried to measure the plate thickness manually with a distance of 10 cm using a micrometer screw gauge. These measurements showed large variations and it was believed that this was due to poor precision of the screw gauge. A measurement device with an electronic screw gauge with serial communication interface was then constructed,

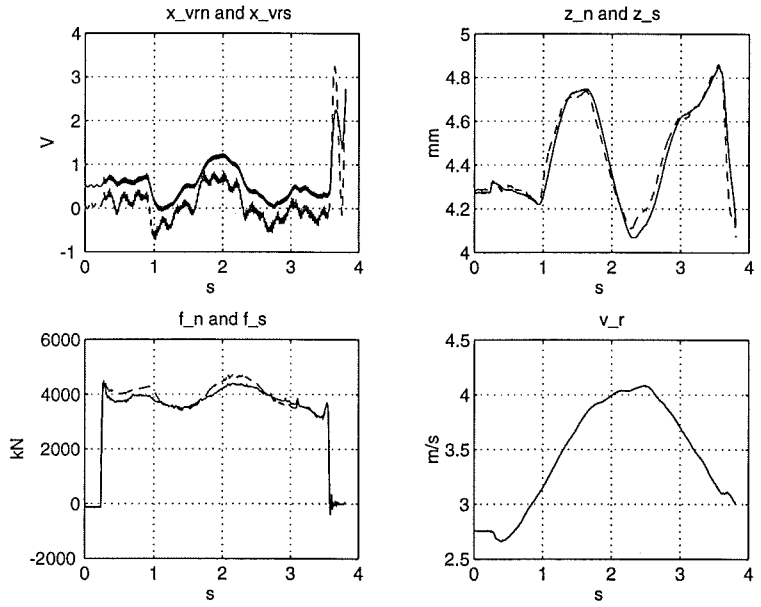

Figure 5.1 An example of the variables which are collected during one pass. Upper left: the references for the north servo valve x_{vrn} (full) and south servo valve x_{vrs} (dashed). Upper right: north position z_n (full) and south position z_s (dashed). Lower left: north rolling force f_n (full) and south rolling force f_s (dashed). Lower right: peripheral speed of the upper work roll v_r.

a pulse encoder for length measurement was also mounted. A constant orientation to the plate when performing the measurements in a more continuous way yielded a higher accuracy. The thickness measurements were collected using a digital controller with the feature that the sampling frequency could be controlled using the pulse encoder, see [Bengtsson, 1994]. Notice that we have *spatial sampling* as a consequence of the measurement procedure.

Before the plate was measured approximately 5 cm were cut off the edges. This was done since the thickness at the edges is not well defined due to various boundary effects. The north edge was first measured, the plate was cut in two and the plate center was measured. Finally the plate was flipped and the south edge was measured. In order not to destroy the plates we choose plates where the cutting is necessary to obtain the specified width. To reduce measurement noise due to dust the plates were swept before measurement was performed. The scale is thicker on the thick plates, since they are finished at higher temperature, this increases the noise level due to holes in the scale.

The roll surface is not straight, as assumed in the modeling. The roll is actually ground in cigar-shape to reduce the plate crown and hereby save material, see Chapter 2. To correct the thickness measurements, the difference between the roll diameter at the center and the edges are added to the center thickness measurement. Assuming that the roll is ground in sine shape the correction is

$$\theta = c(1 - \sin(\frac{\pi(l-w)}{2l}))$$

where c is the thickness difference between the center and the edges of the roll.

An example of the data is shown i Figure 5.2. Note the high-frequency thickness variations, the thickness can vary several tenths of mm within 20 cm. It was found that it was necessary to measure the thickness every 0.5 cm to catch these variations. This is quite surprising since the upper roll pack weighs approximately 200 tonnes. The peaks in the thickness are due to cold zones introduced by cooling from the roller tables. We find that it is important to avoid these to obtain proper thickness tolerances, since the thickness variations are too high frequent to be handled by the thickness control.

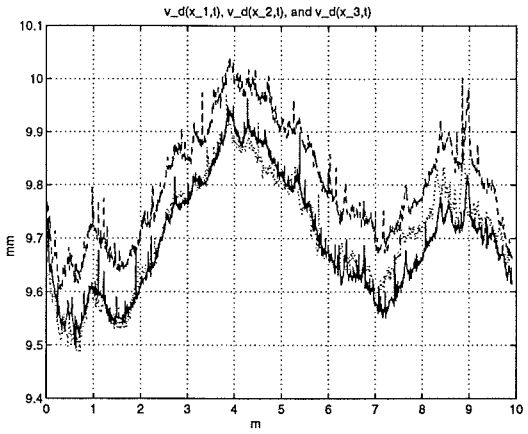

Figure 5.2 Thickness measurements in the length direction of the chosen plate. Solid line: thickness at north edge $v_d(x_1, t)$, dashed line: thickness at center $v_d(x_2, t)$, and dotted line: thickness at south edge $v_d(x_3, t)$. Note that the plate is thicker at the center than at the edges, this phenomenon is called *plate crown*

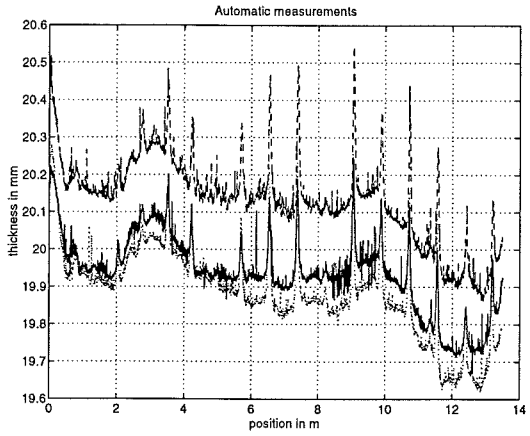

Figure 5.3 An example of the consequences of cooling by the roller tables. Solid line: thickness at north edge $v_d(x_1, t)$, dashed line: thickness at center $v_d(x_2, t)$, and dotted line: thickness at south edge $v_d(x_3, t)$. The peaks are due to the cold zones. Note that the amplitude of the peaks are 0.5 mm.

A more extreme example of the consequences of the cooling by the roller tables is shown in Figure 5.3. This is a 20 mm plate where the amplitude of the peaks is more than 0.5 mm. The typical distance of 1 m between the peaks agrees well with the distance between the rolls of the roller tables. The cold zones are a result of a pause time of approximately 20 s where the plate was not moved. The thickness measurements shown in Figure 5.3 are from a measurement test and will not be used in the system identification.

5.2 Measurements for identification

To obtain representative results for the identification it is chosen to measure 10 plates with 5 different nominal thicknesses and 2 different widths, the dimensions are shown in Table 5.2.

The widths of 2 and 3 m are chosen since they are close to the minimum and maximum of the plates rolled. The chosen thickness interval

Thickness [mm]	Small width [m]	Large width [m]
6	2	3
10	2	3
20	2	3
30	2	3
40	2	3

Table 5.2 Nominal dimensions of the measured plates. The data from these ten plates will the basis for the system identification.

is representative for the plate production since the thickness of 95 % of the produced plates are in this interval. The data were collected during normal production and additional information about plate temperature, roll position and calculated thickness was thus available from the reports from control system planning the rolling, see Chapter 2.

5.3 Estimation of plate position

A fundamental problem when using the data is that the electrically measurable signals are obtained using *time sampling* and the thickness measurements are obtained using *spatial sampling*. To perform the system identification it is necessary that all the data are sampled in time and we therefore have to find the independent variable of the thickness measurements in some way.

Unfortunately the plate speed is not measurable, and is not related to the roll speed v_r in any useful way. The two variables are normally assumed to be related by the equation

$$v_p(t) = (1 + s_f(t))v_r(t)$$

where v_p is the plate speed and s_f is the so called forward slip, see for instance [Cumming, 1972]. Generally, it is hard to calculate the slip, which varies with the rolling geometry. It is therefore not possible to

find the relations between the plate position and measurement time in an analytic way. We therefore have to use an approximate solution.

The mean value of the plate thicknesses at the edges $\overline{v}$ can be estimated the *gaugemeter equation*, which models the rolling mill as a spring, see Chapter 3. Neglecting the roll ovalness and eccentricity the equation can be written as

$$\overline{v}_e(t) = \overline{z}(t) + \frac{\overline{f}(t)}{\overline{K}}$$

where $\overline{v}_e$ is the estimate of the mean value of the plate thickness, $\overline{z}$ is the mean value of the roll positions, and $\overline{f}$ is the mean value of the rolling forces. $\overline{K}$ is the estimate of the mill spring coefficient, see Appendix B. Since the gauge meter principle is also used for calculating the plate thickness at the Danish Steel Works we can here use the value of $\overline{K}$ from the rolling mill control system.

Since there are no time delays involved here we can, using a for the position of the plate, formulate the optimization problem

$$\min_{a_e(t)} \sum_{k=1}^{N} \left(\overline{v}_e(a(k)) - \left[\overline{z}(a_e(k)) + \frac{\overline{f}(a_e(k))}{\overline{K}} \right] \right)$$

where k is sample number and N is the total number of samples. a_e can be seen as an estimate of the plate position a as a function of k. We here model a_e using a spline interpolation of based on 10 points. These points are the parameters of the optimization problem. $\overline{z}(a_e)$ and $\overline{f}(a_e)$ are also found using spline functions, this is done using `interp1` in MATLAB. Before the optimization is done all the signals are low-pass filtered to ensure that the static relation of the gaugemeter equation is valid. To avoid problems with initial conditions the low-pass filtering is done using FIR-filters. The transfer function of the filters are of 50th order and is found using `fir1`. A cut-off frequency of 2 Hz has shown to be a good choice.

A result of the optimization is shown Figure 5.4 and the corresponding a_e is shown in Figure 5.5. The optimization has been performed using `leastsq` and convergence of the problem is generally poor. It is necessary to give the routine a good initial guess for the result to be sensible.

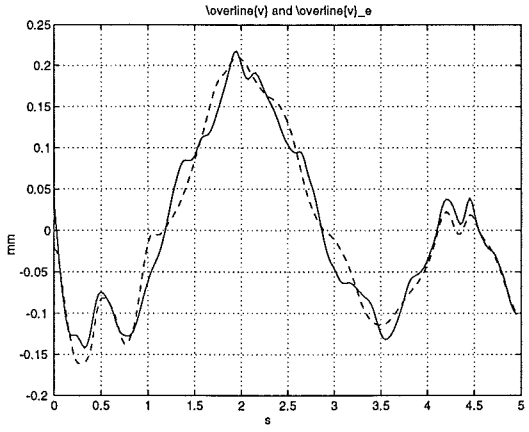

Figure 5.4 Fitting the variables measured during the pass and the thickness measurements. Measured thickness $\overline{v}$ (full) and estimated thickness $\overline{v}_e$ (dashed).

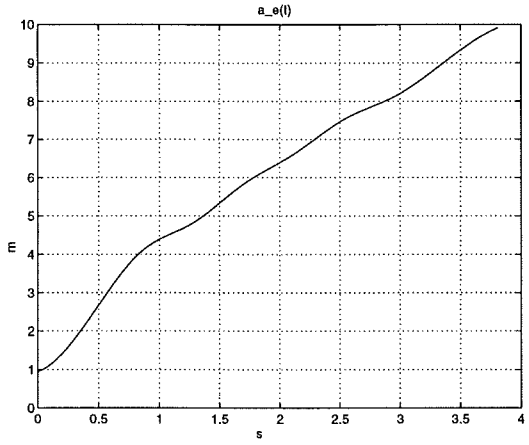

Figure 5.5 The estimate of the plate position a_e when it is rolled.

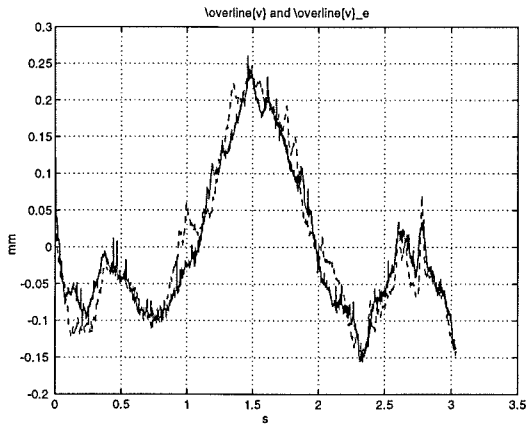

Figure 5.6 Measured thickness $\overline{v}$ (full) and estimated thickness $\overline{v}_e$ (dashed) thickness, when they are not low-pass filtered.

The thickness measurements are transformed to time sampling using the estimated a_e and spline functions, again using `interp1`. A result of this is shown in Figure 5.6. Notice the nice fit. This illustrates that the gaugemeter principle gives a good estimate of the mean value of the plate thickness at the two edges.

5.4 Summary

The inputs and outputs for the model for the rolling mill have now been collected. The data consist of the key variables for the last pass for 10 plates covering the relevant thickness and width intervals.

Since the thickness measurements are found using spatial sampling and the other variables are found using time sampling it is necessary to align the data in some way. This is done by formulating and solving an optimization problem using the gaugemeter equation.

We now have the model and the input and output data represented as a time series. We are thus ready for the system identification which will be carried out in the following chapter.

6

System identification

In this chapter the parameters of the models for the hydraulic systems and the rolling stand will be identified. The purpose of the models is controller design and simulation. Simplicity will be preferred to advanced structure, it will in general, be possible to improve the results by adding more degrees of freedom, but this will imply lack of physical understanding and will therefore be avoided, if possible.

Due to the lack of excitation, nonparametric methods will not be used. Instead we will use restrictive parametrizations, this implies that all constants known in advance will be inserted in the models before the system identification is performed. The main advantage of this is that one is quite sure that the model is correct if only a couple of parameters of a physically derived structure are identified.

Much effort and time has been put into finding appropriate parametrizations and the problem of identifying the mill dynamics have been reduced to finding two parameters. Furthermore, the parameter variations are correlated with key variables. In this way we find parametric model variations which will be useful in the controller design.

The author has found no work on identification of rolling mills and the system identification is therefore described in detail. In the following the model for the hydraulic systems is transformed to discrete time and a parametrization of the model is chosen. After this, identifiability of the model is investigated, the identification method is chosen, and the results of the identification are presented. The procedure for the identification of the rolling stand is similar, with the exception that we here have to find the parameters of both the model and the observer.

6.1 Hydraulic systems

The model for the hydraulic systems was derived in Chapter 4. Here it will be rewritten to a form appropriate for the system identification. This implies a transformation to suitable discrete time form. Since the model is nonlinear we will be working with nonlinear system identification. Only results for the model for the north hydraulic system will be shown here, since the model for the south system is similar.

Rewriting equations

To be able to perform the system identification it is necessary to transform the differential equation to discrete time form. Exploiting an idea given in [Johansson, 1993] we simply integrate the nonlinear differential equations for the north hydraulic system, see (4.7)

$$-\dot{z}_{h_n}(t) = a_{hn1}\xi_n(t) - a_{hn2}(z_t - z_{h_n}(t))\dot{f}_n - a_{hn3}f_n(t), \tag{6.1}$$

where

$$\xi_n(t) = \begin{cases} x_{vn}(t)\sqrt{\overline{P}_s - f_n(t)} & x_{vn}(t) \geq 0 \\ x_{vn}(t)(\sqrt{\eta\overline{P}_s} + \sqrt{\eta\overline{P}_s + f_n(t)}) & x_{vn}(t) < 0. \end{cases}$$

If we furthermore divide by $z_t - z_{h_n}$ (which is always nonzero) before integrating we save a numerical differentiation because the integrand $(z_t - z_{h_n})\frac{d}{dt}f_n$ then can be evaluated analytically. The result is

$$y_n(t_1, t_2) = a_{hn1}\xi_{n_1}(t_1, t_2) + a_{hn2}\xi_{n_2}(t_1, t_2) + a_{hn3}\xi_{n_3}(t_1, t_2), \tag{6.2}$$

where

$$y_n(t_1,t_2) = \ln\frac{z_t - z_{h_n}(t_2)}{z_t - z_{h_n}(t_1)}$$

$$\xi_{n_1}(t_1,t_2) = \begin{cases} \displaystyle\int_{t_1}^{t_2} \frac{\sqrt{\overline{P}_s - f_n(t)}}{z_t - z_{h_n}(t)}dt & x_{vn}(t) \geq 0 \\ \displaystyle\int_{t_1}^{t_2} \frac{(\sqrt{\eta\overline{P}_s + f_n(t)} + \sqrt{\eta\overline{P}_s})}{z_t - z_{h_n}(t)}dt & x_{vn}(t) < 0 \end{cases}$$

$$\xi_{n_2}(t_1,t_2) = f_n(t_2) - f_n(t_1)$$

$$\xi_{n_3}(t_1,t_2) = \int_{t_1}^{t_2} \frac{f_n(t)}{z_t - z_{h_n}(t)}dt.$$

Note that the parameters are unaffected by the discretization and that the system is still linear in the parameters. The integrals which are not possible to evaluate analytically can be calculated numerically.

Parametrization

Different parametrizations of the hydraulic model have been investigated and it is found that the parameterization of (6.2) works well. We thus have the three parameters a_{hn1}, a_{hn2}, and a_{hn3} to estimate.

Identifiability

Identifiability implies that it will be possible to obtain unique estimates of the parameters of the model (6.2) for some inputs and an initial state. Since it is nonlinear we have a non-standard problem on our hands. Furthermore, the data are collected during closed-loop operation. There is therefore a risk for non-unique parameter estimates. We will now argue that the disturbances from the inhomogeneous heating of steel plate provides sufficient excitation to identify the parameters of the hydraulic systems.

Using (4.21) and the model for the mill stand (4.14) the mean value of the force $\overline{f}_c$ and the north rolling force f_{c_n} can be calculated from

$$\overline{f}_c(t) = \overline{G}_{f_c}(p)\overline{z}_h(t) + d(t)$$
$$f_{c_n}(t) = G_{f_{cn}}(p)z_h(t) + d(t),$$

where $d(t)$ is the hardness variations due to the cold zones of the steel plate. It is assumed that it is the same at the two sides of the rolling stand. $\overline{G}_{f_c}$ is a transfer function with one input and one output and $G_{f_{cn}}$ has two inputs and one output.

The thickness control uses $\overline{f}$ and the mean value of the positions $\overline{z}$ as input signals, see Chapter 3, and since the hydraulic systems have separate position controllers the control signal x_{vn} is a function of $\overline{f}$, $\overline{z}$, and z_n

$$x_{vn}(t) = C_z(p)(C_{v_1}(p)\overline{f}_c(t) + C_{v_2}(p)\overline{z}_h(t) - z_{h_n}(t)),$$

where C_{v_1} and C_{v_2} are the transfer functions for the thickness controller and C_z is the transfer function for the position controller. In the above equation we have inserted the values from the models instead of the measured signals.

It is difficult to analytically show the identifiability of the hydraulic systems. By making some simplifying assumptions we will show that we most probably have identifiability.

The identification problem will have an unique parametrization if the regressors of (6.2) are linearly independent, see [Gustavsson *et al.*, 1977]. This will be the case if the sampling time is properly chosen and the integrands are linearly independent. That the integrands are linearly independent implies that

$$\begin{aligned}\alpha_1(t) &= \xi_n(t)\\ \alpha_2(t) &= (z_t - z_{h_n}(t))\dot{f}_n\\ \alpha_3(t) &= f_n(t)\end{aligned}$$

should be linearly independent. ξ_n is defined in (6.1).

To show that the parameters are linearly independent we will show that it is not possible for them to be linearly dependent. If α_1, α_2, and α_3 are linearly dependent there will exist non trivial parameters

of (6.1) such that that $\dot{z}_n = 0$, $\forall t$. This permits us to proceed with

$$\begin{aligned} &\dot{z}_{h_n}(t) = 0 \\ &\Downarrow \\ &z_h(t) = z_{h0} \\ &z_{h_n}(t) = z_{h0_n}, \end{aligned}$$

where z_{h0} and z_{h0_n} are constant. We assume also that $\dot{z}_{h_s} = 0$ and that $z_{h0_n} < z_t$. To model the slow hardness variations of the plate due to the cold zones from the furnace, the disturbance d is chosen to be a sine wave $k_s \sin(\omega_s t)$, this implies that

$$\begin{aligned} \overline{f}_c(t) &= \overline{G}_{f_c}(p)\overline{z}_{h0} + k_s \sin(\omega_s t) \\ &= k_s \sin(\omega_s t) + \overline{k} \\ f_{c_n}(t) &= G_{f_{cn}}(p) z_{h0} + k_s \sin(\omega_s t) \\ &= k_s \sin(\omega_s t) + k_n, \end{aligned}$$

where $\overline{k}$ and k_n are constants. $\overline{z}_{h0}$ is the mean value of z_{h0}.
Introducing f_{c_n} for f_n in (6.1) we obtain the α's for the case of $\dot{z}_{h_n} = 0$:

$$\alpha_{1_0}(t) = \begin{cases} x_{vn}(t)\sqrt{\overline{P}_s - (k_s \sin(\omega_s t) + k_n)} & x_{vn}(t) \geq 0 \\ x_{vn}(t)(\sqrt{\eta \overline{P}_s + (k_s \sin(\omega_s t) + k_n)} + \sqrt{\eta \overline{P}_s}) & x_{vn}(t) < 0 \end{cases}$$

$$\alpha_{2_0}(t) = (z_t - z_{h0_n})\omega_s k_s \cos(\omega_s t)$$

$$\alpha_{3_0}(t) = k_s \sin(\omega_s t) + k_n,$$

where

$$\begin{aligned} x_{vn}(t) &= C_z(p)(C_{v_1}(p)(k_s \sin(\omega_s t) + \overline{k}) + C_{v_2}(p)\overline{z}_{h0} - z_{h0_n}) \\ &= k_{vn_1} \sin(\omega_s t) + k_{vn_2}. \end{aligned}$$

k_{vn_1} and k_{vn_2} are constants.
We see that we can not have linear dependence since α_{2_0} and α_{3_0} are orthogonal and x_v is multiplied by the time varying square root in

α_{1_0}. We therefore see that there exist no non trivial parameter sets yielding $\dot{z}_{h_n} = 0$ and it is therefore not possible for α_1, α_2, and α_3 to be linearly dependent. We therefore conclude that it is not likely that we will have have problems with non unique parameter estimates for the hydraulic systems.

Identification

The performance index used in the identification is

$$V_n = \sum_{k=1}^{N} \varepsilon_n(k)^2,$$

where $\varepsilon_n(k)$ is the prediction error of the model. The model for the north system is

$$y_{h_n}(k) = a_{hn1}\xi_1(k) + a_{hn2}\xi_2(k) + a_{hn3}\xi_3(k), \tag{6.3}$$

where

$$\xi_1(k) = \begin{cases} \displaystyle\int_{k-h}^{k} \frac{\sqrt{\overline{P}_s - f_n(t)}}{z_t - z_n(t)} dt & x_{vn}(t) \geq 0 \\ \displaystyle\int_{k-h}^{k} \frac{(\sqrt{\eta\overline{P}_s + f_n(t)} + \sqrt{\eta\overline{P}_s})}{z_t - z_n(t)} dt & x_{vn}(t) < 0 \end{cases}$$

$$\xi_2(k) = f_n(k) - f_n(k-h)$$

$$\xi_3(k) = \int_{k-h}^{k} \frac{f_n(t)}{z_t - z_n(t)} dt.$$

The model for the south system is analogous and is therefore not shown. For the identification it has been found that a sampling interval of $h = 0.025$ s is a good choice. Using this value of h some of the noise is averaged out while the dynamics of the system is still captured. $\eta = 0.15$ is found to give the best results.

To prevent extensive nonlinear noise transformations and to weight the data in an appropriate frequency interval they are filtered using a

fourth order Butterworth filter with a cut-off frequency of 100 Hz. The relatively high cut off frequency is necessary due to the high frequency nature of ξ_2. The filtering is done using the MATLAB-function `idfilt`. Assuming that the noise can be described as additive filtered white noise implies that the model used for the identification is

$$y_{h_n}(k) = a_{hn1}\xi_1(k) + a_{hn2}\xi_2(k) + a_{hn3}\xi_3(k) + C(q^{-1})e(k),$$

where

$$C(q^{-1}) = 1 + c_1q^{-1} + \cdots + c_nq^{-n}$$

and $e(k)$ is a white noise sequence and q is the forward shift operator. Note that the model has the same structure as an ARMAX-model with $A(q^{-1}) = 1$.

Since we have a non-standard problem we formulate the system identification as an optimization problem. Recalling that the model has ARMAX structure we simply compute the prediction error as

$$\varepsilon_n(k) = \frac{1}{C(q^{-1})}\left(y_n(k) - (a_{hn1}\xi_1(k) + a_{hn2}\xi_2(k) + a_{hn3}\xi_3(k))\right),$$

where

$$y_n(k) = \frac{z_t - z_n(k)}{z_t - z_n(k-1)}.$$

This implies that we use the *Maximum Likelihood method*, see [Åström and Eykhoff, 1971]. It is found that a third order noise polynomial is appropriate in the system identification. The minimum of the performance function is found using the nonlinear least squares function `leastsq` in MATLAB. The integrals in the regressors are computed using the MATLAB-function `trapz`.

Results

The identification is performed on the discrete time model (6.3) using the ten data sets described in Chapter 5. Since the signal for the position of the valve glider is very noisy the reference has been used

	North		**South**
a_{hn1}	$8.9 \times 10^{-1} \pm 5 \times 10^{-2}$	a_{hs1}	$8.1 \times 10^{-1} \pm 5 \times 10^{-2}$
a_{hn2}	$-7.6 \times 10^{-4} \pm 2 \times 10^{-4}$	a_{hs2}	$-9.2 \times 10^{-4} \pm 4 \times 10^{-4}$
a_{hn3}	$-2.6 \times 10^{-2} \pm 2 \times 10^{-2}$	a_{hs3}	$-2.7 \times 10^{-2} \pm 2 \times 10^{-2}$

Table 6.1 Table for nominal values of parameters with deviations for the hydraulic systems. The parameters are found using the 10 available data sets.

instead. Using spectral analysis it has been found that the dynamics of the servo valve is neglectable compared with the dynamics of the process. The change of variables is therefore not expected to affect the system identification.

A plot of a typical result is shown in Figure 6.1. The agreement is quite good considering the assumptions made when deriving the model. Furthermore, the prediction error is close to white noise which indicates that we have an unbiased estimate of the parameters. Note that the beginning and ends of the passes are included in the data – the peak in the prediction error for the north system arises when the plate enters the mill.

An example of a simulation using the original differential equation and the measured system response is shown in Figure 6.2. The implementation of the time derivatives when calculating $\frac{d}{dt}f$ is done using the backward difference approximation. The simulations are performed using the MATLAB-function `ode45` with the reference for the valve glider positions x_{vr} and the rolling forces f as input signals. The parameters used in the model are the ones identified from the data set shown. It is seen that there is good correspondence between the two responses. This shows that the assumption that the supply pressure P_s is constant and the assumptions regarding the pressures at the right and left sides of the common piston at the oil side work well in practice.

The parameters obtained from the identification of all the data sets are shown in Table 6.1. The distribution of the parameters for the two systems are shown in Figures 6.3 and 6.4. For the design in Chapter 7 we want to define a set of nominal parameters. The nominal parameters are chosen to be the center of the interval of the parameter

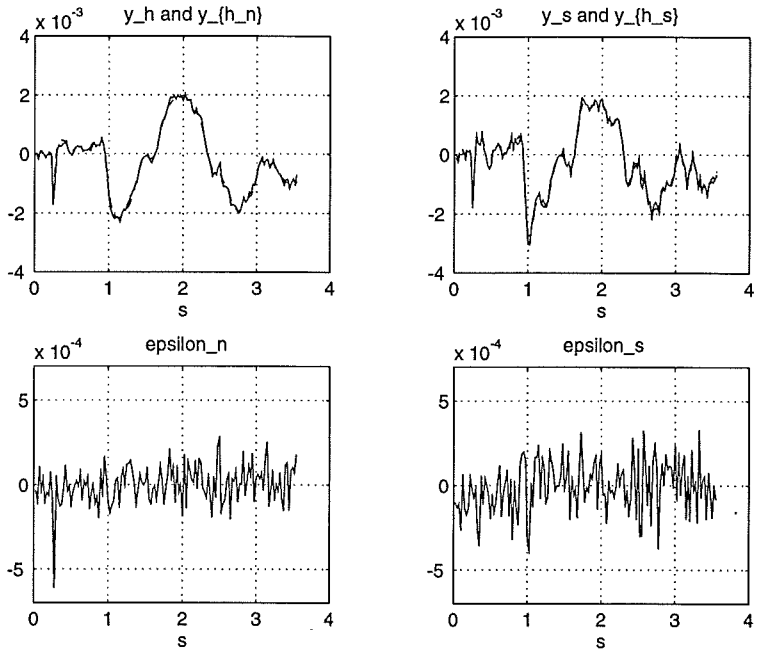

Figure 6.1 Results of the system identification of the hydraulic systems. Left side top: fit of the measured output y_n (full) and the predicted output y_{h_n} (dashed) and bottom: the prediction error ε_n. Right side top: fit of the measured output y_s (full) and and predicted output y_{h_s} (dashed) and bottom: the prediction error ε_s.

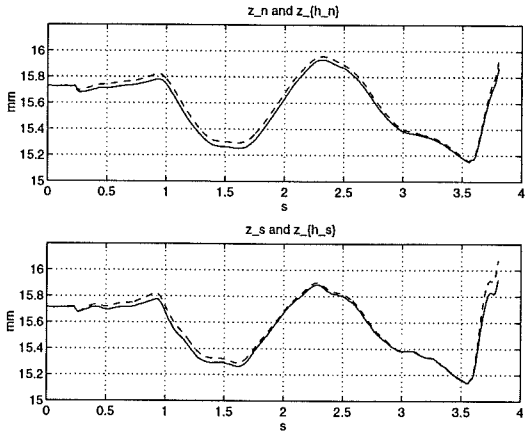

Figure 6.2 Simulation of the positions of the hydraulic systems using the same parameters for identification and simulation. Upper plot, full: measured response for north system z_n and dashed: simulated response for north system z_{h_n}. Lower plot, full: measured response for south system z_s and dashed: simulated response for north system z_{h_s}.

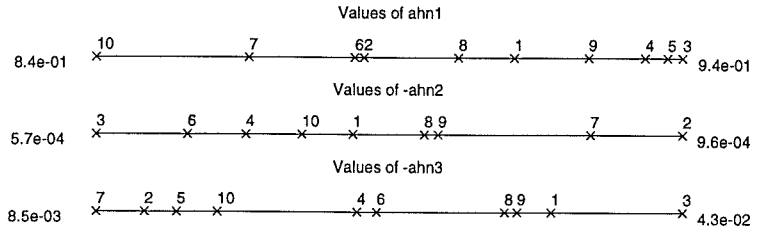

Figure 6.3 The distribution of the parameters for the north hydraulic system. The numbers refer to the ten data sets.

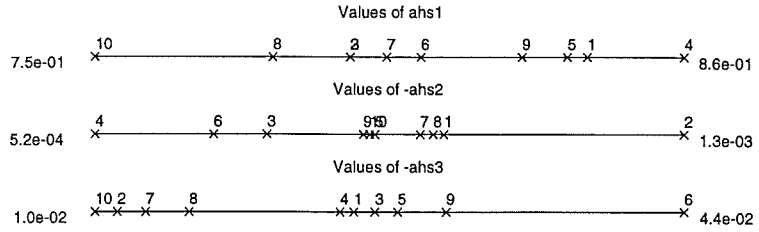

Figure 6.4 The distribution of the parameters for the south hydraulic system. The numbers refer to the ten data sets.

estimates.

When identifying the above parameters the regressors were scaled to be of the same magnitude as the output – this was done to prevent numerical problems. Generally all the regressors are of the same order of magnitude and we thus conclude that it are the parameters a_{hn1}, and a_{hs1} that have major influence. This implies that the model for the hydraulic systems will be close to an integrator if it is linearized. It is seen that these parameters vary less than 10% while the other parameters all vary within the same order of magnitude.

One could expect that the leak flows vary with the positions z_n and z_s due to differences in the wear of the oil cylinders. The variations of the parameters a_{hn3} and a_{hs3} is therefore not surprising. The compressibility of the oil covers many phenomena and it is therefore difficult to say much about the variations of the parameters a_{hn2} and a_{hs2}. The zero point for the servo valve for the southern system varies quite much and it has therefore been necessary to compensate for this. The accuracy of the parameter estimates are apparently not affected by this.

Due to the small variations of the dominating parameters it is expected that parameter variations are of little importance. To confirm this we simulate the differential equation using the nominal parameter values. The result is shown in Figure 6.5. It is seen that the mean value of the simulated output drifts away, this is because the system is close to an integrator. This implies that the model will be sensitive to offsets in the input and since the zero point of the valve glider varies a bit

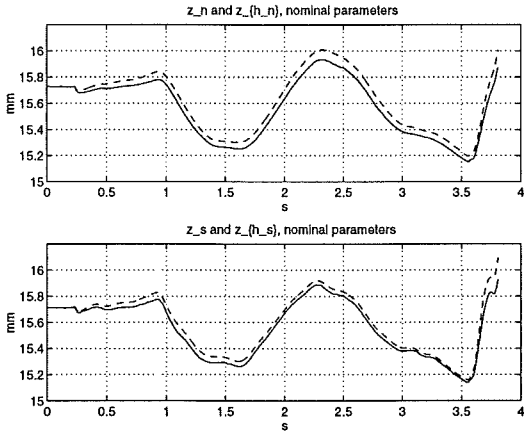

Figure 6.5 Simulation of the positions of the hydraulic systems using the nominal parameters. Upper plot, full: measured response for north system z_n and dashed: simulated response for north system z_{h_n}. Lower plot, full: measured response for south system z_s and dashed: simulated response for north system z_{h_s}.

this introduces the above effect. We solve the above problem by simply including an integrator when designing the controller.

6.2 Rolling stand

The two models for the rolling stand derived in Chapter 4 are linear and we thus have a more or less standard problem. To preserve the structure the parameters of the model and the observer will be identified using the original continuous time state space form. This can be done using the *System identification toolbox* in MATLAB, see [Ljung, 1991].

Not considering estimation of the roll eccentricity, the only reference on identifying rolling mill dynamics found is [Cumming, 1972]. In this reference the parameters of scalar equations are estimated using a correlator, and it is therefore a bit out of date.

Parametrization

Since we use the continuous time state space models (4.14) and (4.20) for the system identification no model transformations are necessary here. We thus proceed with the parametrization of the models.

The model In the system identification it is found that the peripheral speed of the work roll $v_r(t)$ has little or no influence on the plate thickness and this input is therefore removed from the model. This is probably due to the fact the the friction inside the material can be modeled well as static friction, which is independent of the deformation speed. We thus have the model structure

$$\begin{aligned}\left[\begin{array}{c}\dot{y}_c(t)\\ \hline q_c(t)\end{array}\right] &= \left[\begin{array}{c|c}A_c & B_c\\ \hline C_c & D_c\end{array}\right]\left[\begin{array}{c}y_c(t)\\ \hline \frac{1}{2}z(t)\end{array}\right]\\ &= \left[\begin{array}{cc|c}-a_{m2}\Gamma_1 & I & 0\\ -EI\Gamma_2 - a_{m1}\Gamma_1 & 0 & EI(\rho A\Gamma_2\Gamma_3 - \Gamma_4)\\ \hline I & 0 & -\rho A\Gamma_3\end{array}\right]\left[\begin{array}{c}y_c(t)\\ \hline \frac{1}{2}z(t)\end{array}\right],\end{aligned} \tag{6.4}$$

where a_{m1}, a_{m2} are unknown scalar parameters. The state space equations are of fourth order.

The observer Since the influence from the roll position $\frac{1}{2}z$ is well determined, it is only necessary to scale the coefficients of the rolling force f we and we thus introduce the matrix O_{fe}. The model structure then is

$$q_e(t) = O_{fe}\Gamma_6 f(t), \tag{6.5}$$

where

$$O_{fe} = \begin{bmatrix} o_{fe_1} & 0 \\ 0 & o_{fe_2} \end{bmatrix}.$$

The two unknown parameters in the observer are o_{fe_1}, and o_{fe_2}.

Identifiability

Analysis of the identifiability of (6.4) is relevant since it ensures that there is no redundancy in the parametrization of the model. Normally, when working with SISO transfer functions, identifiability is ensured, see [Bellman and Åström, 1970], but in this case we have a MIMO state space model and it is therefore relevant to investigate if identifiability is present.

Identifiability implies that different parameter sets yields different outputs for some inputs and initial states, see [Grewal and Glover, 1976]. Using this reference a local test for linear systems is that the functional matrix of the elements of the Markov parameters should have full rank. This implies that there is an injective relationship between the parameters and the impulse response. The criterion is

satisfied for (6.4) since the functional matrix is

$$\frac{\partial}{\partial \Delta_c}\begin{bmatrix} D_c(:,1) \\ D_c(:,2) \\ C_c B_c(:,1) \\ C_c B_c(:,2) \\ C_c A_c^1 B_c(:,1) \\ C_c A_c^1 B_c(:,2) \\ C_c A_c^2 B_c(:,1) \\ C_c A_c^2 B_c(:,2) \\ C_c A_c^3 B_c(:,1) \\ C_c A_c^3 B_c(:,2) \end{bmatrix} = \begin{bmatrix} 0 & 0 \\ \vdots & \vdots \\ 0 & 0 \\ 0 & -\frac{EI}{\rho A}\beta_1^4\gamma_{3_1} \\ 0 & -\frac{EI}{\rho A}\beta_1^4\gamma_{3_1} \\ 0 & -\frac{EI}{\rho A}(\beta_2^4\gamma_{3_2} - \gamma_{4_2}) \\ 0 & \frac{EI}{\rho A}(\beta_2^4\gamma_{3_2} - \gamma_{4_2}) \\ -\frac{EI}{\rho A}\beta_1^4\gamma_{3_1} & \frac{EI}{(\rho A)^2}2a_{m2}EI\beta_1^4\gamma_{3_1} \\ -\frac{EI}{\rho A}\beta_1^4\gamma_{3_1} & \frac{EI}{(\rho A)^2}2a_{m2}EI\beta_1^4\gamma_{3_1} \\ -\frac{EI}{\rho A}(\beta_2^4\gamma_{3_2} - \gamma_{4_2}) & \frac{EI}{(\rho A)^2}2a_{m2}(\beta_2^4\gamma_{3_2} - \gamma_{4_2}) \\ \frac{EI}{\rho A}(\beta_2^4\gamma_{3_2} - \gamma_{4_2}) & -\frac{EI}{(\rho A)^2}2a_{m2}(\beta_2^4\gamma_{3_2} - \gamma_{4_2}) \end{bmatrix},$$

where $\Delta_c = [\, a_{m1} \; a_{m2} \,]$. The functional matrices obviously have full rank for all parameter values. The model is therefore locally identifiable for all parameter values. We can thus state that there is no general linear dependence among the parameters.

Since the data are collected during normal operation there is a risk of feedback in the data. This can add extra algebraic relations to the system and thus lead to non-unique parameter estimates, see [Gustavsson *et al.*, 1977]. The effect can be seen as linear dependence among the regressors which implies that the control signal is proportional to the output or its derivatives. Problems due to this are not expected here since the output used for the control is found using the *gaugemeter principle*. This output is therefore only an estimate of the plate thickness and there is thus little risk that the control signal will be proportional to the plate thickness or its derivatives.

The key subject left is the excitation of the input signals. As seen in Chapter 5 the position sometimes is close to a sine wave, which will be considered as the worst case here. Introducing the input signals $\bar{z}(t)$ for the mean value of the roll positions and $\dot{z}(t)$ for the difference of

the roll positions it is possible to reduce the model to two SISO models

$$q_{c_1}(t) = \overline{G}_{q_c}(p) = \left(\frac{\rho AEI\beta_1^4\gamma_{3_1}}{\rho Ap^2 + a_{m2}p + (a_{m1} + EI\beta_1^4)} - \rho A\gamma_{3_1}\right)\overline{z}(t)$$
$$q_{c_2}(t) = \grave{G}_{q_c}(p)\left(\frac{\rho AEI(\beta_2^4\gamma_{3_2} - \gamma_{4_2})}{\rho Ap^2 + a_{m2}p + (a_{m1} + EI\beta_2^4)} - \rho A\gamma_{3_2}\right)\grave{z}(t).$$

Using this fact we see that a sinusoidal variation of the mean value of the roll position $\overline{z}$ or the skewness of the roll position $\grave{z}$ is sufficient for identifying a_{m1} and a_{m2}, see [Åström and Wittenmark, 1995]. We thus do not expect problems with identifying the parameters in this case.

Since the observer is a static model and the matrix Γ_6 have full rank, it is sufficient that the mean value of the rolling force $\overline{f}$, the difference of the forces $\grave{f}$, and the normal coordinates q are different from zero. This is the case for all the data sets, and we therefore expect no problems here either.

Identification

Since we have a multivariable problem we use the performance function

$$V = \det\left(\sum_{k=1}^{N}\varepsilon(k)\varepsilon(k)^T\right),$$

which implies that we are using multivariable maximum likelihood identification, see [Åström and Eykhoff, 1971]. Introduction of noise models does generally not improve the results and we therefore work with the state space structure

$$\begin{aligned}\dot{y}_c(t) &= A_c y_c(t) + B_c\tfrac{1}{2}z(t) + e(t)\\ q(t) &= C_c y_c(t) + D_c\tfrac{1}{2}z(t) + e(t),\end{aligned}$$

where e is white noise and q are the normal coordinates used in the series expansion of the solution. The normal coordinates can be deter-

mined using the thickness measurements at the three different positions across the plate width and the equation

$$\tfrac{1}{2}v_d(x,t) = \varepsilon(x)\tfrac{1}{2}z(t) + \sum_{i=1}^{2}\phi_i(x)q_i(t), \tag{6.6}$$

which is found by combining (4.10) and (4.13). Inserting the thicknesses of the three measurement tracks at the north edge, center, and south edge with positions x_1, x_2, and x_3 yields

$$\begin{bmatrix} \frac{1}{2}v_d(x_1,t) \\ \frac{1}{2}v_d(x_2,t) \\ \frac{1}{2}v_d(x_3,t) \end{bmatrix} = \begin{bmatrix} \varepsilon(x_1) \\ \varepsilon(x_2) \\ \varepsilon(x_3) \end{bmatrix} \tfrac{1}{2}z(t) + \begin{bmatrix} \phi_1(x_1) & \phi_2(x_1) \\ \phi_1(x_2) & \phi_2(x_2) \\ \phi_1(x_3) & \phi_2(x_3) \end{bmatrix} \begin{bmatrix} q_1(t) \\ q_2(t) \end{bmatrix}. \tag{6.7}$$

The above equation system is overdetermined and is therefore solved in a least squares sense in MATLAB.

To obtain a well conditioned problem, all the signals are scaled to have amplitudes of the same order of magnitude. In the identification a fourth order Butterworth filter with a cut-off frequency of 10 Hz is used for filtering the position $\frac{1}{2}z$, the rolling force f, and the normal coordinates q. To obtain agreement between the mean thickness calculated by the model and the measurements, the mean value of the thickness at the plate edges is set to the value calculated using the gaugemeter equation, see Chapter 3. The procedure for the observer is similar to the above and is therefore not repeated here.

Results

The identification has been performed directly on the state space structure using `pem` in MATLAB. Since the sampling interval is small we can assume that the input signals are constant between the sampling instants when transforming the model to discrete time. Using the values found in Appendix B for the mill spring coefficient $2K$, the stiffness of the roll pack EI, the mass of the roll pack ρA, and the value for the plate width w, we calculate β_1 and β_2, and the two first eigenfunctions ϕ_1 and ϕ_2. The eigenfunctions are computed in advance and are not involved in the system identification, where they enter through the Γ_i-matrices.

Time-invariant results for the model The identification is based on the model with the parametrization shown in (6.4), the position of the hydraulic system $\frac{1}{2}z$ and the normal coordinates q found using (6.7). We obtain the results shown in Figure 6.6. The results are representative for all 10 data sets.

As seen from the figure, the agreement is not very good, this is because the parameter a_{m1} is time varying. The mean values of the normal coordinates are however estimated quite well. The variations of a_{m1} will be investigated in more detail in the next section, we will here be satisfied with estimating the mean values of the parameters. Note that the difference between the thickness at the two sides is predicted quite well considering the time varying parameter. This indicates that the plane strain assumption works well in our case.

Trial and error tests show that the precise value of the damping a_{m2} is not critical for the result of the identification. This is probably because of the low frequency excitation of the roll positions z. We thus fix it at the value $a_{m2} = 200$, which is the mean value found in the identification. The parameter a_{m1} is considered to be the most important parameter since it, together with β_1, determines both the undamped natural frequency and the stationary gain of the system. When identifying the parameter for the 10 data sets, we find that a_{m1} varies one order of magnitude. Trying to correlate it with key parameters for the rolling process we find that a_{m1} varies systematicly with the plate hardness k_p.

It is a well known fact that the material parameters varies with the plate temperature and the reduction, see [Roberts, 1983]. This reference gives the following formula for the deformation resistance k_p which can be seen as the "specific hardness" of the plate

$$k_p = -1.429 + 4.98\left(\frac{T(t)}{1000}\right)^{-2} - 21.36\sqrt{r_t(t)} + 33.08\sqrt{r_t(t)}\left(\frac{T(t)}{1000}\right)^{-1}. \tag{6.8}$$

T is the plate temperature in ° C and

$$r_t(t) = \frac{\overline{v}(t) - \overline{v}_{-1}(t)}{\overline{v}_{-1}(t)}$$

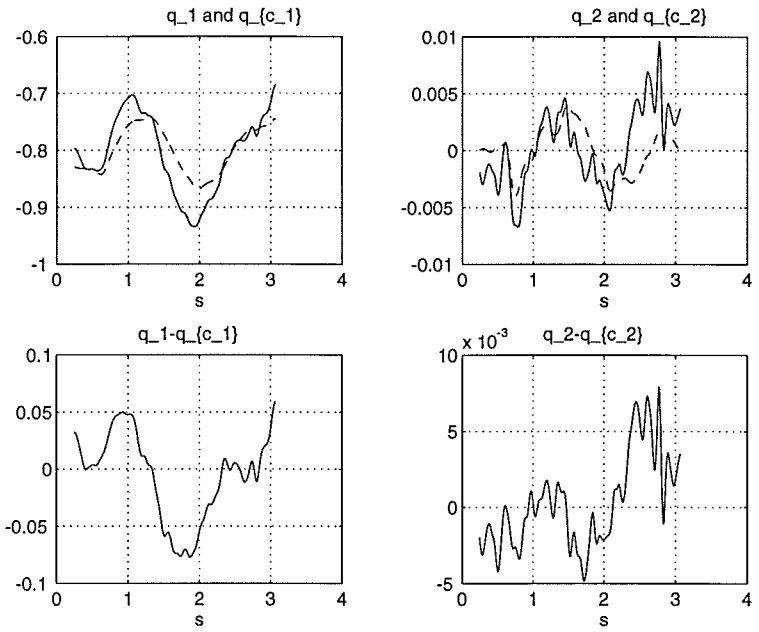

Figure 6.6 Identification results for the model. Left side, top: measured value of the normal coordinate q_1 (full) and estimated value of the normal coordinate q_{c_1} (dashed), bottom: prediction error for q_{c_1}. Right side, top: measured value of the normal coordinate q_2 (full) and estimated value for the normal coordinate q_{c_2} (dashed), bottom: prediction error for q_{c_2}. The results are not very good due to a time varying parameter a_{m1}.

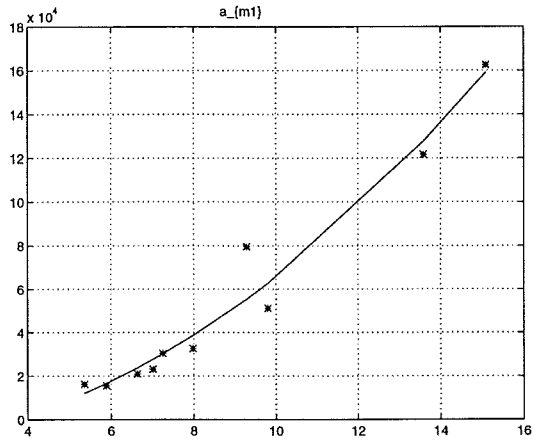

Figure 6.7 The parameter a_{m1} as a function of material hardness k_p.

is the *reduction*. Since the parameter a_{m1} is the spring coefficient for the steel plate k_p is closely related to a_{m1} in the model. The correlation between a_{m1} and k_p can be seen from Figure 6.7. From the figure we find that $a_{m1} \sim k_p$ is an acceptable model for parameter.

Note that the temperature used for calculating k_p is an estimated value – this might explain some of the deviations. An other reason for some of the deviations is that there is a phase shift for the material in the temperature interval between 723°C, and 870°C. In this interval there will be variations in hardness which can not be calculated by the formula for k_p.

Performing the identification on all 10 data sets we find the parameters shown in Table 6.2. Due to the known variations of a_{m1}, which are well correlated with k_p, we introduce no nominal data sets here.

A relevant question in connection with the variation of the parameter a_{m1} is: *How does this influence the dynamics of the rolling stand?*. To investigate this we have seen that the dynamics of the model for the rolling stand can be divided into two SISO transfer functions. When transforming from normal coordinates q_c to plate thickness v_c the di-

a_{m1}	$1.55 \times 10^4 - 1.62 \times 10^5$
a_{m2}	2.00×10^3

Table 6.2 Parameters for the model found using all 10 data sets.

rect term almost disappears. Neglecting this yields the relationships

$$\begin{aligned}
\overline{v}_c(t) &= \overline{G}_{v_c}(p)\overline{z}(t) \\
&= \frac{\phi_1(\mu)\rho A\gamma_{3_1}EI\beta_1^4}{\rho Ap^2 + a_{m2}p + EI\beta_1^4 + a_{m1}}\overline{z}(t) \\
\grave{v}_c(t) &= \grave{G}_{v_c}(p)\grave{z}(t) \\
&= \frac{\phi_2(\mu)\rho A\gamma_{3_2}EI\beta_2^4}{\rho Ap^2 + a_{m2}p + EI\beta_2^4 + a_{m1}}\grave{z}(t)
\end{aligned}$$

We see that $\overline{G}_{v_c}$ and $\grave{G}_{v_c}$ have no zeros and it therefore only is necessary to investigate the locations of the poles of the transfer functions. Inserting the values of a_{m1} and a_{m2} found in the system identification yields the pole locations shown in Figures 6.8 and 6.9.

We see that the poles tend to become faster and less damped when the plate hardness a_{m1} increases. Unfortunately the steady state gain of $\overline{G}_{v_c}$ and $\grave{G}_{v_c}$ also decreases with increasing plate hardness a_{m1} and it can therefore not be concluded that is becomes easier to control the plate thickness for the hard plates.

Time varying results for the model As seen in the last section the agreement between the model and the collected data were not satisfactory. Is was assumed that this was because of variations of the parameter a_{m1}. We saw that a_{m1} was correlated with the plate hardness k_p which could be calculated using (6.8). Using this equation we see that two things introduce time variations in k_p and thus a_{m1}:

- the reduction r_t;
- the plate temperature T.

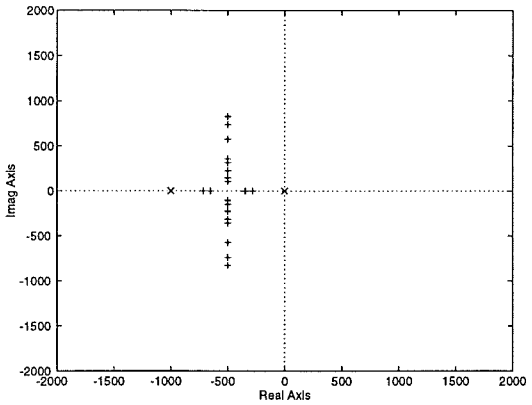

Figure 6.8 The pole locations for $\overline{G}_{v_c}$ as a function of a_{m1}. The crosses corresponds to $a_{m1} = 0$ and the poles with the largest imaginary part corresponds to the maximal value of a_{m1}. It is seen that the poles are real when a_{m1} is small and becomes faster and less damped when the value of a_{m1} increases.

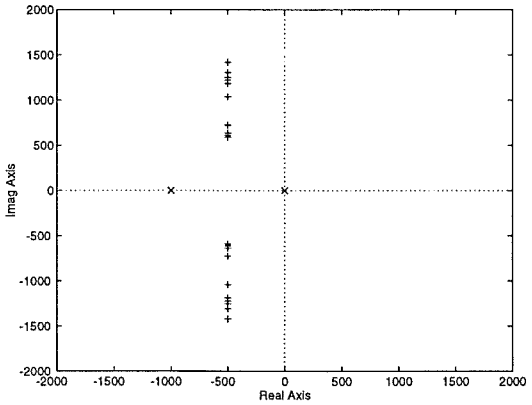

Figure 6.9 The pole locations for $\hat{G}_{v_c}$ as a function of a_{m1}. The crosses corresponds to $a_{m1} = 0$ and the poles with the largest imaginary part corresponds to the maximal value of a_{m1}. It is seen that the poles becomes faster and less damped when the value of a_{m1} increases.

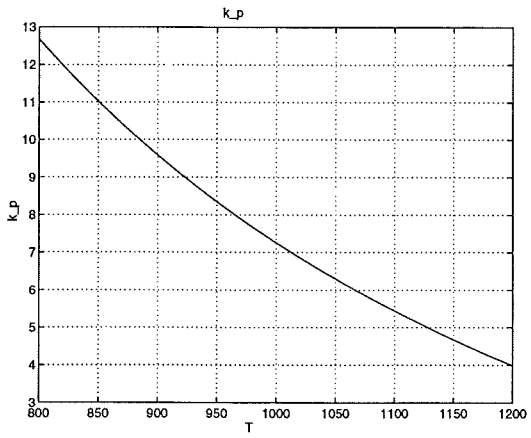

Figure 6.10 The plate hardness k_p as a function of the plate temperature T, for a reduction r_t of 0.1.

Typically the reduction r_t does not vary much during the pass, since the thickness control tends to keep the thickness constant. On the other hand the temperature can vary due to several factors:

- wide cold zones from the reheat furnace, which gives slow temperature variations;
- narrow cold zones from cooling by the roller tables, which gives fast temperature variations.

The temperature variations and their effect on the thickness controllers are well known in the literature, see for instance [Davies *et al.*, 1983], [Atori *et al.*, 1992], and [Nishikawa *et al.*, 1986]. A plot of k_p as a function of the temperature T in a representative interval and for $r_t = 0.1$ is shown in Figure 6.10. It is seen that k_p varies approximately a factor ten in the relevant temperature interval. The additional variation of a_{m1} is because the reduction r_t also varies.

To investigate the time variations during one measurement series a discrete time *recursive least squares estimator*, described in [Åström and Wittenmark, 1995] is implemented in OMSIM. Finding the transfer

function for the model and using the mean value of the position $\bar{z}$ as input, the MIMO transfer function reduces to the SISO transfer function

$$\bar{f}_c(t) = \left(\frac{2K\phi_1(0)\rho A\gamma_{3_1} EI\beta_1^4}{\rho Ap^2 + a_{m2}p + EI\beta_1^4 + a_{m1}(t)} - 2K\phi_1(0)\rho A\gamma_{3_1} \right) \bar{z}(t).$$

Introducing the new output variable $f_z = \bar{f}_c + 2K\phi_1(0)\rho A\gamma_{3_1}\bar{z}$ the problem is on standard form, and it is straight forward to estimate the plate hardness a_{m1} keeping the other parameters constant

$$y_z(t) = (\rho Ap^2 + a_{m2}p + EI\beta_1^4) f_z(t) - 2K\phi_1(0)\rho A\gamma_{3_1} EI\beta_1^4 \bar{z}(t) = a_{m1} f_z(t).$$

Using y_z as output and f_z as regressor, it is possible to estimate a_{m1}. Unfortunately the mill spring constant $2K$ can not be estimated since this parameter is used for finding ϕ_1, γ_{3_1}, and β_1. Note that the material coefficients can be estimated without knowledge of the plate thickness.

The results of the recursive system identification is shown in Figure 6.11. The estimation is done with a forgetting factor of 0.90 and a sampling time of 0.0025 s, which gives an estimator memory of 0.025 s, see [Johansson, 1993]. With a rolling speed of 4 m/s this implies that the length of the memory is approximatively 0.1 m. The variations shown are representative for other measurements investigated. It is seen that we have both slow and fast variations with an amplitude of approximately ±20 % of the nominal value of a_{m1}. It is seen that the amplitude of the fast variations is small compared to the amplitude of the slow variations.

The value for the parameter a_{m1} obtained using the time invariant methods is also shown in Figure 6.11. It is seen that there is good agreement between the two values considering that the fixed value is calculated using the thickness measurements, while the time varying value is found using the rolling force measurement.

If excessive cooling by the roller tables occur we will have significant fast time variations and there is a risk of that we can no longer consider the system as time invariant. This is fortunately not the case for any

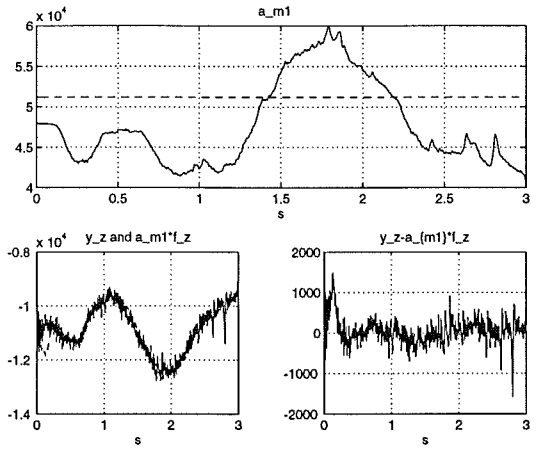

Figure 6.11 Upper plot: variations of a_{m1} (full), found using recursive system identification. The dotted line shows the constant value of 5.12×10^4 obtained in connection with the regular system identification. Lower left plot: the measured and predicted output in connection with the system identification. Lower right plot: the prediction error obtained in connection with the recursive system identification.

of the measurements used for the system identification. When we have a time varying system the working point may also vary with time. It is therefore important that we do not use working points in connection with the system identification and this has therefore been avoided.

Using the model (6.4) and (6.7) it is possible to calculate the thicknesses at the center and edges for the plate from the normal coordinates q_c, the roll positions $\frac{1}{2}z$ and the time varying value for the plate hardness a_{m1}. The result is shown in Figure 6.12. It is seen that the agreement between the model and the measurements is quite good. Note that the difference between the thickness at the edges and center, the plate crown, is captured quite well by the model. The good agreement shows that the linerization of the material model at a working point works well in practice. That the thickness control ensures that the thickness variations are small, helps to make the linear model valid in practice.

Since we use the relationship between the normal coordinates q and the rolling forces f in the simulations we also here investigate how well the model is able to predict f. Using (4.21) we obtain the relationship

$$\begin{bmatrix} f_{c_n}(t) \\ f_{c_s}(t) \end{bmatrix} = 2K \begin{bmatrix} \phi_1(0) & \phi_2(0) \\ \phi_1(w) & \phi_2(w) \end{bmatrix} \begin{bmatrix} q_{c_1} \\ q_{c_2} \end{bmatrix}.$$

Using the model (6.4) with the time varying plate hardness a_{m1} we obtain the results shown in Figure 6.12. It is again seen that there is quite good agreement. The deviations between the measured and calculated thicknesses are probably due to variations of the material hardness in the sidewise direction which is not covered by the model. These deviations are to small to have noticeable effect on the calculation of the plate thickness and can therefore not be seen here.

Time invariant results for the observer Using the observer given by (6.5), the rolling force f and q found from (6.7) we perform the system identification for the observer. A typical result is shown in Figure 6.13. Note that we now are able to predict the normal coordinates q quite well since we have knowledge of the variations of the plate hardness a_{m1} through the rolling force measurement. The results shown are representative for all 10 data sets.

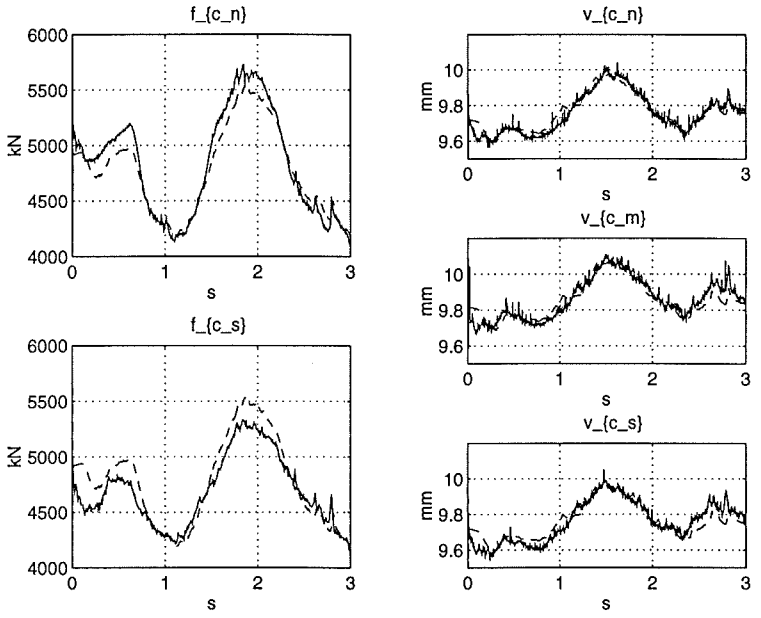

Figure 6.12 Calculation of rolling force and plate thickness using the model and the time varying results for a_{m1}. Left side, upper plot: the measured north rolling force f_n (full) and the calculated value f_{c_n} (dashed). Lower plot: the measured south rolling force f_s (full) and the calculated value f_{s_n} (dashed). Right side, upper plot: the north thickness measurement $v_d(x_1)$ (full) and the calculated value v_{c_n} (dashed). Middle plot: the center thickness measurement $v_d(x_2)$ (full) and the calculated value v_{c_m} (dashed). Lower plot: the south thickness measurement $v_d(x_3)$ (full) and the calculated value v_{c_s} (dashed). It is seen that there is considerably better agreement between measurements and model output than in Figure 6.6.

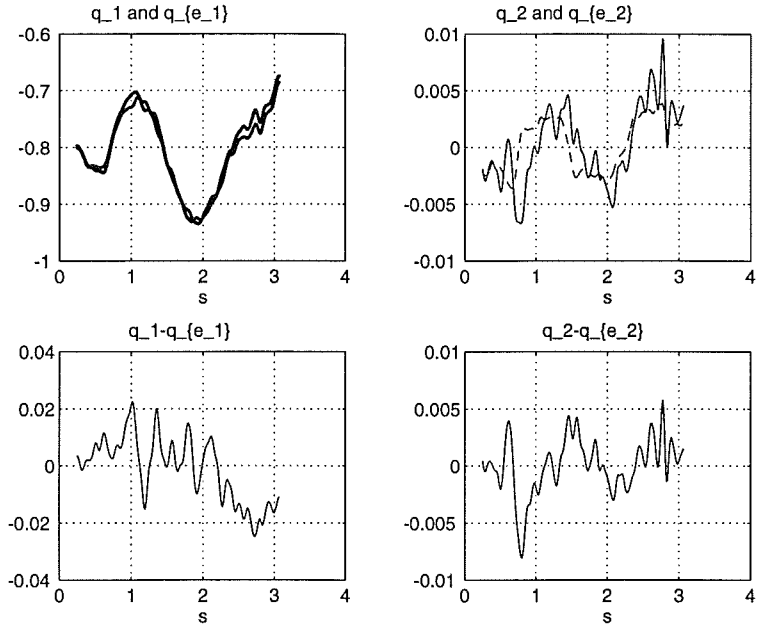

Figure 6.13 Identification results for the observer. Left side, top: measured value for the normal coordinate q_1 (full) and estimated value for the normal coordinate q_{e_1} (dashed), bottom: prediction error for q_{e_1}. Right side, top: measured value for the normal coordinate q_2 (full) and estimated value for the normal coordinate q_{e_2} (dashed), bottom: prediction error for q_{e_2}.

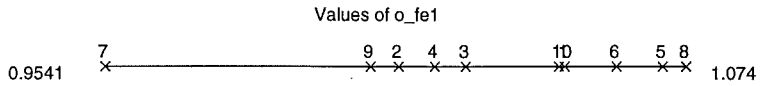

Figure 6.14 Distribution of the parameter o_{fe_1} for the observer. The nominal value of the parameter is 1.

The values of the parameter o_{fe_1} are shown in Figure 6.14. It is seen here that $o_{fe_1} \approx 1$, as expected. Ideally the parameters o_{fe_2} should also have the value 1, but from the system identification we find that $o_{fe2} \approx 0.2$ for the plate width $w = 2.15$ and $o_{fe2} \approx 0.4$ for $w = 3.15$. The reason that we only have data for two values of the plate width w is that the ten data sets are from plates with only two different widths.

Inspecting the force measurements we find that the boundary conditions

$$
\begin{aligned}
f_n(t) &= 2Ku(0,t) \approx 2K(q_1(t)\phi_1(0) + q_2(t)\phi_2(0)) \\
f_s(t) &= 2Ku(w,t) \approx 2K(q_1(t)\phi_1(w) + q_2(t)\phi_2(w)) \\
&\Downarrow \\
\overline{f}(t) &\approx 2K\phi_1(0)q_1(t) \qquad (6.9) \\
\grave{f}(t) &\approx 2K\phi_2(0)q_2(t), \qquad (6.10)
\end{aligned}
$$

where $\grave{f}(t)$ is the difference of the forces, are not fulfilled. The plots of the left and right sides of (6.9) and (6.10) are shown in Figure 6.15. Here we see that the left and right side of (6.9) agrees quite well but that there is a significant deviation between the left and right side of (6.10). The amplitude of the difference of the roling forces $\grave{f}$ is too large – this explains why o_{fe_2} becomes smaller than 1.

One explanation to the above could be that the connection between the two legs of the rolling stand is not included in the physical model. It is quite possible that the above difficulty could be avoided by inserting a spring between the two sides of the physical model. Another possibility that the force measurement is inaccurate. If this is found to be the case, an improvement of the force measurements is necessary to obtain a better agreement between model and data.

Using the results from the identification we arrive at the values for the nominal parameters shown in Table 6.3. Since the identification is based on a fixed value of the parameter o_{fe_2} and the variation of o_{fe_1} is small, no simulations of the nominal model is shown, since they will be similar to the results of Figure 6.13.

Using (6.6) the thickness predicted by the observer at the measurement points can be calculated. The results are shown in Figure 6.16. We note that now the predicted and measured thicknesses agree quite

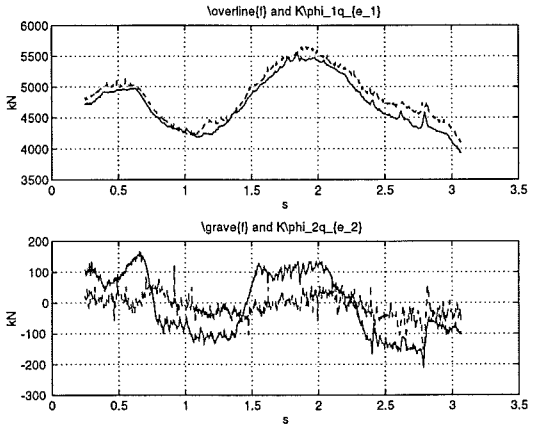

Figure 6.15 Illustration of that the rolling force measurements do not fulfill the boundary conditions. Upper plot: mean value of the rolling forces $\overline{f}$ full and $2K\phi_1(0)q_1$ (dashed). Lower plot: difference between the rolling forces $\hat{f}$ full and $2K\phi_2(0)q_2$ (dashed).

	w = 2.15	w = 3.15
o_{fe_1}	1	1
o_{fe_2}	0.2	0.4

Table 6.3 Parameters of the observer as functions of the plate width w. The parameters are found using all the 10 data sets

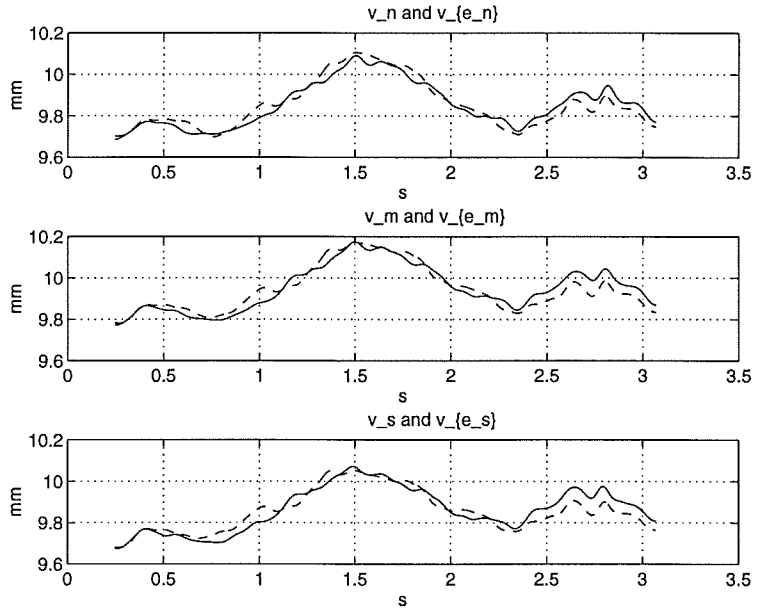

Figure 6.16 The thickness at the plate edges and center calculated using the observer. Upper plot: the measured value $v_d(x_1)$ (full) and the calculated value v_{e_n} (dashed) of the thickness at the northern edge. Center plot: the measured value $v_d(x_2)$ (full) and the calculated value v_{e_m} (dashed) of the thickness at the center. Lower plot: the measured value $v_d(x_3)$ (full) and the calculated value v_{e_s} (dashed) of the thickness at the southern edge v_s.

well due to the rolling force measurement. Also for the observer the calculated plate crown is close to its measured value.

6.3 Total model

In Chapter 4 we derived a total model including both the hydraulic systems and the rolling stand. The models for the hydraulic systems, the model for the rolling stand, and the observer for the rolling stand are implemented in OMSIM using (6.1) and (6.4), see [Andersson, 1994].

This simulation environment is well equipped for handling discrete event systems, such as the hydraulic positioning systems where the structure of the differential equations changes at $x_{vn} = 0$ and $x_{vs} = 0$.

The parameters used for the simulations are the ones found from the system identification. An exception is that the parameter of the observer o_{fe_2} is set back to 1, for the model and the observer to match. Note that this only affects the estimation of the states of the model.

The results of a simulation of the total model are shown in Figure 6.17. The input signals are chosen as

$$x_{vrn}(t) = \begin{cases} 10 & 0 \geq t < 0.1 \\ 0 & t > 0.1 \end{cases}$$

$$x_{vrs}(t) = \begin{cases} 10 & 0\ geqt < 0.2 \\ 0 & t > 0.2. \end{cases}$$

At $t = 0$ the outgoing thickness is equal to the ingoing thickness of the plate, which is 11.64 mm and the rolling force is zero. Then the hydraulic positioning systems movie downwards, the rolling force increases and the outgoing thickness decreases. At $t = 0.1$ the north system stops, but it is seen that the rolling force and the thickness at the north side continue to change due to the movement of the position of the south system. This illustrates the multivariable structure of the system.

It is seen that the hydraulic systems act as integrators. They move with a slightly different speed for the same input due to the different values of the parameters a_{hn1} and a_{hs1}. The states of the model y_c and the states of the observer y_e are shown in Figure 6.18. The simulation here is the same as the one shown in Figure 6.17. It is seen that the states of the model and the states of the observer agrees well. One problem in connection with the estimation of y_c is that it is necessary to know the parameter a_{m2} which is hard to find, unless better excitation is present.

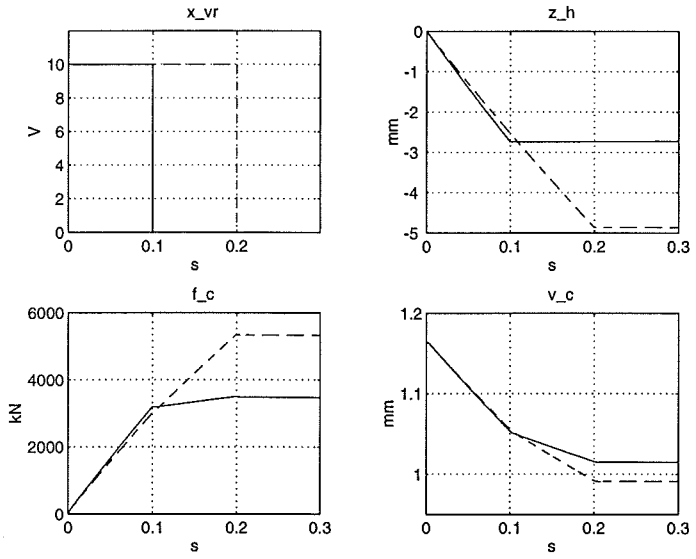

Figure 6.17 Simulations of total model for rolling mill. Upper left: control signal for valve glider positions for north x_{vrn} (full) and south x_{vrs} (dashed) hydraulic system. Upper right: Positions of north hydraulic system z_{h_n} (full) and south hydraulic system z_{h_s} (dashed). Lower left: north rolling force f_{c_n} (full) and south rolling force f_{c_s} (dashed). Lower right, plate thickness north edge v_{c_n} (full) and plate thickness south edge v_{c_s} (dashed).

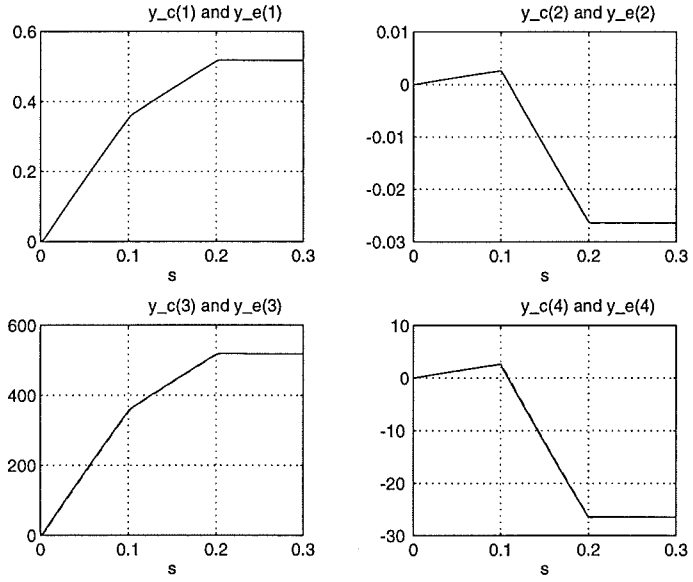

Figure 6.18 Comparison of the four states of the model y_c (full) and the state estimate found by the observer y_e (dashed). It is seen that the agreement between the real and estimated value is good.

6.4 Summary

In this chapter we have found the parameters of the model for the rolling mill. For the hydraulic systems we have found a set of nominal parameters and for the model for the rolling stand we have found one constant and one time varying parameter. For the observer we have found two parameters, one constant and one which varies with the plate width. The agreement between model and data are all satisfactory, it was however necessary to introduce extra parameters in the observer since two of the four boundary conditions used for calculating the plate thickness were not fulfilled.

The models have been implemented in a suitable simulation environment and we are now ready to do and evaluate the controller design. This will be done in the next chapter.

7

Controller design

The purpose of this chapter is to design a thickness controller for the rolling mill, which consists of the hydraulic positioning systems and the rolling stand. The purpose of the controller is to ensure that the desired plate thickness is obtained with as small deviations as possible, despite the process disturbances.

The performance specifications of the control systems are first given, this includes description of typical disturbances and the multivariable nature of the system. Then the controlled outputs are chosen and the multivariable structure, the dynamics of the system, and the steady state gains are analyzed.

The above forms the basis for the choice of methods for controlling the rolling mill. The controllers are then designed using the models and parameters found in the previous chapters. In general, time invariant methods will be used for the controller design and we therefore assume that the material parameters are constant during the pass in the following. The effects of the variations of the material parameters will be investigated in the simulations.

Due to variation of several central parameters and the fact that it is not possible to measure the process output, stability is an important issue in connection with the thickness control. Therefore, the stability of the closed loop system will be analyzed and bounds on the parameter variations will be found. In the last section of this chapter the performance of the control system is investigated using computer simulations. Here the effects of reference changes and typical disturbances are found and commented.

No work on multivariable thickness control of hot rolling mills has been found. Several descriptions of the single-input single-output case are given in [Kokai *et al.*, 1985], [Saito *et al.*, 1981], [Teoh *et al.*, 1984], [Ferguson *et al.*, 1986] and many more. Furthermore, advanced control and estimation methods have been used in connection with the elimination of the effects of roll eccentricity, see [Yeh *et al.*, 1991], [Teoh *et al.*, 1984], and [Asada *et al.*, 1986]. For further details see Chapter 3.

7.1 Performance specifications

As described in Chapters 2 and 3 the purpose of the thickness control is to obtain a specified constant thickness, despite disturbances such as:

- variations of the plate hardness;
- variations of the ingoing thickness.

The thickness control problem is thus a regulator problem, see [Åström and Wittenmark, 1990]. A central goal of the control is to minimize the thickness variations of the rolled plates. The quality level possible to obtain depends on saturation of the control signal and the amplitude of the variations. It might therefore be necessary to minimize the variations by other means to obtain the desired value of the thickness variations.

The rolling process is a multivariable system, this has to be taken into consideration when controlling the process. A natural demand is to be able to control the thickness at the north and south edge independently of each other. This will make it possible to handle reference changes and control errors at one edge with minimal effect on the thickness at the other edge. Furthermore, the controller has to be able to compensate for asymmetric material conditions. This is not possible with the existing control, see Chapter 3.

A third important issue is the stability of the thickness control system. The stability is disturbed by two effects:

- variations of the material characteristics;

- the controlled variable (the thickness) has to be estimated.

This has lead to a detuning of the compensation for mill deflection in traditional thickness control systems, see Chapter 3. An analysis of the stability of the thickness control system is therefore relevant in connection with the design.

In system identification of the hydraulic systems in Chapter 6 we found that the models of the hydraulic systems were sensitive to offsets in the control variable. It was concluded that including an integrator in the controller would solve this problem when controlling the roll position. We therefore include an integrator in the controller design. It will bee seen later that using an integrator will also be a good idea in connection with the control of the plate thickness.

The handling of the start and the end of the pass will not be discussed in the following. Since the plate ends usually are curved, the physical model for the rolling stand does not cover this case, since the plate will not have full width when entering the roll gap. The plate ends furthermore tends to be colder than the rest of the plate. To ensure a proper start up and shut down of the control it is likely that a special control strategy is necessary to handle the beginning and end of the passes.

7.2 Analysis of model

The first natural question that arises is, at how many points in the width direction is it possible to control the tickness of the plate using the two hydraulic actuators. We do this to choose the number of outputs we want to control. Looking at the state equations of the model we see that in steady state we have that

$$\begin{aligned} \dot{y}_c(t) = 0 &= A_c y_c(t) + B_c \tfrac{1}{2} z(t) \\ &\Downarrow \\ y_c(t) &= -A_c^{-1} B_c \tfrac{1}{2} z(t), \end{aligned}$$

noting that the system matrix A_c is invertible. The above implies that we are only able to control the state vector in stationarity within a

two dimensional plane. We can therefore not control more than two outputs in stationarity with the thickness control. The thicknesses of a plate are normally measured at a distance μ from the plate edges. Our outputs are thus chosen as

$$\begin{bmatrix} v_n(t) \\ v_s(t) \end{bmatrix} = \begin{bmatrix} v(\mu,t) \\ v(w-\mu,t) \end{bmatrix}$$
$$= 2\begin{bmatrix} \phi_1(\mu) & \phi_2(\mu) \\ \phi_1(w-\mu) & \phi_2(w-\mu) \end{bmatrix}\begin{bmatrix} q_1(t) \\ q_2(t) \end{bmatrix} + \begin{bmatrix} \varepsilon(\mu) \\ \varepsilon(w-\mu) \end{bmatrix} z(t).$$

Using our physical insight we choose the north position z_n for controlling the north thickness v_n and the south thickness z_s for controlling the south thickness v_s.

Investigating the multivariable structure of the system we apply a step of 1 mm at the north position z_n. The open-loop step response is shown in Figure 7.1. We see that the thickness at both edges are affected by the position change at one of the sides. Furthermore, it can be seen from the step responses that two systems with different dynamics are involved. This is due to the fact that the dynamics for for the normal coordinates q_{c_1} and q_{c_2} are different. Note the direct term, which is the result of inaccuracies in connection with the state transforms used in the modeling. The direct term is small compared to the steady state gain of the system and it will be neglected in the controller design. It will though be included in the simulations.

The multivariable effect illustrated in Figure 7.1 causes trouble when controlling the thickness at the two sides independently. If the thickness at the north side deviates from the specified value while the south thickness does not, it is not possible to obtain the right thickness by just adjusting the hydraulic position at the north side. It is thus necessary to consider the multivariable nature of the system when designing the controller. Ideally it should be possible to control the thicknesses at the two sides independently of each other.

Looking at the mean values for position $\overline{z}$ and thickness $\overline{v}$, and neglecting the direct term, the relationship is

$$\overline{v}(t) = \overline{G}_{v_c}(p)\overline{z}(t) = \frac{\phi_1(\mu)\rho A\gamma_{3_1} EI\beta_1^4}{\rho Ap^2 + a_{m2}p + EI\beta_1^4 + a_{m1}}\overline{z}(t).$$

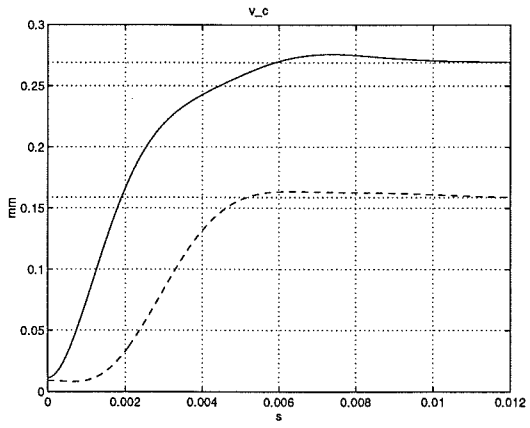

Figure 7.1 Open-loop result of a step change of 1 mm in the north position z_n. Full: thickness at north edge v_{c_n} and dashed: thickness at south edge v_{c_s}. It is seen that the position change at one side affects the thickness at both sides of the rolling stand

The dynamics of this transfer function varies due to the variations of a_{m1}. A similar transfer function $\grave{G}_{v_c}$ can be derived for the skewness of the position $\grave{z}$ and the skewness of the thickness $\grave{v} = \frac{1}{2}(v_n - v_s)$. Using the values obtained from the system identification the undamped natural frequencies of the two transfer functions $\overline{\omega}_n$ and $\grave{\omega}_n$ are in the intervals

$$\overline{\omega}_n \in [200,\ 432] \text{ rad/s}$$
$$\grave{\omega}_n \in [342,\ 658] \text{ rad/s}.$$

The steady state gains of the rolling stand $\overline{k}_g$ and $\grave{k}_g$ are in the intervals

$$\overline{k}_g \in [0.136,\ 0.404]$$
$$\grave{k}_g \in [-0.0142,\ 0.287],$$

that is, they vary a factor 3. Generally, $\overline{k}_g$ will lie in the interval between zero and one. If the plate hardness is close to 0, $\overline{k}_g$ will be close to 1 and when the plate becomes very hard $\overline{k}_g$ will be close to zero. This illustrates why an important part of the optimization of the rolling mill is to do the rolling in minimal time to keep the plate as hot as possible.

Since the hydraulic positioning systems are the actuators of the thickness control system, they set the limits of achievable performance. The variables that mainly affect the limitations of the positioning systems are:

- the supply pressure $\overline{P}_s$;
- the valve glider positions x_v.

This introduces limits on the values of the rolling forces f, the roll positions z and the reduction r_t. The maximal mill deflection is determined by the maximal rolling force and thus by $\overline{P}_s$. Since this limit is smaller than the maximal position z_t it is the above limitations and not the structure of the hydraulic systems that set the limits for the positions z.

The hydraulic systems operate under very different conditions. The rolling force, which determines the gain of the system, varies from 0 to the value of the supply pressure $\overline{P}_s$ and this should be taken into consideration, when designing the controller for the hydraulic systems.

Using small closed loop step responses for the hydraulic systems we find that they have a damping factor of $\zeta = 0.7$ and a peak time $t_p = 0.07$. This yields a undamped natural frequency of the hydraulic systems of

$$\omega_{nh} = 24.6 \text{ rad/s}.$$

We see that the dynamics of the hydraulic systems are considerably slower than the dynamics of the mill stand. This is one of the reasons why it is difficult to eliminate the high frequency variations of the plate thickness. Making the hydraulic system faster is of course a question about saturation of the control signal, but according to the constructor of the existing control system it is possible to make it considerably faster when implementing a digital controller.

7.3 Choice of control methods

The controller design will be done in continuous time. This is necessary to utilize the structure of the physical models we have derived and identified in the previous chapters. It will be necessary to implement the control strategies using digital equipment and the control strategy therefore has to be transformed to discrete time. This can be done using the approximate methods described in [Åström and Wittenmark, 1990]. The price to be paid for this procedure is that it is necessary to implement the controller using a higher sampling frequency than if the design was done in discrete time.

To make the hydraulic systems work well at all operating points, it is necessary to use a non-linear control strategy. Since we only have a first order system and all states and inputs can be measured or estimated, it is chosen to use feedback linearization for controlling the hydraulic systems, see [Slotine and Li, 1991].

The responses of the two sides of the rolling mill are separated using eigenspace design as described in [Harvey and Stein, 1978]. This de-

sign method makes it possible to assign specified values to the eigenvectors of the closed loop system. The additional eigenvectors and eigenvalues for which we have no specifications are furthermore placed in a "nice" way.

The variation of the material hardness a_{m1} changes the steady state gain of the system and it is necessary to compensate for this in some way. The plate thickness can, despite the parameter variations, be estimated using the observer. Using an integrator it is possible to ensure that the closed loop steady state gain is not affected by the parameter variations. The variations of the plate hardness a_{m1} will still affect the dynamics and the stability of the system.

The parameter variations make adaptive control relevant. Since we use an advanced control strategy the adaptive control will though be complicated. It will therefore in simulations be investigated if the performance of the above strategy is satisfactory or if a truly adaptive controller is needed.

7.4 Design of controllers

In the following sections the controllers for the hydraulic systems and the rolling stand will be designed. The hydraulic systems will be controlled using feedback linearization and the rolling stand will be controlled by a state feedback, found using eigenspace design.

Hydraulic systems

Since we have a first order system it is quite easy to derive a control law which linearizes the system. Even if some of the usual assumptions on the input function such as independence of the control variable and smoothness are not fulfilled it is still possible to do the feedback linearization. As usual we only show the results for the north system since the procedure of the south system is the same. To increase number of the degrees of freedom in the eigenspace design we give the hydraulic systems a time constant κ when doing the feedback linearization. κ is then used as a design parameter in the eigenspace design.

We choose the control signal as

$$x_{vrn}(t) = \frac{1}{-a_{hn1}\xi_1(t)}(-a_{hn2}\xi_2(t) - a_{hn3}\xi_3(t) + r_{l_n}(t) - \kappa z_n(t)),$$

where

$$\xi_1(t) = \begin{cases} \sqrt{\bar{P}_s - f_n(t)} & x_{vn}(t) \geq 0 \\ \sqrt{\eta \overline{P}_s} + \sqrt{\eta \overline{P}_s + f_n(t)} & x_{vn}(t) < 0 \end{cases}$$

$$\xi_2(t) = (z_t - z_n(t))\frac{d}{dt}f_{c_n}(t)$$

$$\xi_3(t) = f_n(t).$$

r_{l_n} is the control signal from the thickness controller. The north position z_n, the position of the valve glider x_{vn}, and the north rolling force f_n can be measured directly and $\frac{d}{dt}f_{c_n}$ can be estimated using the relationship

$$\frac{d}{dt}f_{c_n}(t) = 2KF\frac{d}{dt}q_c(t),$$

found in Section 4.3. To determine the derivative of the normal coordinates $\frac{d}{dt}q_c$ we can use the model for the rolling stand and the differential equation for $\dot{z}_{h_n}$. This is not trivial since a good estimate of the plate hardness a_{m1} is necessary to do this. An alternative is to use approximative numerical differentiation of the rolling force f to find $\frac{d}{dt}f$.

We note that the control strategy demands that $f_n < \overline{P}_s$. When the pressure due to the rolling force f_n gets close to the supply pressure $\overline{P}_s$ the thickness control will in any case be switched off to prevent overload of the hydraulic system. It is therefore not necessary to worry about the case $f_n = \overline{P}_s$.

Using the above strategy the model for the hydraulic system reduces to

$$\dot{z}_{h_n}(t) = -\kappa z_{h_n}(t) + r_{l_n}(t)$$

and can thus be inserted as an extra state in the state space equations for the rolling stand.

Rolling stand

We now proceed with the design of the controller for the rolling stand. The design will be performed on the model for the rolling stand combined with the now linear hydraulic systems and two additional integrator states. The main idea in the eigenspace principle is that, in addition to the desired closed loop poles, a set of desired closed loop eigenvectors is also specified – this is possible since we are working with a multivariable system, see [Kailath, 1980] and [Moore, 1976].

The response of the closed loop system due to the initial conditions q_{c_o} can be written as

$$v_c(t) = \sum_{j=1}^{n} C_c v_j (v_{ij}^T q_{c_o}) e^{\lambda_j t}, \tag{7.1}$$

where the λ_j's are the closed loop eigenvalues and v_j are the closed loop eigenvectors defined by

$$(I\lambda_j - (A_c - B_c L))v_i = 0 \tag{7.2}$$

and

$$[\, v_{i_1} \quad v_{i_2} \quad \cdots \quad v_{i_n} \,]^T = [\, v_1 \quad v_2 \quad \cdots \quad v_n \,]^{-1}.$$

It is possible to affect the eigenvectors by the choice of the feedback matrix L. It is here assumed that the closed loop eigenvalues are simple, this implies that the closed loop eigenvectors all are linearly independent. Assuming that the closed loop eigenvalues $\lambda_j \neq \mathrm{sp}(A_c)$ we can rewrite (7.2) as

$$\begin{aligned} v_j &= (I\lambda_j - A_c)^{-1} B_c \mu_j \\ \mu_j &= -L v_j. \end{aligned} \tag{7.3}$$

The idea of the eigenspace design is then to choose the feedback matrix L to obtain the desired eigenvectors, if possible.

The desired closed loop eigenvalues for the new thickness controller are chosen to give the same magnitudes of the control signals as used by the existing control system. There are two reasons for this:

- It is hard to say when the hydraulic positioning systems saturate since this depends on the nature of the disturbances and the characteristics of the supply equipment. It is therefore more natural to adjust the response speed of the controller when it is implemented.
- It will be possible to compare the performance of our control system to the performance of the existing control system.

Using the eigenspace design approach first described in [Harvey and Stein, 1978] and later generalized in [Stein, 1979] we find that by choosing the weighting matrices for a LQG controller in a special way it is possible to obtain a set of specified closed loop eigenvalues and eigenvectors. The eigenvalues and eigenvectors are obtained asymptotically as the control weight σ tends to zero. The number of design parameters are thus reduced to one when the eigenvalues and eigenvectors are chosen.

Using the general approach it is possible to assign $p < n - m$ finite eigenvalues with the associated eigenvectors

$$v_i \to (\lambda_i I - A_c)^{-1} B_c \mu_i, \quad i = 1, \ldots, p \tag{7.4}$$

and for the $n - p$ asymptotically infinite eigenvalues the eigenvectors can be chosen as

$$\begin{array}{l} [\, v_{1+(j-1)k} \quad \cdots \quad v_{jk} \,] \to [\, B_c(:,j)\mu_j \quad \cdots \quad A_c^k B_c(:,j)\mu_j \,], \\ j = 1, \ldots, m, \; k = 1 + \frac{n-p}{m} \end{array} . \tag{7.5}$$

Here n is the number of states and m is the number of inputs and outputs. There will be m sets of infinite eigenvalues. Each set goes toward infinity in the Butterworth pattern

$$\lambda \sim \left(\frac{1}{\sqrt{\sigma}} \right)^{1/k}$$

and has the eigenvectors

$$[\, B_c(:,j)\mu_j \quad \cdots \quad A_c^k B_c(:,j)\mu_j . \,]$$

The generalized approach makes it possible to handle the case where multiple closed loop eigenvalues are needed, this will be exploited in our case. The point now is to choose the desired finite and infinite eigenvectors and to do this we need a state space representation of the whole system.

Using the control law found in the previous section the hydraulic systems can be included as a part of the state space model. Since it is half of the position $\frac{1}{2}z$ that is used in the model for the rolling stand it is most convenient to use half of the position as a state. As seen in the previous section the steady state gain of the open loop system varies due to the variations of the plate hardness a_{m1}. The simplest way of avoiding this for the closed loop system is to calculate the plate thickness

$$v_c(t) = [\,\Phi \quad 0\,]\, y_c(t)$$

and introducing two integral states i

$$i(t) = \tfrac{1}{2}r(t) - v_c(t)$$

where $r^T = [\,r_n \quad r_s\,]$ are the references for the plate thickness. The state space representation including the hydraulic positions and the integral states is

$$\left[\begin{array}{c} \dot{y}_c(t) \\ \frac{1}{2}\dot{z}_h(t) \\ i(t) \\ \hline v_c(t) \end{array}\right] = \left[\begin{array}{c|c} A_{ch} & B_{ch} \\ \hline C_{ch} & D_{ch} \end{array}\right] \left[\begin{array}{c} y_c(t) \\ \frac{1}{2}z_h(t) \\ i(t) \\ \hline r_l(t) \\ \frac{1}{2}r(t) \end{array}\right]$$

$$= \left[\begin{array}{cccc|cc} -a_{m2}\Gamma_1 & I & 0 & 0 & 0 & 0 \\ -EI\Gamma_2 - a_{m1}\Gamma_1 & 0 & EI(\rho A\Gamma_2\Gamma_3 - \Gamma_4) & 0 & 0 & 0 \\ 0 & 0 & -\kappa I & 0 & I & 0 \\ -\Phi & 0 & 0 & 0 & 0 & I \\ \hline \Phi & 0 & 0 & 0 & 0 & 0 \end{array}\right] \left[\begin{array}{c} y_c(t) \\ \frac{1}{2}z_h(t) \\ i(t) \\ \hline r_l(t) \\ \frac{1}{2}r(t) \end{array}\right] \tag{7.6}$$

where $r_l = [\, r_{l_n} \quad r_{l_s} \,]$ The state space representation has 8 states. For convenience we define

$$B_{ch_1} = [\, 0 \quad 0 \quad I \quad 0 \,]^T$$
$$B_{ch_2} = [\, 0 \quad 0 \quad 0 \quad I \,]^T.$$

Using the PBH rank test, see [Kailath, 1980], it is possible to show that the system $(A_{ch}, B_{ch_1}, C_{ch}, D_{ch})$ is controllable. It is therefore not necessary to worry about uncontrollable modes in the following.
We now perform the eigenspace design on the new state space description. Using (7.3) and (7.6) we find that the possible directions of the two finite eigenvectors are

$$[\, \nu_1 \quad \nu_2 \,] \sim \begin{bmatrix} \Pi(\lambda_f)\rho AEI(\rho A\Gamma_2\Gamma_3 - \Gamma_4) \\ \Pi(\lambda_f)(\rho A\lambda_i + a_{m2})EI(\rho A\Gamma_2\Gamma_3 - \Gamma_4) \\ \Pi(\lambda_f)\begin{bmatrix} p_{c_2}(\lambda_i) & 0 \\ 0 & p_{c_1}(\lambda_i) \end{bmatrix} \\ (1/\lambda_f)\Pi(\lambda_f)EI\rho A\Phi\begin{bmatrix} p_{c_2}(\lambda_i) & 0 \\ 0 & p_{c_1}(\lambda_i) \end{bmatrix}(\rho A\Gamma_2\Gamma_3 - \Gamma_4) \end{bmatrix} [\, \mu_1 \quad \mu_2 \,], \tag{7.7}$$

where

$$p_{c_1}(p) = \rho Ap^2 + a_{m2}p + EI\beta_1^4 + a_{m1}$$
$$p_{c_2}(p) = \rho Ap^2 + a_{m2}p + EI\beta_2^4 + a_{m1}$$

and

$$\Pi(\lambda_f) = \begin{bmatrix} p_{c_1}(\lambda_i) & 0 \\ 0 & p_{c_2}(\lambda_i) \end{bmatrix}.$$

The main objective of the eigenspace design is to separate the two sides of the rolling stand. Using (7.1) we find that the output is given by

$$v_c(t) = \sum_{j=1}^{8} C_{ch}\nu_j e^{\lambda_j t}(\nu_{i_j}^T q_{c_o}).$$

Looking at the response for two finite eigenvectors and choosing $\lambda_f = \lambda_1 = \lambda_2$ we end up with

$$v_c(t) = C_{ch}[\, v_1(v_{i_1}^T q_{c_o}) \quad v_2(v_{i_2}^T q_{c_o})\,] e^{\lambda_f t}.$$

Looking at the directions of the two eigenvectors we build the matrix

$$\begin{bmatrix} v_{c_{nn}} & v_{c_{ns}} \\ v_{c_{sn}} & v_{c_{ss}} \end{bmatrix} \approx [\,\Phi \quad 0 \quad 0 \quad 0\,][\, v_1 \quad v_2\,].$$

Tor the two sides to be decoupled it is necessary that

$$\begin{bmatrix} v_{c_{nn}} & v_{c_{ns}} \\ v_{c_{sn}} & v_{c_{ss}} \end{bmatrix} \sim \begin{bmatrix} 1 & 0 \\ 0 & 1 \end{bmatrix},$$

a choice of the eigenvectors should then be

$$[\, v_1 \quad v_2\,] = \begin{bmatrix} \Phi^{-1} \\ * \\ * \\ * \end{bmatrix},$$

where $*$ indicates that we do not care about that submatrix. We see that if we choose

$$[\, \mu_1 \quad \mu_2\,] = \left(\begin{bmatrix} p_{c_1}(\lambda_f) & 0 \\ 0 & p_{c_2}(\lambda_f) \end{bmatrix} \rho AEI(\rho A \Gamma_2 \Gamma_3 - \Gamma_4) \right)^{-1} \Phi^{-1}$$

then the two desired finite eigenvectors are obtained. Note that the above choice for μ_1 and μ_2 also separates the integrator states.

A natural demand would be also to try to separate the rolling forces of the two sides. Using the same procedure as above we find the matrix

$$\begin{bmatrix} f_{c_{nn}} & f_{c_{ns}} \\ f_{c_{sn}} & f_{c_{ss}} \end{bmatrix} = [\, 2KF \quad 0 \quad 2K\rho AF\Gamma_3 \quad 0\,][\, v_3 \quad v_4\,]$$

and the desired eigenvectors are thus

$$[\nu_3 \quad \nu_4] = \begin{bmatrix} (2KF)^{-1} \\ * \\ -(2K\rho AF\Gamma_3)^{-1} \\ * \end{bmatrix}.$$

Looking at (7.7) we see that there is no choice of closed loop eigenvalues λ_3, λ_4, and $[\mu_3 \quad \mu_4]$ that yields the above set of eigenvectors. The only thing we demand from the force in the following is therefore that it should be well damped to avoid unnecessary exceeding of the force limit.

Since we only have demands for two eigenvectors we choose to have 2 finite eigenvectors and the system is of 8th order we will thus have 6 infinite eigenvectors. We find these using (7.5) and (7.6) with $k = 2$

$$[\nu_3 \quad \nu_6] = \begin{bmatrix} 0 \\ 0 \\ I \\ 0 \end{bmatrix} [\mu_3 \quad \mu_4]$$

$$[\nu_4 \quad \nu_7] = \begin{bmatrix} 0 \\ EI(\rho A\Gamma_2\Gamma_3 - \Gamma_4) \\ -\kappa I \\ 0 \end{bmatrix} [\mu_3 \quad \mu_4]$$

$$[\nu_5 \quad \nu_8] = \begin{bmatrix} EI(\rho A\Gamma_2\Gamma_3 - \Gamma_4) \\ -\kappa EI(\rho A\Gamma_2\Gamma_3 - \Gamma_4) \\ \kappa^2 I \\ 0 \end{bmatrix} [\mu_3 \quad \mu_4].$$

The only demand on the infinite eigenvectors is that the symmetry of the system should be preserved, this is obtained by chosing

$$[\mu_3 \quad \mu_4] = \begin{bmatrix} 1 & 0 \\ 0 & 1 \end{bmatrix}.$$

Choosing the weighting matrices as described in [Stein, 1979] we obtain the weighting matrices

$$R = \sigma I$$
$$Q = H^T H.$$

Noting that the chosen eigenvectors are linearly independent, H is found by solving the equation

$$H = [0 \quad I \quad 0 \quad 0][\nu_1 \quad \cdots \quad \nu_8]^{-1}$$

which gives

$$H = \begin{bmatrix} 0 \\ \begin{bmatrix} \psi_1(\lambda_f)-\psi_2(\lambda_f) & \psi_2(\lambda_f) \\ \psi_2(\lambda_f) & \psi_1(\lambda_f)-\psi_2(\lambda_f) \end{bmatrix} (\rho A \Gamma_2 \Gamma_3 - \Gamma_4)^{-1} \\ I \\ (\rho AEI\Phi(\rho A\Gamma_2\Gamma_3 - \Gamma_4))^{-1} \end{bmatrix}^T,$$

where

$$\psi_1(\lambda_f) = \lambda_f(\kappa(\rho A\lambda_f + a_{m2}) + p_{c_1}(\lambda_f))$$
$$\psi_2(\lambda_f) = \tfrac{1}{2}\lambda_f EI(\beta_1^4 - \beta_2^4),$$

This, together with the algebraic Riccati equation

$$0 = PA_{ch} + A_{ch}^T P + Q + PB_{ch_1}R^{-1}B_{ch_1}^T P/\sigma \tag{7.8}$$

can be used for finding the feedback matrix

$$L = R^{-1}B_{ch_1}^T P/\sigma.$$

Unfortunately it is difficult to solve the Riccati equation algebraicly and we therefore have to use numerical tools for finding L. An example of the results of the design with closed loop eigenvalues $\lambda_f = 125$, a time constant for the linearized hydraulic systems $\kappa = 50$, and a control weight $\sigma = 1\times10^{-4}$ are shown in Figure 7.2. Note that the two sides are not entirely decoupled,. Full decoupling requires large gains

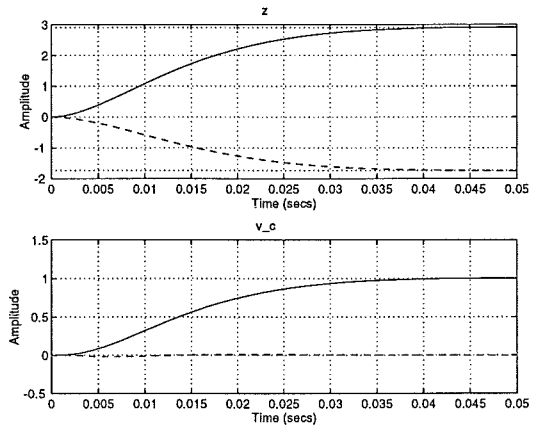

Figure 7.2 Result of eigenspace design, response for step reference change of the thickness at the north edge. Upper plot, full: north position z_n and dashed: south position z_s. Lower plot, full: thickness at north edge v_n and dashed: thickness at south edge v_s. Note that the south thickness is almost unaffected by the change of the thickness at the north edge.

of the feedback matrix. This is not a good idea considering saturation and stability aspects.

When computing the steady state gain of the closed loop system we find that

$$C_{ch}(-A_{ch} + B_{ch_1}L)^{-1}B_{ch_2} \approx I.$$

This indicates that the separation of the two sides has been successful since a reference change for one of the sides does not affect the other side in stationarity.

As stated earlier it is not possible to measure the process output, and we can therefore not use a traditional observer. Instead we use the static relationships found in Section 4.2 and extend it with the position

measurement $\frac{1}{2}z$ and the integral states i

$$\begin{bmatrix} y_e(t) \\ \frac{1}{2}z(t) \\ i(t) \end{bmatrix} = D_{eh} \begin{bmatrix} \frac{1}{2}z(t) \\ f(t) \\ i(t) \end{bmatrix} = \begin{bmatrix} \rho A \Gamma_3 & \Gamma_6 & 0 \\ a_{m2}\Gamma_3 & a_{m2}\Gamma_1\Gamma_6 & 0 \\ I & 0 & 0 \\ 0 & 0 & I \end{bmatrix} \begin{bmatrix} \frac{1}{2}z(t) \\ f(t) \\ i(t) \end{bmatrix}. \quad (7.9)$$

The advantage of this approach is that we capture the variations of a_{m1} using the rolling force measurement. Introducing f_c instead of f and z_h instead of z in (7.9) we find that

$$\begin{aligned} \begin{bmatrix} y_e(t) \\ \frac{1}{2}z_h(t) \\ i(t) \end{bmatrix} &= \Upsilon_o \begin{bmatrix} y_c(t) \\ \frac{1}{2}z_h(t) \\ i(t) \end{bmatrix} \\ &= D_{eh} \begin{bmatrix} 0 & 0 & I & 0 \\ 2KF & 0 & -2K\rho AF\Gamma_3 & 0 \\ 0 & 0 & 0 & I \end{bmatrix} \begin{bmatrix} y_c(t) \\ \frac{1}{2}z_h(t) \\ i(t) \end{bmatrix} \end{aligned} \quad (7.10)$$

which gives the connection between the estimate of the observer and the states of the model. Setting y_e equal to y_c the state space description of the closed loop system is given by

$$\begin{aligned} \left[\begin{array}{c} \dot{y}_c(t) \\ \frac{1}{2}\dot{z}_h(t) \\ i(t) \\ \hline v_c(t) \end{array}\right] &= \left[\begin{array}{c|c} A_{cl} & B_{cl} \\ \hline C_{cl} & D_{cl} \end{array}\right] \left[\begin{array}{c} y_c(t) \\ \frac{1}{2}z_h(t) \\ i(t) \\ \hline r(t) \end{array}\right] \\ &= \left[\begin{array}{c|c} A_{ch} - B_{ch_1}L\Upsilon_o & B_{ch_2} \\ \hline C_{ch} & D_{ch} \end{array}\right] \left[\begin{array}{c} y_c(t) \\ \frac{1}{2}z_h(t) \\ i(t) \\ \hline r(t) \end{array}\right], \end{aligned}$$

which will be used for the stability analysis.

The controller structure is shown in Figure 7.3. Note that the principal structure is the same as the traditional one described in Chapter 3.

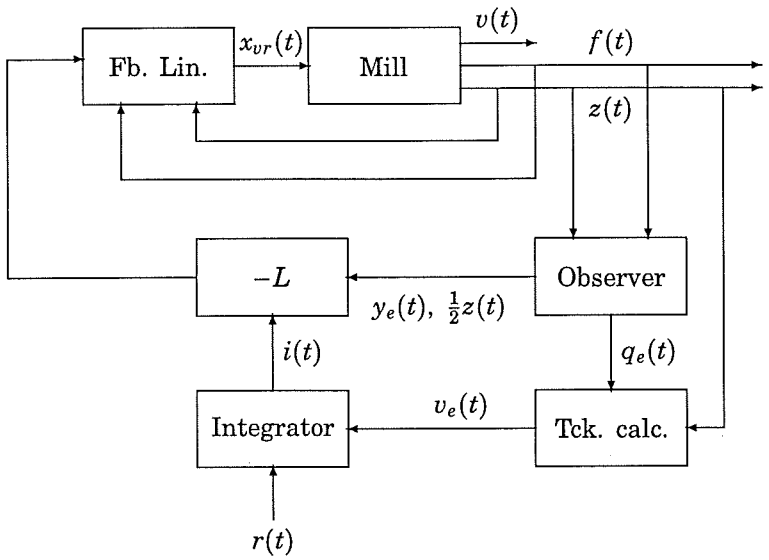

Figure 7.3 The structure of the total controller, including feedback linearization, state feedback and integrator. Note that here the direct term is included when calculating v_e.

7.5 Robustness considerations

Until now we have considered the model as time invariant, but we have already seen that some of the parameters of the model vary with time. In the following analysis we consider variations of the material parameter a_{m1}, the mill spring coefficient $2K$, and the stiffness of the roll pack EI. The variation of a_{m1} and $2K$ is a well known problem in rolling mill control, see the description in Chapter 3. We will here find that they are allowed to vary more than 20% before the stability is affected.

To keep the stability analysis simple we assume that the feedback linearization works well and we can approximate the hydraulic systems with the linear models from the previous section. Further we do not consider the fact that the controller will be implemented in discrete time – if the sampling frequency is large compared to the bandwidth of the system this will be neglectable, see [Åström and Wittenmark, 1990]. We thus work with the linear continuous time state space model for the closed loop system in the following.

We have the time varying parameters:

$$\begin{aligned} a_{m1}(t) &= (1+\delta_p(t))\overline{a}_{m1} \\ 2K(t) &= (1+\delta_m(t))\overline{2K} \\ EI(t) &= (1+\delta_m(t))\overline{EI}, \end{aligned} \tag{7.11}$$

where $\delta_p \in [-r_p, r_p]$ and $\delta_m \in [-r_m, r_m]$. $\overline{a}_{m1}$, $\overline{2K}$, and $\overline{EI}$ are the nominal values of the parameters used for finding the observer. In the following it is assumed that it is the mean values of $2K$ and EI during the pass that are used for finding $\overline{2K}$ and $\overline{EI}$. We vary $2K$ and EI together since we in this way ensure that the eigenfunctions are not affected by the time variations.

It is hard to say anything about the nature of the variations of δ_m and δ_p. Since the variations of the mill spring coefficient $2K$ are mainly caused by variations of the rolling force f and therefore the variations of the material hardness a_{m1}, δ_m varies with δ_p. As seen from the system identification in Chapter 6, a_{m1} contains both high and low frequency variations and it is therefore chosen to do the stability analysis for arbitrary time variations.

The parameter variations can be divided into two main groups:

- large variations over the entire rolling;
- small variations during the pass.

Generally, $2K$ and EI belongs to the last category since it only varies around its mean value while the material hardness a_{m1} belongs to both categories. From the system identification we found that a_{m1} varies $\pm 20\%$ during the pass. For the variations over the entire rolling the maximal value found for $\overline{a}_{m1}$ is 2×10^5 and the minimal value for $\overline{a}_{m1}$ is chosen to be 0 since the thickness also should also be able to handle very soft plates. Using the mill spring curve we find that the mill spring coefficient $2K$ is able to vary $\pm 20\%$ around its mean value for all values of the rolling force f.

The purpose of the stability analysis will be to find bounds on the variations δ_p and δ_m. If these bounds are larger than the actual parameter variations the thickness control system will be stable. The parameter $\overline{a}_{m1}$ varies much during the entire rolling and the thickness control system should be stable for all values of the parameter. The bounds on δ_p and δ_m will therefore be found for all the actual values of $\overline{a}_{m1}$. Normally the thickness control system is detuned to avoid instability, see Chapter 3. Making a proper stability analysis may therefore make it possible to improve the performance of the controller by avoiding the detuning.

To investigate the stability of the system it is sufficient to look at the system matrix for the closed loop system A_{cl}. Using a state transformation it is possible to separate the algebraic Riccati equation (7.8) into two separate equations. It is then easy to show that the state feedback L has the structure

$$L = \begin{bmatrix} l_1 & l_2 & l_3 & l_4 & l_5 & l_6 & l_7 & l_8 \\ l_1 & -l_2 & l_3 & -l_4 & l_6 & l_5 & l_8 & l_7 \end{bmatrix}.$$

Inserting the time varying parameters (7.11) into the model for the rolling stand – the variables of the observer is of course constant –

and using the state transformation matrix

$$T_s = \begin{bmatrix} 1 & 0 & 0 & 0 & 0 & 0 & 0 & 0 \\ 0 & 0 & 1 & 0 & 0 & 0 & 0 & 0 \\ 0 & 1 & 0 & 0 & 1 & 1 & 0 & 0 \\ 0 & 0 & 0 & 0 & 0 & 0 & \frac{1}{2} & \frac{1}{2} \\ 0 & 1 & 0 & 0 & 0 & 0 & 0 & 0 \\ 0 & 0 & 0 & 1 & 0 & 0 & 0 & 0 \\ 0 & 0 & 0 & 0 & 1 & -1 & 0 & 0 \\ 0 & 0 & 0 & 0 & 0 & 0 & \frac{1}{2} & -\frac{1}{2} \end{bmatrix}$$

make it possible to give A_{cl} block diagonal structure. We therefore have two 4×4 matrices

$$A_{cl_1}(t) = \begin{bmatrix} -\frac{a_{m2}}{\rho A} & 1 & 0 & 0 \\ -\frac{a_{m1}(t)+EI(t)\beta_1^4}{\rho A} & 0 & EI(t)\beta 1^4 \gamma_{3_1} & 0 \\ -\frac{2K(t)}{2K}\frac{d_1}{\rho A} & 0 & -\kappa + \delta_m(t)\gamma_{3_1} d_1 - (l_5 + l_6) & -2(l_7 + l_8) \\ -\phi_1 & 0 & 0 & 0 \end{bmatrix}$$

$$A_{cl_2}(t) = \begin{bmatrix} -\frac{a_{m2}}{\rho A} & 1 & 0 & 0 \\ -\frac{a_{m1}(t)+EI(t)\beta_2^4}{\rho A} & 0 & EI(t)\beta 1^4 (\gamma_{3_2} - \gamma_{4_2}) & 0 \\ -\frac{2K(t)}{2K}\frac{d_2}{\rho A} & 0 & -\kappa + \delta_m(t)\gamma_{3_2} d_2 - (l_5 - l_6) & -2(l_7 - l_8) \\ -\phi_2 & 0 & 0 & 0 \end{bmatrix},$$

where

$$d_1 = 2(l_1 \rho A + l_3 a_{m2})$$
$$d_2 = 2(l_2 \rho A + l_4 a_{m2})$$

A simple method for investigating the stability of A_{cl_1} and A_{cl_2} is to use the small gain theorem, see [Desoer and Vidyasagar, 1975]. It is

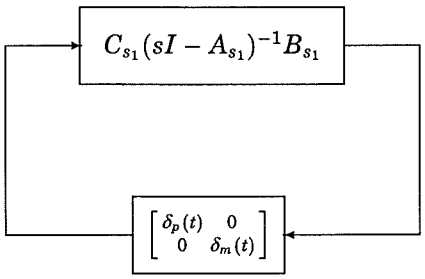

Figure 7.4 The standard representation of a system with time varying parameters. The representation is used in connection with the stability analysis.

possible to implement this stability test using relatively simple numerical routines. Since it only gives sufficient conditions for stability, the bounds found using the small gain theorem can be rather conservative. The conservatism can be reduced by introducing scaling factors in the description of the parameter variations. The stability bounds will further be investigated using simulations.

To be able to use the small gain theorem we first transform A_{cl_1} and A_{cl_2} to a standard form used in stability analysis. This standard representation is a transfer function with a feedback of the time varying parameters, see Figure 7.4. The standard representations of A_{cl_1} and A_{cl_2} are

$$\left[\begin{array}{c|c} A_{s_1} & B_{s_1} \\ \hline C_{s_1} & D_{s_1} \end{array}\right] = \left[\begin{array}{ccccc|cc} -\frac{a_{m2}}{\rho A} & 1 & 0 & 0 & 0 & \\ -\frac{\bar{a}_{m1}+\overline{EI}\beta_1^4}{\rho A} & 0 & \overline{EI}\beta 1^4\gamma_{3_1} & 0 & \frac{\bar{a}_{m1}}{s_1\rho A} & -\frac{\overline{EI}\beta_1^4}{\rho A} \\ -\frac{d_1}{\rho A} & 0 & -\kappa-(l_5+l_6) & -2(l_7+l_8) & 0 & -\frac{d_1}{\rho A} \\ -\phi_1 & 0 & 0 & 0 & 0 & 0 \\ \hline -s_1 & 0 & 0 & 0 & 0 & 0 \\ 1 & 0 & -\rho A\gamma_{3_1} & 0 & 0 & 0 \end{array}\right] \tag{7.12}$$

$$\left[\begin{array}{c|c} A_{s_2} & B_{s_2} \\ \hline C_{s_2} & D_{s_2} \end{array}\right] =$$

$$\left[\begin{array}{cccc|ccc} -\frac{a_{m2}}{\rho A} & 1 & 0 & 0 & 0 & 0 & 0 \\ -\frac{\overline{a}_{m1}+\overline{EI}\beta_2^4}{\rho A} & 0 & \overline{EI}(\beta 2^4\gamma_{3_2}-\gamma_{4_2}) & 0 & \frac{\overline{a}_{m1}}{s_2\rho A} & -\frac{\overline{EI}(\beta_2^4-\frac{\gamma_{4_2}}{\gamma_{3_2}})}{\rho A} & \frac{\overline{EI}\gamma_{4_2}}{\rho A\gamma_{3_2}} \\ -\frac{d_2}{\rho A} & 0 & -\kappa-(l_5-l_6) & -2(l_7-l_8) & 0 & -\frac{d_2}{\rho A} & 0 \\ -\phi_2 & 0 & 0 & 0 & 0 & 0 & 0 \\ \hline -s_2 & 0 & 0 & 0 & 0 & 0 & 0 \\ 1 & 0 & -\rho A\gamma_{3_2} & 0 & 0 & 0 & 0 \\ -1 & 0 & 0 & 0 & 0 & 0 & 0 \end{array}\right] \tag{7.13}$$

s_1 and s_2 are scaling factors used for finding the least conservative estimate for the stability bounds.

Using the small gain theorem and ensuring that A_{s_1} is stable for all nominal values of a_{m1}, we will have stability for the arbitrary time variations δ_p and δ_m if

$$\gamma_1 \geq \sup_{s=j\omega} \overline{\sigma}\left(C_{s_1}(sI - A_{s_1})^{-1}B_{s_1}\right)$$

$$\gamma_2 \geq \max(\sup_t |\delta_m(t)|, \sup_t |\delta_p(t)|)$$

$$\gamma_1\gamma_2 < 1,$$

where $\overline{\sigma}$ denotes the maximal singular value. When γ_1 has been found the bound on the δ_m and δ_p are found by setting $\gamma_2 = 1/\gamma_1$. The results will in principle be the same for the other system and they are therefore not shown here.

That A_{s_1} is stable is ensured by computing the eigenvalues of the matrix for the values of $\overline{a}_{m1}$ used in the stability analysis. The norm for finding γ_1 can be calculated using the state space description and MATLAB. If such advanced numerical tools are not available it is possible to use the Frobenius norm which is the square root of the sum of squares of the numerical values of the elements of the transfer function matrix. The result will be a polynomial which can be evaluated using simpler tools. The Frobenius norm is more conservative than the above, but is not found to be of major importance in this case.

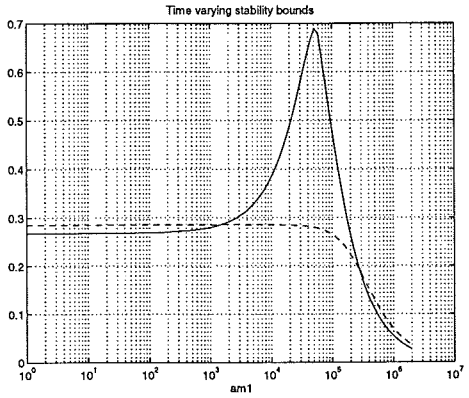

Figure 7.5 The limits on the variations of δ_p and δ_m. Full: the limit for A_{s_1} and dashed: the limit for A_{s_2}.

Using the small gain theorem on (7.12) and (7.13) we find the results shown in Figure 7.5. The figure shows γ_2 as a function of the nominal value of the plate hardness $\overline{a}_{m1}$. To cover also very hard plates the maximal value of the analysis has been chosen to 2×10^6 even if the maximal value found in the identification is 2×10^5. The best choice of the scaling factors have been found to be $s_1 = 1.5$ and $s_2 = 1$. Simulations show that for $a_{m1} = 5 \times 10^4$ the system will be stable for $\delta_m = 0.2$ and unstable for $\delta_m = 0.3$, this indicates that the results not are very conservative.

The results of Figure 7.5 shows that the system is stable for all mean values of the plate hardness during the pass $\overline{a}_{m1} \in [0, 2 \times 10^5]$ found in the system identification. It is seen from the figure that $\overline{a}_{m1} > 2 \times 10^5$ smaller and smaller variations of δ_m and δ_p are permitted. When $\overline{a}_{m1}$ is large the plate is cold and we can here also expect large temperature variations during the pass, it is therefore not sure that the control will be stable when the plate is very hard. It should be mentioned that it is likely that the plate will be rejected due to poor metallurgical properties when the plate hardness $\overline{a}_{m1}$ is above the values found in the system identification. The above results indicate that it will not

be necessary to detune the thickness compensation system. This will make a better thickness control possible.

7.6 Evaluation of performance

Several questions can be asked in connection with the performance of the thickness control. The two usual main concerns are:

- response to reference changes;
- effects of typical disturbances.

Both subjects will be investigated in the following. The performance of the new control system will be compared to the performance of the existing control system, when possible. A central question is whether it is necessary to redesign the controller and how often this should be done. This will also be investigated below. Again we simulate the whole system in continuous time, that is we assume that the control law is implemented using a high sampling frequency.

The linear transfer functions for the existing controllers for the hydraulic systems and the thickness controller used in the computer simulations have been provided by the constructor of the control system on the rolling mill at The Danish Steel Works. To be able to compare the new and existing controllers the existing control is adjusted to compensate fully for the mill spring.

The feedback linearization is implemented using the mean values of the parameters for the north and south sides. To keep the implementation simple $\frac{d}{dt}f$ is found using $\frac{d}{dt}q_c$ from the model used for simulating the rolling stand.

Simulations

To investigate the response to reference changes and the effect of typical disturbances we will perform a number of simulations using the simulation model described in Chapter 6. The dynamics, static gain, and the decoupling of the two sides can be investigated using a step change of the reference at one and both sides. Even if the integrator ensures that the static gain is unity despite the variations of the plate

hardness a_{m1}, the dynamics of the system varies with this parameter. From the system identification it is found that $a_{m1} \in [2\times10^4,\ 2\times10^5]$. The controller is designed for $a_{m1} = 5 \times 10^4$. It is therefore chosen to simulate the responses for mean values of the plate hardness $\overline{a}_{m1} = \{2\times10^4,\ 5\times10^4,\ 2\times10^5\}$ to investigate the effects of the parameter variations on the dynamics of the closed loop system and the decoupling of the two sides. The above values of $\overline{a}_{m1}$ can be considered representative for the values where it is important that the thickness control operates well.

The simulations of changes of the thickness reference at both sides and at one side subsequently are shown in Figures 7.6 and 7.7. It is chosen to show the control signals for the servo valves x_{vr} and the plate thicknesses at the edges v_c. The reference at both sides r is changed from 11.64 mm to 10.5 mm at $t = 0$ s and the reference at the north side r_n is changed from 10.5 to 10.25 at $t = 0.5$ s. Since it is not possible to control the two sides independently with the existing control system, r_n is not changed at $t = 0.5$ in this case.

From the simulations of the reference changes it is seen that the magnitudes of the control signals are similar. The existing control system is less damped and has a considerably longer settling time than the new one. Furthermore the integrator of the existing control is considerably slower, which is not desirable. It should be noted here that the existing control system is tuned on line and it might turn out that the less damped dynamics are desirable here. It will be natural to investigate this in connection with the implementation of the control system.

From Figure 7.7 it is seen that the time constant of the new control system varies quite much with the plate hardness a_{m1}. The separation of the two sides works well when the value for $\overline{a}_{m1}$ used for the design. In the other cases the thickness at the south side varies a couple of hundredths of a mm when the thickness at the north sides is changed. The damping of the control system is satisfactory for all three values of $\overline{a}_{m1}$. Since the limits on the control signal are the same for all values of a_{m1}, not much will be gained from redesigning the controller.

From the above simulations we conclude that it is not necessary to redesign the controller because of the variations of a_{m1} unless very hard demands on damping and separation of the two sides are present.

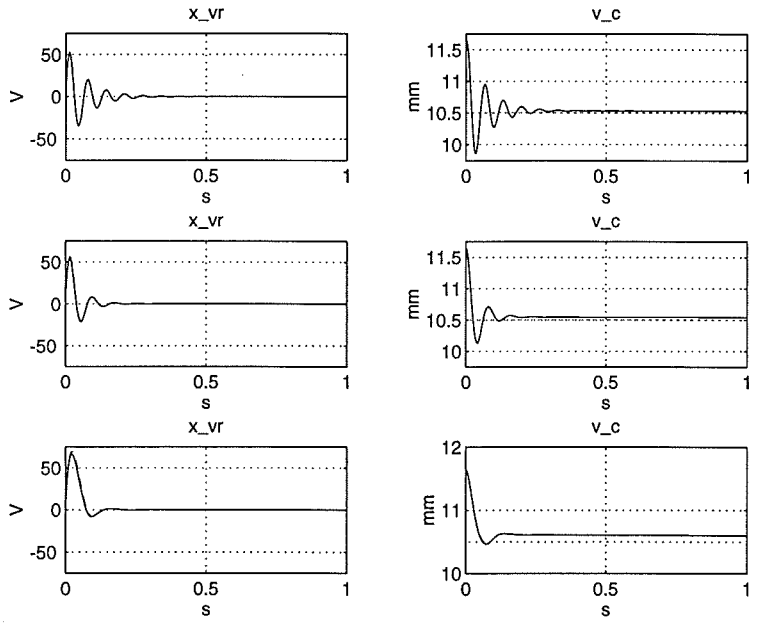

Figure 7.6 Simulation of the existing control system. A step change of the thickness references for both sides to 10.5 mm is done at $t = 0$. Left plots, full: control signal for north servo valve x_{vrn} and dashed: control signal for north servo valve x_{vrs}. Right plots, full: the thickness at the north edge v_{c_n} and dashed: the thickness at the south edge v_{c_s}. The top plots show a simulation for a soft plate and the lower plot a simulation for a hard plate. The plots in the middle are for the value used for the design of the eigenspace controller. Since we are not able to change the thickness at only one side two responses are similar and can therefore not be distinguished. It is seen that it will take a while before the thicknesses reach the desired value of 10.5 mm.

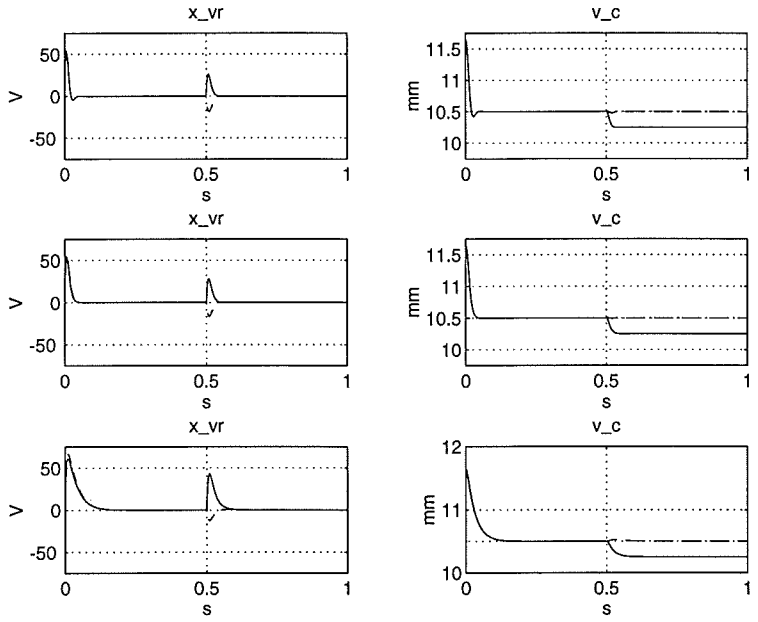

Figure 7.7 Simulation of the new control system. A step change of the thickness references for both sides to 10.5 mm is done at $t = 0$, and a step change of the thickness reference for the north side is done at $t = 0.5$. Left plots, full: control signal for north servo valve x_{vrn} and dashed: control signal for north servo valve x_{vrs}. Right plots, full: the thickness at the north edge v_{c_n} and dashed: the thickness at the south edge v_{c_s}. The top plots show a simulation for a soft plate and the lower plot a simulation for a hard plate. The plots in the middle are for the value used for the design of the eigenspace controller.

Note that, because of the variation of the model parameters with the plate width w, it will only be necessary to design the controller when w changes. Since the plate width does not change significantly during the rolling of one plate, it will only be necessary to redesign the controller once for each plate.

We now proceed with investigating the effects of the variations of a_{m1} during the pass. As mentioned before these variations mainly consist of slow variations due to cold zones from the reheat furnaces and fast variations from the cooling by the roller tables. It is here chosen to use step changes of the plate hardness to be able to investigate the dynamics and the steady state characteristics of the response to the variations of the plate hardness a_{m1}. The variations of a_{m1} are divided into

- changes in the mean value;
- changes in the value across the plate width.

In the first type of variations the symmetry of the rolling process is preserved, this is not the case for the second type of variations.

In the modeling in Chapter 5 it is assumed that material characteristics are symmetric, but it is quite easy to introduce asymmetric material conditions in the model for the rolling stand. This can be done assuming that that the plate hardness across the plate width is

$$a_{m1}(x,t) = a_{m1}(t)\left(1 + \tau(t)\frac{2x-w}{w}\right),\ x \in [0,\ w].$$

The last term represent a linear variation of the plate hardness across the plate width and τ is a unit step. Inserting the above in the model we find that the only thing that changes is Γ_1 which becomes

$$\Gamma_1(t) = \begin{bmatrix} \frac{1}{\rho A} & \tau(t)\int_0^w \phi_2(x)\frac{2x-w}{w}dx \\ \tau(t)\int_0^w \phi_2(x)\frac{2x-w}{w}dx & \frac{1}{\rho A} \end{bmatrix}.$$

Inserting the above in the simulation program we are able to investigate the effects of asymmetric material conditions.

The simulations of the variations of the plate hardness a_{m1} during the pass are shown in Figures 7.8 and 7.9. Again the simulations are

done for mean values $\overline{a}_{m1} = \{2 \times 10^4,\ 5 \times 10^4, 2 \times 10^5\}$ to investigate the responses for different plate hardnesses. The reference is changed from 11.64 mm to 10.5 mm at $t = 0$, a_{m1} is changed to $0.8a_{m1}$ at $t = 0.5$ and τ is changed from 0 to 0.2 at $t = 1$. The variations of mean value and the skewness of a_{m1} are both set to 20%, this is inspired by the system identification where we found that a_{m1} varies ±20% in the length direction. Similar variations are expected in the width direction. In the traditional controller the start value of the plate thickness differs from 10.5, this is due to the rather slow integrator.

From the simulations we see that the impact of the hardness variations is most significant for large plate hardnesses a_{m1}. For $\overline{a}_{m1} = 2 \times 10^4$ the effect of the variations are hardly noticeable, for $\overline{a}_{m1} = 5 \times 10^4$ they have some effects on the plate thickness, and for $\overline{a}_{m1} = 2 \times 10^5$ they have a major impact on the plate thickness. The settling time and damping of new control is better than for the traditional control. Again similar values of the control signal are used for the new and the existing control.

Note that the new control is able to handle the asymmetric material conditions while the traditional controller is not. Generally, it is for the thin, and therefore hard, plates the most strict demands on the plate thickness are present and the deviations shown for the traditional controller will result in a rejection of the plate. Additional problems with different length of the plate edges and the following problems with the plate shape can also be expected.

More simulations to investigate the effects of variations of the mill spring coefficient $2K$ and the roll stiffness EI could be done. The variations of these parameters do not affect the symmetry of the rolling process. Furthermore, the variations mostly affect the estimation of the plate thickness and the responses of the new and existing control systems will therefore be similar. It is therefore chosen not to show the simulations of this case.

7.7 Summary

We have designed new controllers for the hydraulic positioning systems and the rolling stand. The hydraulic systems are linearized using feed-

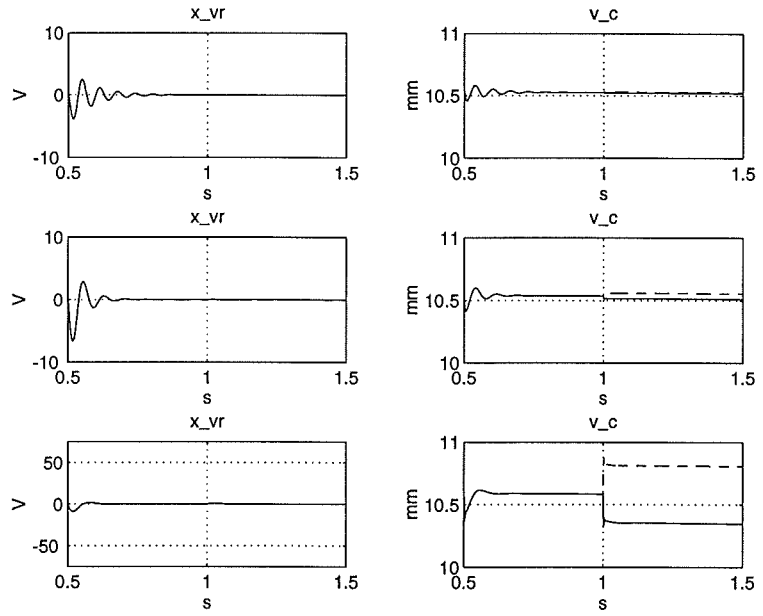

Figure 7.8 Simulation of the existing control system with a desired thickness of 10.5 mm. A step change of the mean value of the plate hardness a_{m1} is done at $t = 0.5$ and asymmetric hardness conditions are introduced by a step change of τ at $t = 1$. Left plots, full: control signal for north servo valve x_{vrn} and dashed: control signal for north servo valve x_{vrs}. Right plots, full: the thickness at the north edge v_{c_n} and dashed: the thickness at the south edge v_{c_s}. The top plots show a simulation for a soft plate and the lower plot a simulation for a hard plate. The plots in the middle are for the value used for the design of the eigenspace controller.

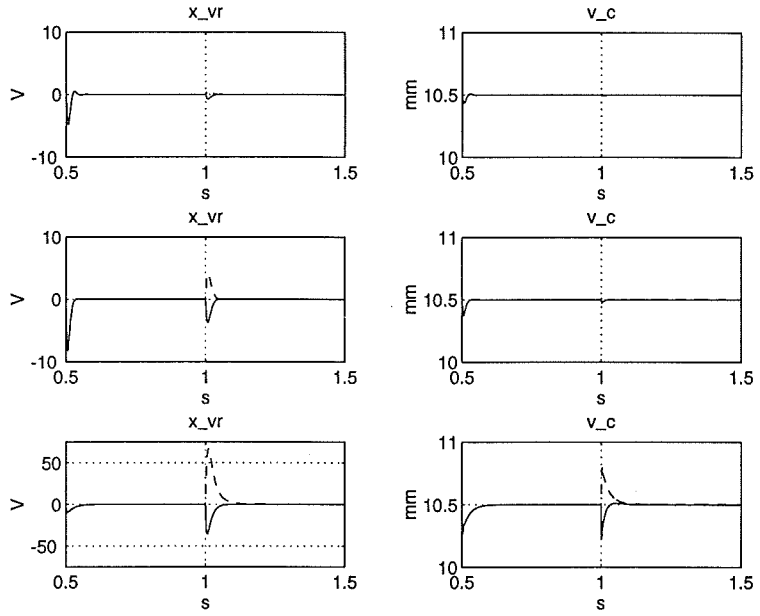

Figure 7.9 Simulation of the new control system with a desired thickness of 10.5 mm. A step change of the mean value of the plate hardness a_{m1} is done at $t = 0.5$ and asymmetric hardness conditions are introduced by a step change of τ at $t = 1$. Left plots, full: control signal for north servo valve x_{vrn} and dashed: control signal for north servo valve x_{vrs}. Right plots, full: the thickness at the north edge v_{c_n} and dashed: the thickness at the south edge v_{c_s}. The top plots show a simulation for a soft plate and the lower plot a simulation for a hard plate. The plots in the middle are for the value used for the design of the eigenspace controller.

back linearization and included in the model for the rolling stand. A state feedback for the now linear system is designed using eigenspace control. The main objective in connection with the eigenspace design is to separate the response of the thicknesses at the two sides. The dynamics of the new control system are chosen to obtain the same magnitude of the control signals as used by the existing controller. To ensure that the steady state gain of the system will be unity despite the variations of the material parameters two integral states are introduced in the controller.

The stability of the linear control system is investigated and it is found that it will be stable for the expected parameter variations. The performance of the new and existing control systems are compared using simulations. It is found that the dynamic performance of the new control system is better than the one of the traditional control system. The new control system is, furthermore, able to handle asymmetric material conditions and differences in the thickness references for the two sides, this is not the case with the existing control system.

8

Conclusions

As stated in the introduction the main purposes of this report are to develop a physical model for the hot rolling process, to find the parameters of this model, and to design a controller for the thickness control on the basis of the model. This has all been done and it is now time for making the final conclusions.

8.1 What has been done?

The main effort has been spent on developing the model for the rolling mill and identifying the parameters of this model. As stated in the introduction, the modeling is a recursive procedure and after the first iteration several changes of the model were necessary to obtain proper results. Since there are many things to vary in the model and in the way of doing the system identification, it is a complicated procedure to find the right set-up. The model and the results of the system identification shown in the report are the result of one and a half years work. Both the literature study to find the state of the art and the controller design have taken half a year to complete each. It is therefore natural that we are able to conclude the most from the modeling and identification part of the thesis.

The model developed is dynamical and multivariable, as stated in the introduction. The model is found by dividing the hot rolling mill into two subsystems:

- the hydraulic positioning systems;

- the rolling stand.

and building physical models for how these systems work. The mathematical descriptions of the subsystems are found from these physical models. The models for the positioning systems are nonlinear while the model for the rolling stand is linear. Since it is not possible to measure the plate thickness and an additional signal is available when implementing the controller, a thickness observer is built in addition to the model to be used for the controller design. Because physical modeling is used, the number of unknown parameters of the models for the subsystems are kept at a minimum.

It was chosen to collect the data for the system identification during normal operation of the rolling mill. Since it is not possible to measure the plate thickness during rolling, it was necessary to measure the inputs when the plate was rolled and the output – the plate thickness – after the rolling. A large number of data were necessary to obtain proper measurements for the system identification and a device for measuring and recording the thickness was therefore designed and constructed by the author. The input measurements and the thickness measurements have been joined by formulating and solving an optimization problem. It is believed that these collected data are unique and have made it possible to obtain a good model.

The parameters of the two submodels for the rolling mill are found using the collected data. Using nonlinear system identification a set of constant nominal parameters are found for the hydraulic positioning systems, where good agreement between model and data is obtained. Due to the time variant nature of the mill stand, there is poor agreement between model and data when time invariant methods are used for the system identification. The parameter values obtained can be seen as a mean value for that pass and they are well correlated with a theoretically found plate hardness. Using a time varying value of the parameter found using recursive system identification good agreement between model and data were obtained. Since the time variations are included in the extra signal available for the observer, good agreement between model and data is obtained in this case.

Analyzing the models for the rolling mill, it is found that the dynamics of the mill stand are considerably faster than the dynamics of the

hydraulic positioning systems. This means that it will be hard to compensate for the fast variations of the plate thickness using the hydraulic positioning systems. Using methods suitable for handling nonlinear and multivariable systems a controller for the thickness control is found. The controller is designed to use the same control effort as the existing equipment on the rolling mill at The Danish Steel Works. Using computer simulations it is found that the new controller is able to handle the asymmetric case and yields a more accurate thickness control compared to the existing control system. The new control strategy is furthermore found to be stable for the relevant parameter variations. The performance is also acceptable for the different material characteristics of the steel plate found in the system identification.

Seen in the light of my work the existing control system performs quite well. The existing observer is able to predict the thickness quite accurately and the controller appears well tuned. Since it has been found that the rolling stand is considerably faster than the hydraulic systems the static models for the rolling stand also works well. If a controller yielding a faster response of the hydraulic systems was introduced, dynamic models of the rolling stand could be used to do a better design. The main disadvantage of the existing system is therefore that it is not able to handle the asymmetric case.

One should recognize, that besides the development of mathematical models and controllers, additional knowledge and understanding of the hot rolling process have been gained in connection with this work. We were, for instance, surprised by the impact of the parameter variations on the plate thickness. The main factor was the temperature variations induced by inhomogeneous cooling by the roller tables used for transporting the plates. These variation are too fast to be handled by the thickness control and therefore additional precautions are necessary to remove these disturbances.

One major problem in connection with the system identification of the model for the rolling stand is the lack of excitation in the input signals. This is the price paid for using data collected during normal operation. To obtain data with a better excitation additional experiments are necessary. This needs careful planning and will induce additional costs, but will yield an additional verification of the model.

8.2 Future work

In my opinion there are two main directions of further work:

- improving the model for the rolling stand;
- using the results in practice.

The physical model used, only covers a few main features of the rolling stand and many improvements of the model are therefore possible. For instance, introduction of a more advanced model for the material, including models of the friction in the rolling mill, identifying the asymmetric material characteristics, and getting data with better dynamic and asymmetric excitation would all result in an improvement of the model. Better models for the noise and disturbance characteristics of the rolling stand would also be a helpful tool in improving the performance of the control system.

As suggested in the system identification in Chapter 6, inclusion of an extra spring in the physical model will also yield a possible improvement of the results. Furthermore, explicit handling of the time variations in the modeling, system identification and controller design would also be a good idea.

The responses of the plate thickness at the north and south sides of the rolling mill are separated by the controller design. Besides the handling of the asymmetric material conditions this can also be used for controlling the plate shape in the length direction. This is due to the fact that the length of the plate edges is dependent of the thickness reduction at the edges. One one way of implementing the straightness control is to measure the plate straightness using a camera and then using this measurement for finding the references for the thicknesses at the edges.

As mentioned in the introduction it is not straight forward to implement the controller. Much additional work is needed to do this. An other way of using the model is to use it for optimizing the adjustment of the existing control system. This can for instance be done by using the methods described in [Abildgaard, 1991]. Additional improvements can be done by removing the high frequency disturbances induced by the cooling of the roller tables. This can be done by implementing a

different control strategy for the roller tables.

9

Bibliography

Abildgaard, O. (1991): *Issues in Unified Optimization of Systems and Controllers.* PhD thesis, Control Engineering Institute, Technical University of Denmark.

Andersson, M. (1994): *Object-Oriented Modeling and Simulation of Hybrid Systems.* PhD thesis, Department of Automatic Control, Lund Institute of Technology.

Asada, Y. *et al.* (1986): "New feed forward gauge control method for cold tandem mills." *IFAC Proceedings of the 1986 automation in mining mineral and metal processing conference.*

Åström, K. J. and P. Eykhoff (1971): "System identification – a survey." *Automatica*, **7**, pp. 123 – 162.

Åström, K. J. and B. Wittenmark (1990): *Computer Controlled Systems.* Prentice-Hall.

Åström, K. J. and B. Wittenmark (1995): *Adaptive control.* Addison-Wesley Publishing Company.

Atori, H. *et al.* (1992): "Application of two-degree-of-freedom control system to automatic gauge control." *American Control Conference.*

Bellman, R. and K. J. Åström (1970): "On structural identifiabillity." *Mathematical Biosciences*, **7**, pp. 329 – 339.

Bengtsson, G. (1994): *Manual for μ-controller.* First Control Systems AB, Västerås, Sweden.

Bryant, G. F., P. D. Spooner, and J.M.Caley (1975): "Design of tandem mill dynamic control schemes." *Proceedings of the 5th IFAC world congress.*

Burr-Brown Corporation, Tucson, Arizona, USA (1986): *The Burr-Brown PCI-20000 personal computer intelligent instrumentation system*, 1.9 edition.

Choi, S. G., M. A. Johnson, and M. J. Grimble (1994): "Polynomial lqg control of back-up-roll eccentricity gauge variations in cold rolling mills." *Automatica*, **30:6**, pp. 975–992.

Crandall, S. H., N. C. Dahl, and T. J. Lardner (1978): *An Introduction to the Mechanics of Solids.* McGraw Hill.

Cumming, I. G. (1972): "On-line identification of a steel mill." *Automatica*, **8**, pp. 531 – 541.

Davies, D. A. *et al.* (1983): "Control of gage, width, profile and shape on rautatuukki's 3.6-meter plate mill." *Iron and Steel Engineer*, December.

Desoer, C. A. and M. Vidyasagar (1975): *Feedback Systems: Input-Output Properties.* Academic Press.

Edwards, W. J. (1978): "Design of entry strip thickness controls for tandem cold mills." *Automatica*, **14**, pp. 429–441.

Edwards, W. J. *et al.* (1987): "Roll eccentricity control for strip rolling mills." *Proceedings of the IFAC 10th Triennial World Congress.*

Fenner, R. T. (1989): *Mechanics of Solids.* Blackwell Scientific Publications.

Ferguson, J. J. *et al.* (1986): "Modern hot-strip mill thickness control." *IEEE Transactions on industry applications 1986*, September/October.

Foda, S. and P. Agathoklis (1992): "Control of the metal rolling process. a multidimensional system approach." *Journal of the Franklin Institute*, **329:2**, pp. 317–332.

Fujii, S. and M. Saito (1975): "A new mathematical model for plate mill control." *Proceedings of the 5th IFAC world congress.*

Ginzburg, V. B. (1984): "Dynamic characteristics of automatic control system with hydraulic actuators." *Iron and Steel Engineer.*

Gou, R.-M. (1991): "Evaluation of dynamic characteristics of hagc system." *Iron and Steel Engineer*, July.

Grewal, M. S. and K. Glover (1976): "Identifiability of linear and nonlinear dynamical systems." *IEEE Transactions on Automatic Control*, December, pp. 833 – 837.

Grimble, M. J. and M. A. Johnson (1988): *Optimal Control and Stocastic Estimation. Theory and Applications.*, volume II, chapter 13.4 Gauge Control and the Back-up Roll Eccentricity Problem. John Wiley & Sons.

Guo, R.-M. (1994): "Material damping effect in cold rolling process." *Iron and Steel Engineer*, December.

Gustavsson, I. (1975): "Survey of applications of identification in chemical and physical processes." *Automatica*, **11**, pp. 3–24.

Gustavsson, I. *et al.* (1977): "Identification of processes in closed loop – identifiability and accuracy aspects." *Automatica*, Vol. 13, pp. 59 – 75.

Hansen, E. B. (1993): *Variationsregning (Eng: Calculus of Variations).* Polyteknisk Forlag.

Harvey, C. A. and G. Stein (1978): "Quadratic weights for asymptotic regulator properties." *IEEE Transactions on Automatic Control*, **AC-23:3**, pp. 378 – 387.

Huzyak, P. and T. L. Gerber (1984): "Design and application of hydraulic gap control systems." *Iron and Steel Engineer*, August.

Johansson, R. (1993): *System Modeling and Identification.* Prentice Hall.

Kailath, T. (1980): *Linear Systems.* Prentice-Hall.

Kitamura, A. *et al.* (1987): "Recursive identification technique for roll eccentricity control." *IFAC Proceedings of the 10th Triennial World Congress.*

Kokai, K. *et al.* (1985): "Factors affecting the accuracy of plate tickness and their influences on plate flatness." *Transactions ISIJ, vol. 25.*

Ljung, L. (1991): *System Identification Toolbox.* The Math Works, Inc.

Meirovitch, L. (1980): *Computational Methods in Structural Dynamics.* Sijthoff & Noordhoff.

Middleton, R. H. and G. G. Goodwin (1990): *Digital Control and Estimation. An Unified Approach.*, chapter 15 An Industial Case Study. Prentice Hall.

Mizuno, K. "Multivariable nonlinear control system design for multistand rolling mill." *Hitachi Review.*

Moore, B. C. (1976): "On the flexibility offered by state feedback in multivariable system beyond closed loop eigenvalue assignment." *IEEE Transactions on Automatic Control*, October, pp. 689 – 692.

Nakagawa, S. *et al.* (1990): "Gauge control system for hot strip finishing mill." *Proceedings of the IEEE Conference on Decision and Control, vol. 3.*

Nishikawa, Y. *et al.* (1986): "Advanced control in hot strip finishing mill." *IFAC Proceedings of the 1986 automation in mining mineral and metal processing conference.*

Paul, F. W. (1975): "A mathematical model for evaluation of hydraulic controlled cold rolling mills." *Proceedings of the 5th IFAC world congress.*

Pedersen, L. M. (1993): "Plate thickness control of hot rolling mills." Technical Report ISRN LUTFD2/TFRT--7513--SE, Department of Automatic Control, Lund Institute of Technology.

Pedersen, L. M. (1994): "Identification of hydraulic system on rolling mill." In *Preprints ot the 10th IFAC Symposium on System Identification*, volume 3, pp. 337 – 342.

Pedersen, L. M. (1995): "Modeling and identification of hot rolling mill." In *Proceedings of 1995 American Control Conference*, volume 5, pp. 3674 – 3678.

Pedersen, L. M. (1996): "Multivariable model for a hot rolling mill.". The Institute of Materials. To appear at the conference "The Control of Profile and Flatness" 1996.

Pedersen, L. M. and B. Wittenmark (1996): "Multivariable controller design for hot rolling mill." Submitted for IFAC '96 in San Francisco.

Roberts, W. L. (1983): *Hot Rolling of Steel*, volume 10 of *Manifacturing Engineering and Materials Processing*. Marcel Dekker.

Saito, M. *et al.* (1981): "High-accuracy plate thickness control." *Proceedings of the IFAC 8th Triennial World Congress.*

Slotine, J.-J. E. and W. Li (1991): *Applied Nonlinear Control.* Prentice Hall, Inc.

Stein, G. (1979): "Generalized quadratic weights for asymptotic regulator properties." *IEEE Transactions on Automatic Control*, **AC-24:4**, pp. 559 – 565.

Stone, M. D. (1969): "Backup roll bending – for crown and gauge control." *Iron and Steel Engineer*, December, pp. 69 – 87.

Teoh, E. K., G. C. Goodwin, W. J. Edwards, and R. G. Davies (1984): "An improved strip thickness controller for a rolling mill." *Proceedings of the IFAC 9th Triennial World Congress, vol. 4.*

Trostmann, E. (1987): *Hydraulisk Styring (Eng: Hydraulic Control).* Instituttet for Styreteknik, DTH.

Wood, G. E. *et al.* (1977): "Mill modulus variation and hysteresis – their effect on hot strip mill agc." *Iron and Steel Engineer*, January.

Yamashita, A., Y. Misaka, N. Hase, and R. Takahashi (1976): "Development of feed formward agc for 70" hot strip mill at kashima steel works." *The Sumitomo Search, no. 16*, November, pp. 34–39.

Yeh, T.-H. *et al.* (1991): "The development of new backup roll eccentricity compensation system for the plate mill." *China Steel; Technical Report.*

Zeltkalns, A. *et al.* (1977): "Force sensing in rolling mills." *Iron and Steel Engineer*, January.

A

Notations

A: cross sectional area of roll pack
A_1: area of common piston corresponding to p_1
A_2: area of common piston corresponding to p_2
A_3: area of common piston corresponding to f_n/A_4
A_4: area of grease piston
A_c, B_c, C_c, D_c: state space matrices for model for rolling stand
A_{ch}, B_{ch}, C_{ch}, D_{ch}: extended model for rolling stand
A_{cl}, B_{cl}, C_{cl}, D_{cl}: closed loop system for new thickness control
A_{s_1}, B_{s_1}, C_{s_1}: matrices used in stability analysis
A_{s_2}, B_{s_2}, C_{s_2}: matrices used in stability analysis
$C_v(p)$: transfer function for existing thickness controller
$C_z(p)$: transfer function for existing position controller
D_e: matrix for static observer used for estimating y_c
D_{eh}: observer for estimating states of extended model
E: Youngs modulus for steel
F: matrix used for calculating f_c
$G_h(p)$: transfer function for hydraulic systems controlled by C_z
$G_t(p) = \frac{G_h(p)C_v(p)}{1+G_h(p)C_v(p)}$
I: second moment of area for the work roll
$K(f,w)$: mill spring coefficient
$\overline{K}(f,w)$: estimate of K
L: state feedback matrix for new thickness controller

P_s: supply oil pressure for hydraulic systems
Q: weighting matrix for states in eigenspace design
$Q_1(t)$: flow into left side of oil cylinder
$Q_2(t)$: flow into right side of oil cylinder
R: weighting matrix for control signal in eigenspace design
$T(t)$: plate temperature
$\Gamma_1, \ldots, \Gamma_6$: matrices found in the modeling of the rolling stand
Φ: matrix used for calculating v_c and v_e
β_1, β_2: solution of equation for finding ϕ_1 and ϕ_2
δ: unit pulse
$\delta_m(t)$: variable describing variations of EI and K during pass
$\delta_p(t)$: variable describing variations of a_{m1} during pass
$\varepsilon(x)$: function used in state transform to obtain u
$\varepsilon(t)$: prediction error for model for rolling stand
$\varepsilon_n(t)$: prediction error for model for north hydraulic system
$\varepsilon_s(t)$: prediction error for model for south hydraulic system
η: scaling factor for $\overline{P}_s$ to find p_2
γ_{ij}: $(j, 1)$ entry of Γ_i
$\grave{G}_{q_c}(p)$: transfer function relating q_{c_2} to $\grave{z}$
$\grave{G}_{v_c}(p)$: transfer function relating $\grave{v}_c$ to $\grave{z}$
$\grave{\omega}_n$: undamped natural frequency for $\grave{G}_{v_c}$
$\grave{f}(t) = \frac{1}{2}(f_n(t) - f_s(t))$
$\grave{k}_g$: steady state gain for $\grave{G}_{v_c}$
$\grave{v}_c(t) = \frac{1}{2}(v_{c_n}(t) - v_{c_s}(t))$
$\grave{z}(t) = \frac{1}{2}(z_n(t) - z_s(t))$
$\hat{u}(x, t)$: approximate solution for u
κ: time constant for feedback linearized hydraulic systems
λ_1, λ_2: eigenvalues for finite eigenvectors
λ_f: desired finite eigenvalues for the new thickness control
μ: distance from edge for output thicknesses
μ_1, μ_2: vectors used to obtain the desired finite eigenvectors
μ_3, μ_4: vectors used to obtain the desired infinite eigenvectors
ν_1, ν_2: finite closed loop eigenvectors for rolling stand

$v_3, \ldots, v_8$: infinite closed loop eigenvectors for rolling stand
ω_{nh}: undamped natural frequency for G_h
$\overline{EI}$: mean value of EI during a pass
$\overline{G}_{f_c}(p)$: transfer function relating $\overline{f}_c$ to $\overline{z}$
$\overline{G}_{q_c}(p)$: transfer function relating q_{c_1} to $\overline{z}$
$\overline{G}_{v_c}(p)$: transfer function relating $\overline{v}_c$ to $\overline{z}$
$\overline{K}$: mean value of K during a pass
$\overline{P}_s$: oil supply pressure transformed to grease side
$\overline{\omega}_n$: undamped natural frequency for $\overline{G}_{v_c}$
$\overline{a}_{m1}$: mean value of a_{m1} during a pass
$\overline{f}(t) = \frac{1}{2}(f_n(t) + f_s(t))$
$\overline{f}_c(t) = \frac{1}{2}(f_{c_n}(t) + f_{c_s}(t))$
$\overline{k}_g$: steady state gain for $\overline{G}_{v_c}$
$\overline{r}(t)$: reference value for $\overline{v}$ in traditional control
$\overline{v}(t) = \frac{1}{2}(v_n(t) + v_s(t))$
$\overline{v}_c(t) = \frac{1}{2}(v_{c_n}(t) + v_{c_s}(t))$
$\overline{v}_e(t)$: estimate of $\overline{v}$
$\overline{v}_{-1}(t) = \frac{1}{2}(v_{-1n}(t) + v_{-1s}(t))$
$\overline{z}(t) = \frac{1}{2}(z_n(t) + z_s(t))$
$\overline{z}_r(t)$: reference for $\overline{z}$ in traditional thickness control
$\phi_1(x)$, $\phi_2(x)$: eigenfunctions obtained in series expansion of u
ρ: mass density of steel
σ: scalar control weight in eigenspace design
θ: correction for roll crown
$\varphi(t) = \frac{K(f,w)}{\overline{K}(f,w)} \frac{a_m(t)}{a_m(t)+K(f,w)}$
$\overline{\omega}(t)$: variation of v_d relative to v_{d-1}
$\xi_1(t), \ldots, \xi_3(t)$: variables of model for hydraulic systems
$\xi_{n_1}(t), \ldots, \xi_{n_3}(t)$: regressors for identification of hydraulic systems
^{i}: i times partial derivation with respect to x
$a(t)$: position of plate when rolled
$a_e(t)$: estimate of $a(t)$
$a_m(t)$: plate hardness used in traditional modeling

a_{hn1}: parameter for flow through servo valve for north system
a_{hn2}: parameter for oil compressibility of north system
a_{hn3}: parameter for leak flow for north system
a_{hs1}: parameter for flow through servo valve for south system
a_{hs2}: parameter for oil compressibility for south system
a_{hs3}: parameter for leak flow for south system
$a_{m1}(t)$: plate hardness
$a_{m2}(t)$: plate damping
$a_{m3}(t)$: parameter for v_r in p_d
c: roll crown
$f(t) = [\, f_n(t) \quad f_s(t) \,]^T$
$f_c(t) = [\, f_{c_n}(t) \quad f_{c_s}(t) \,]^T$
$f_n(t)$: rolling force at north side
$f_s(t)$: rolling force at south side
$f_z(t)$: regressor in recursive identification of a_{m1}
$f_{c_n}(t)$: north rolling force found using model for the rolling stand
$f_{c_s}(t)$: south rolling force found using model for the rolling stand
$i(t)$: integral states in extended model for rolling stand
k: sample number
$k_p(r_t, T)$: plate hardness
l: width of work roll
$l_1, \ldots, l_8$: elements of L
m: number of inputs and outputs of extended rolling stand model
n: number of states in extended model for rolling stand
$o(t)$: roll eccentricity and ovalness
$o_e(t)$: estimate of o
o_{fe_1}, o_{fe_2}: parameters of observer
p: differential operator $\frac{d}{dt}$
$p_1(t)$: pressure at left side of oil cylinder
$p_2(t)$: pressure at right side of oil cylinder
$p_d(x,t)$: pressure distribution across plate width
$p_{c_1}(p)$: characteristic polynominal for $\overline{G}_{c_v}$
$p_{c_2}(p)$: characteristic polynominal for $\grave{G}_{c_v}$

q: forward shift operator
$q(t) = [\, q_1(t) \quad q_2(t) \,]^T$
$q_1(t)$, $q_2(t)$: normal coordinates in series expansion for $\hat{u}$
$q_c(t) = [\, q_{c_1}(t) \quad q_{c_2}(t) \,]^T$
$q_e(t) = [\, q_{e_1}(t) \quad q_{e_2}(t) \,]^T$
$q_{c_1}(t)$, $q_{c_2}(t)$: normal coordinates found using model for rolling stand
q_{c_o}: initial conditions for q_c
$q_{e_1}(t)$, $q_{e_2}(t)$: estimates of q_{c_1} and q_{c_2} found using observer
$r(t) = [\, r_n(t) \quad r_s(t) \,]^T$
$r_d(x,t)$: reduction across plate width
$r_l(t) = [\, r_{l_n}(t) \quad r_{l_s}(t) \,]^T$
$r_n(t)$: reference for plate thickness at north edge
$r_s(t)$: reference for plate thickness at south edge
$r_{l_n}(t)$: input for feedback linearization of north hydraulic system
$r_{l_s}(t)$: input for feedback linearization of south hydraulic system
r_t: reduction
s_1, s_2: scaling factors used in the stability analysis
$s_f(t)$: forward slip relating roll and plate speed
t: time
$u(x,t) = \frac{1}{2} v_d(x,t) - \varepsilon(x)\frac{1}{2} z(t)$
$v_c(t) = [\, v_{c_n}(t) \quad v_{c_s}(t) \,]^T$
$v_d(x,t)$: plate thickness across plate width
$v_e(t) = [\, v_{e_n}(t) \quad v_{e_s}(t) \,]^T$
$v_m(t)$: plate thickness at the center
$v_n(t)$: plate thickness at north edge
$v_p(t)$: speed of plate when rolled
$v_r(t)$: rotational speed of work roll
$v_s(t)$: plate thickness at south edge
$v_{-1n}(t)$: ingoing plate thickness at north edge
$v_{-1s}(t)$: ingoing plate thickness at south edge
$v_{c_m}(t)$: center thickness found using model for the rolling stand
$v_{c_n}(t)$: north thickness found using model for the rolling stand

$v_{c_s}(t)$: south thickness found using model for the rolling stand
$v_{d-1}(x,t)$: ingoing thickness across plate width
$v_{e_m}(t)$: plate thickness at the center found using observer
$v_{e_n}(t)$: plate thickness at the north edge found using observer
$v_{e_s}(t)$: plate thickness at south edge found using observer
w: plate width
x: independent variable in width direction
$x_1, \ldots, x_3$: positions for measurement of plate thickness v_d
$x_v(t) = [\, x_{vn}(t) \quad x_{vs}(t) \,]^T$
$x_{vn}(t)$: position of servo valve glider of north hydraulic system
$x_{vrn}(t)$: control signal for north hydraulic system
$x_{vrs}(t)$: control signal for south hydraulic system
$x_{vr}(t) = [\, x_{vrn}(t) \quad x_{vrs}(t) \,]^T$
$x_{vs}(t)$: position of servo valve glider of south hydraulic system
$y_c(t)$: states of the model for the rolling stand
$y_e(t)$: estimate of y_c found using observer
$y_n(t)$: output used in the identification of north system
$y_s(t)$: output used in the identification of south system
$y_z(t)$: output in recursive identification of a_{m1}
$z(t) = [\, z_n(t) \quad z_s(t) \,]^T$
$\bar{z}_h$: output of linear model for hydraulic systems
$z_h(t) = [\, z_{h_n}(t) \quad z_{h_s}(t) \,]^T$
$z_d(x,t)$: roll position across plate width
$z_{h_n}(t)$: position of north common piston found using hydraulic model
$z_{h_s}(t)$: position of south common piston found using hydraulic model
$z_n(t)$: position of north common piston
$z_s(t)$: position of south common piston
z_t: maximal value of position of common piston

B

Physical constants

Below the physical constants of the PDE are found. The numerical values are used for the system identification, the controller design and the simulations.

K

The mill spring coefficient K is a nonlinear function of the rolling force f and the plate width w. The nonlinear characteristics of K are dominating below a certain force level, over the force level K is constant. Since we mostly work with forces in the linear area we can approximate the mill deflection using a linear term K and an offset z_K

$$\frac{\overline{f}(t)}{K(f,w)} \approx z_K(w) + \frac{\overline{f}(t)}{K(w)}$$

Since we only have data for the widths w = 2.15 m and w = 3.15 m we can reduce the necessary figures to the ones shown in Table B.1. When using the mill spring curve z_K is added to the roll position and K is used as a constant mill spring coefficient.

The above K and z_K give the total deflection of the entire rolling mill when using the mean value of the force $\overline{f}$ as input. In the physical model for the rolling stand, half the deflection of the rolling mill is used with the forces f_n and f_s as inputs. Therefore $2K$ and $2z_K$ are used in this case.

	w = 2.15 m	w = 3.15 m
K	2.02×10^9 N/m	2.05×10^9 N/m
z_K	0.570×10^{-3} m	0.525×10^{-3} m

Table B.1

ρ

The work and backup rolls are made from steel coated cast iron. To maintain simplicity we here assume that they are made from solid steel, this has shown to work well in practice. The mass density ρ for steel is

$$\rho = 7.85 \times 10^3 \text{ kg/m}^3$$

see [Fenner, 1989].

A

The total area of the roll pack A is given by

$$A = \pi(r_w^2 + r_b^2) = 2.33\text{m}^2$$

where r_w is the radius of the work roll with a value of 0.425 m and r_b is the radius of the backup roll with a value of 0.750 m

E

Youngs modulus E for steel is:

$$E = 2.07 \times 10^{11} \text{ N/m}^2$$

see [Fenner, 1989].

I

When calculating the second moment of area I for the bending of the roll pack it is normally only necessary to include the second moment

of area for the work roll, see [Roberts, 1983]. Using [Fenner, 1989] we find that I for a member with circular cross section is

$$I = \frac{\pi(2r_w)^4}{64} = 2.56 \times 10^{-2} \text{ m}^4$$

where r_w is the radius of the work roll which has a value of 0.425 m.